

NASA  
Reference  
Publication  
1292, Vol. I

March 1993

The Atmospheric Effects  
of Stratospheric Aircraft:  
Report of the 1992 Models  
and Measurements Workshop

*Volume I—Workshop Objectives  
and Summary*

(NASA-RP-1292-Vol-1) THE  
ATMOSPHERIC EFFECTS OF  
STRATOSPHERIC AIRCRAFT. REPORT OF  
THE 1992 MODELS AND MEASUREMENTS  
WORKSHOP. VOLUME 1: WORKSHOP  
OBJECTIVES AND SUMMARY (NASA)  
132 p

N93-25157

Unclas

H1/45 0158807

IN-45  
158807

p. 132

NASA



**NASA  
Reference  
Publication  
1292, Vol. I**

1993

**The Atmospheric Effects  
of Stratospheric Aircraft:  
Report of the 1992 Models  
and Measurements Workshop**

*Volume I—Workshop Objectives  
and Summary*

*Edited by  
Michael J. Prather  
NASA Office of Space Science and Applications  
Washington, D.C.*

*Ellis E. Remsberg  
Langley Research Center  
Hampton, Virginia*



National Aeronautics and  
Space Administration  
Office of Management  
Scientific and Technical  
Information Program



Contributing Authors:

G. Anderson  
C. Bruhl  
B. Connor  
A. Douglass  
R. Eckman  
D. Fahey  
D. Fisher  
I. Folkins  
R. Garcia  
C. Granier  
W. Grose  
M. Hitchman  
C. Jackman

R. Kawa  
J. Kaye  
J. Kinnersley  
D. Kinnison  
M. Ko  
M. Kurylo  
R. McPeters  
C. Miller  
R. Nagatani  
P. Newman  
G. Pitari  
C. Rinsland  
R. Rood

J. Rosenfield  
T. Sasaki  
U. Schmidt  
R. Seals  
M. A. Smith  
R. Stolarski  
K.-K. Tung  
D. Weisenstein  
H. Wesoky  
D. Wuebbles  
G. Yue  
Y. Yung  
J. Zawodny

PRECEDING PAGE BLANK NOT FILMED

11  
INTERNATIONALLY SLANT

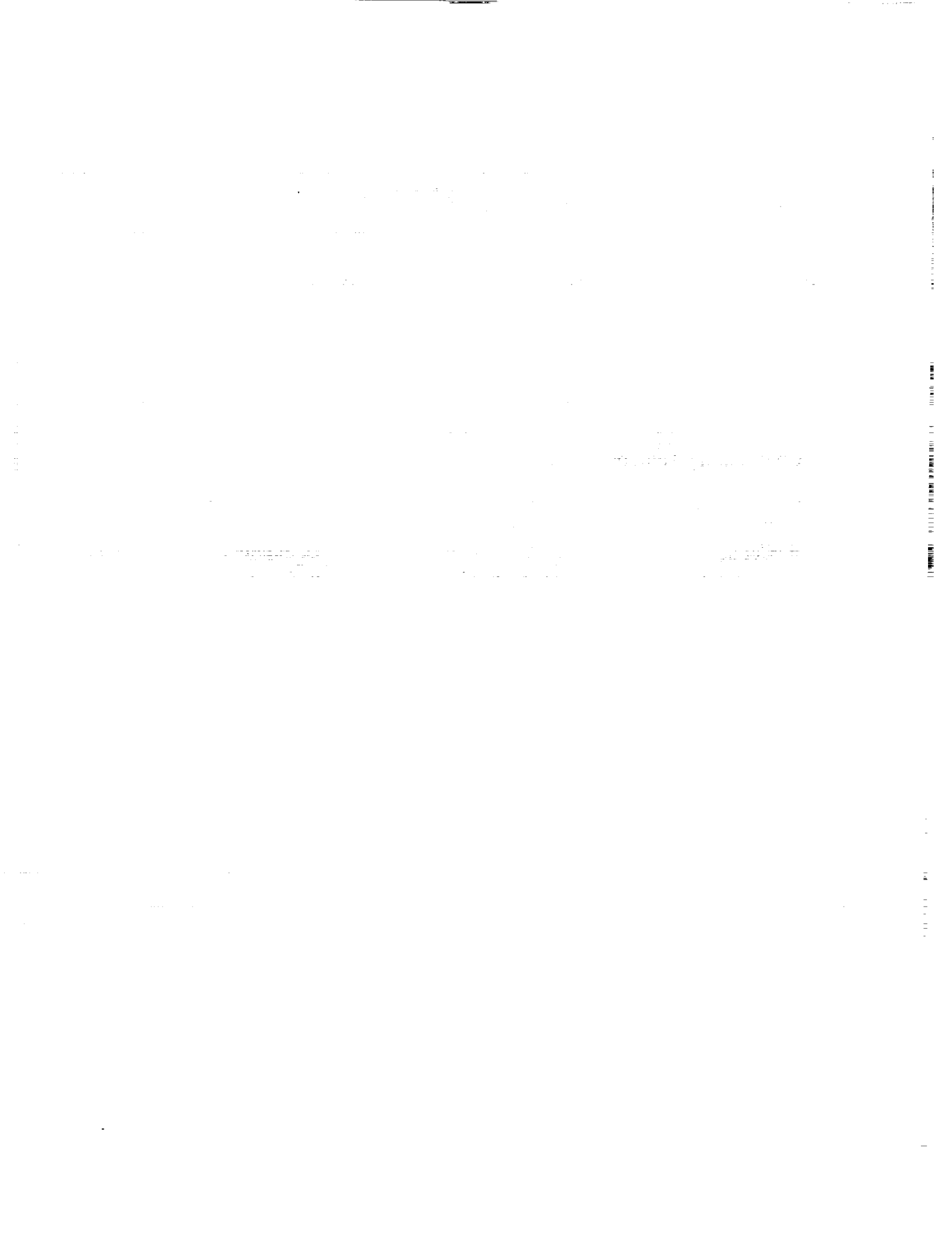


# TABLE OF CONTENTS

## VOLUME I

<b>Preface</b> .....	vii
<b>Executive Summary</b> .....	ix
<b>Chapter 1 Workshop Objectives</b> .....	1
A. Introduction .....	3
B. Experiment Definition .....	5
C. Workshop Participants .....	32
<b>Chapter 2 Summary of Findings</b> .....	39
A. Comparisons with Global Atmospheric Measurements .....	41
B. Special Diagnostic Studies .....	47
<b>Chapter 3 Upper Atmosphere Data Base and Model Submission</b> .....	55
<b>Chapter 4 Update of Model Descriptions</b> .....	61
AER Two-Dimensional Photochemical Transport Model.....	63
CALJPL Two-Dimensional Model .....	67
CAMED-theta Two-Dimensional Model.....	70
DUPONT Two-Dimensional Model .....	73
GISS Photochemical Model.....	76
GISS Three-Dimensional Stratospheric Tracer Model .....	86
GSFC Fast Two-Dimensional Model .....	90
ITALY Two-Dimensional Model .....	95
LLNL Two-Dimensional Chemical-Radiative-Transport Model .....	98
MPIC Two-Dimensional Model .....	103
MRI Two-Dimensional Photochemical Model.....	105
NCAR Model .....	106
NOCAR Two-Dimensional Model .....	110
OSLO Two-Dimensional Transport Chemistry Model .....	111
WASH Two-Dimensional Model .....	112
<b>Chapter 5 Commentary on Models and Measurements Intercomparison</b> .....	115

## VOLUME II

	Key to Model Data in Plots .....	vii
A.	Temperature, Net Heating and Circulation .....	A-1
B.	Water Vapor .....	B-1
C.	Integrated Column Ozone .....	C-1
D.	Ozone Profiles .....	D-1
E.	Global Distributions of N <sub>2</sub> O and CH <sub>4</sub> .....	E-1
F.	Abundances and Distribution of NO <sub>y</sub> Species .....	F-1
G.	Column Abundances of HF, HCl, HNO <sub>3</sub> , ClONO <sub>2</sub> and NO <sub>2</sub> .....	G-1

## VOLUME III

	Key to Model Data in Plots .....	vii
H.	Simultaneous Observations of Long-Lived Species .....	H-1
I.	Radionuclides as Exotic Tracers .....	I-1
J.	Mt. Ruiz Volcanic Cloud .....	J-1
K.	Overview to K, L and M .....	K-i
K.	Photodissociation Rates .....	K-1
L.	Photochemistry of Radicals and Rates .....	L-1
M.	Species Comparisons with ATMOS at Sunset .....	M-1
N.	Transport Fluxes .....	N-1
O.	Model-Model Comparison of Idealized Tracers, X1 and X2 .....	O-1

# Preface

The continuing need for intercomparison and evaluation of the stratospheric models used in environmental assessments was made clear at the first annual Atmospheric Effects of Stratospheric Aircraft component of NASA's High-Speed Research Program (HSRP/AESA) meeting (January 1991). The predictions of ozone perturbations in response to aircraft injections of nitrogen oxides were diverse (see chap. 5, NASA ref. public. 1272, Prather, et al., Jan 1992), there was no ready explanation of these differences and, more importantly, there were no clear indicators as to which of the simulations might be more accurate. At the urging of Bill Grose, the modeling community met in the halls during this meeting and agreed to participate in a "major-effort" modeling workshop to be conducted within a year.

The Stratospheric Models and Measurements (M&M) Workshop was held on 3-7 February 1992 in Satellite Beach, Florida. Substantial revisions and review of the Workshop occurred at the Second AESA Annual Meeting in May 1992, and the editing and reviewing of the document were completed over the summer. Model workshops have been held since the mid-1970s, generally under the auspices of NASA's Upper Atmosphere Programs, when it became important to make predictions of O<sub>3</sub> depletion expected from chlorofluorocarbon emissions. The resources for this study were provided by three NASA programs: the Atmospheric Chemistry, Modeling and Analysis Program (successor of the Upper Atmosphere Theory Program, Jack Kaye), the Upper Atmosphere Research Program (Michael Kurylo), and the AESA studies (Michael Prather and Howard Wesoky).

This study is the first of these efforts to focus on comparison and "verification" of the models with stratospheric measurements. The detailed planning of the Workshop agenda involved members of the atmospheric sciences community who take and analyze measurements: many of these individuals were not directly involved in the AESA effort and gave their time as part of an overall interest in understanding the stratosphere. The AESA program is indebted to their scientific contributions. Results from 14 different modeling groups were evaluated at the Workshop, which was attended by 35 scientists. This report presents the results of that evaluation, including many of the plots used to derive the findings. The report also includes an Executive Summary by the editors. The complete report, including data sets, will be published on CD-ROM. The model results and measurements included in this report and on the CD-ROM are in the public domain. Nevertheless, researchers using any of these data sets are strongly urged to contact and work with the principal investigators involved before republishing any of these data. Both model results and measurements must be regarded as dated material from 1991: measurements rely on retrieval algorithms and calibrations which can change and models are continually developed (e.g., in response to this report), and up-to-date results would likely differ from those reported here.

Many scientists and professionals contributed to the success of the M&M study. Karen Sage and Linda Hunt of Lockheed, Inc. at NASA Langley compiled the models and measurements data sets for the Workshop and for the CD-ROM. Richard Eckman, Robert Seals, and Mary Ann Smith of NASA Langley Research Center provided administrative support for that effort. Kathy Wolfe and staff at Atlantic Research Corporation organized the Florida meeting and prepared the final report. Special thanks for this publication go to Cindy Alami, Nancy Brown, Rose Kendall and Aylene Kovensky.

Michael J. Prather and Ellis E. Remsberg, editors  
30 November 1992

1. The first part of the document discusses the importance of maintaining accurate records of all transactions and activities. It emphasizes that proper record-keeping is essential for ensuring transparency and accountability in financial operations. This section also highlights the role of internal controls in preventing fraud and errors.

2. The second part of the document focuses on the implementation of robust risk management strategies. It outlines various risk assessment techniques and provides guidance on how to identify, measure, and mitigate potential risks. The text stresses the need for a proactive approach to risk management to protect the organization's assets and reputation.

3. The third part of the document addresses the importance of effective communication and reporting. It discusses the need for clear and concise communication channels and the role of regular reporting in keeping stakeholders informed. This section also touches upon the importance of maintaining accurate financial statements and providing timely updates to investors and other interested parties.

4. The fourth part of the document discusses the importance of maintaining accurate records of all transactions and activities. It emphasizes that proper record-keeping is essential for ensuring transparency and accountability in financial operations. This section also highlights the role of internal controls in preventing fraud and errors.

5. The fifth part of the document focuses on the implementation of robust risk management strategies. It outlines various risk assessment techniques and provides guidance on how to identify, measure, and mitigate potential risks. The text stresses the need for a proactive approach to risk management to protect the organization's assets and reputation.

6. The sixth part of the document addresses the importance of effective communication and reporting. It discusses the need for clear and concise communication channels and the role of regular reporting in keeping stakeholders informed. This section also touches upon the importance of maintaining accurate financial statements and providing timely updates to investors and other interested parties.

# Executive Summary

This Workshop on Stratospheric Models and Measurements (M&M) marks a significant expansion in the history of model intercomparisons. It provides a foundation for establishing the credibility of stratospheric models used in environmental assessments of chlorofluorocarbons, aircraft emissions, and climate-chemistry interactions. The core of the M&M comparisons involves the selection of observations of the current stratosphere (i.e., within the last 15 years): these data are believed to be accurate and representative of certain aspects of stratospheric chemistry and dynamics that the models should be able to simulate.

Stratospheric assessments of a decade ago relied predominantly on one-dimensional (1-D) models. The limited observations of the stratosphere then available were often used to define the 1-D diffusive transport. Discrepancies were often explained away as something that a 1-D "globally averaged" model could not be expected to represent! With the development of two-dimensional (2-D) and three-dimensional (3-D) stratospheric models for use in these assessments, it has become increasingly difficult to dismiss these discrepancies between models and observations. Further, the number and diversity of observations make it almost impossible to compare a model with all of them. Another consequence of this wealth of not-always-consistent observations is the publication of papers documenting and "validating" a particular model in which comparisons are made with a selection of data sets that do not always overlap with those in other model publications.

Thus, we selected a single set of measurements that all of the stratospheric models should be asked to simulate. These benchmarks were developed by scientists involved in the taking and analysis of atmospheric measurements from satellites, balloons, and aircraft, with the help of the global modeling community. The final selection of case studies (Sections A through O of this M&M Report) was based on the accuracy and representativeness of the measurements, as well as the ability to test the different components of the stratospheric models. We summarize here what we have learned about the models' ability, as a class, to simulate the stratosphere.

We recognize that there are additional research groups using stratospheric models to assess, for example, chemical changes with climate models and polar ozone depletion with trajectory or assimilation models. In addition to the 2-D and 3-D stratospheric chemistry models evaluated in this M&M Workshop, these other models play important roles in environmental assessments. The M&M effort must expand to include an evaluation of the performance of these more diverse models (e.g., by comparing with the experiments presented here) in order to establish better measures of uncertainty for assessments by all of the stratospheric models.

## PHOTOCHEMICAL PROCESSES

There is strong evidence that the most important photochemical processes are included in the models to an accuracy of approximately 40%. The relative abundances of the odd-nitrogen and chlorine species in the altitude range of 20 and 40 km from selected ATMOS profiles are reasonably simulated over a large range of photochemical conditions. For example, the observed ratios  $\text{NO}:\text{NO}_2:\text{HNO}_3$  at sunset change from 1:4:12 near 20 km to 20:10:1 near 40 km, and are well matched by the models. Similarly, the correlations of  $\text{N}_2\text{O}$  and  $\text{CH}_4$ , for example, show that the relative destruction rates, photolysis of  $\text{N}_2\text{O}$  versus OH reaction with  $\text{CH}_4$ , are reasonably modeled. There still remain some problems with the photochemical balance of  $\text{O}_3$  in the upper stratosphere (systematic underprediction by 20 to 40%).

In the 15-20 km altitude region, where most ozone depletion is observed, we are hampered by the lack of suitable measurements of the chemical partitioning. This region of the stratosphere also

shows the largest differences among the photochemical models, often more than a factor of 2 or more for key species such as OH.

Modeling of transmission of sunlight in the Schumann-Runge bands of molecular oxygen has improved, and we now have a new standard for comparison. Scattered sunlight is a significant component in photolysis of  $\text{NO}_2$ ,  $\text{NO}_3$ ,  $\text{HNO}_3$ ,  $\text{ClONO}_2$ , and  $\text{N}_2\text{O}_5$  in the lower stratosphere. The equation of radiative transfer in a scattering atmosphere, however, is poorly approximated in some of the models and adds to the divergence of model calculations, especially for  $\text{HO}_x$  in the lower stratosphere.

The detailed comparison of photolysis rates and chemical cycles among the models has always been and still remains unsatisfactory: when adopting a prescribed atmosphere, differences should be less than 10% instead of the 30% and more noted here. The modeling groups have agreed that they are solving the same basic equations using the same chemical and physical constants, and, thus, it is difficult to understand how the models could differ as much as reported here. Although uncertainty in the physical "constants" may in some cases exceed these model differences, it cannot be used to explain inaccurate calculations.

## HETEROGENEOUS CHEMICAL PROCESSES

The inclusion of heterogeneous chemical reactions on the global sulfate-layer as a standard feature in the assessment models began with the 1991 World Meteorological Organization/United National Environmental Program (WMO/UNEP) ozone assessment. At first these reactions (i.e.,  $\text{N}_2\text{O}_5$  and  $\text{ClONO}_2$  reacting with the  $\text{H}_2\text{O}$  on the sulfate droplets) appeared to have little impact on the predicted "mean" ozone abundance, but upon closer examination of the models, these reactions shift the chemical destruction of  $\text{O}_3$  in the mid-latitude lower stratosphere from  $\text{NO}_x$  catalytic cycles to those involving  $\text{HO}_x$  and  $\text{Cl}_y$  with little net change in the balance between transport and photochemical loss. Thus, predicted trends in  $\text{O}_3$  become more sensitive to increases in stratospheric chlorine. The modeled trends over the decade 1980-1990 are similar to those measured, but point to missing processes at high latitudes in wintertime (i.e., polar stratospheric clouds, which are not included in most of these models).

Global-scale observations support the inclusion of heterogeneous processing of  $\text{NO}_x$  into  $\text{HNO}_3$  at rates similar to those adopted here. The seasonality of stratospheric  $\text{NO}_2$  concentrations (at sunset from SAGE II) indicates removal of  $\text{NO}_2$  around wintertime coincident with the sulfate layer. Models using only gas-phase reactions could not reproduce this large winter-summer difference in  $\text{NO}_2$  between 20 and 26 km in the mid latitudes of both hemispheres. In addition, the LIMS  $\text{HNO}_3$  profiles and the column  $\text{HNO}_3$  observations support this process of more rapid conversion to  $\text{HNO}_3$  at high latitudes with low sun angles.

Further observations of  $\text{NO}_y$  and  $\text{Cl}_y$  partitioning in the lower stratosphere, especially below 20 km, should become available from the recent 1992 ATMOS flights and the extensive ER-2 campaigns (1991-92 AASE-II and 1992-93 SPADE). It is hoped that when UARS data become publicly available, they will further add to our understanding. These new data would allow a more rigorous evaluation of the modeling of heterogeneous processes.

## STRATOSPHERIC TEMPERATURES AND CIRCULATION

The large differences between the models' and the observed (NMC) temperatures are worrisome for several reasons. Temperatures in the models are important for calculating both the chemical and heating rates used to derive the circulation. The sensitivity of the gas-phase photochemistry to temperature is known, and the differences found here are not consequential. Errors in absolute

temperature of, for example, 5K in the lower stratosphere, can be extremely important for heterogeneous reactions (i.e., the formation of polar stratospheric clouds and the weight % of H<sub>2</sub>O in the sulfate layer droplets, which control the rate of ClONO<sub>2</sub> hydrolysis). The concern over calculation of heterogeneous chemistry in 2-D monthly averaged, zonally averaged models focusses on the real variations of temperature, and hence heterogeneous rates, over a month around a latitude circle that must be averaged. Thus, the hydrolysis of N<sub>2</sub>O<sub>5</sub> -- the most important heterogeneous reaction in these calculations -- should be representable in these models, whereas PSCs and the hydrolysis of ClONO<sub>2</sub> cannot be represented by a monthly zonal-mean temperature.

The derived 2-D circulation is, for most models, based on the net heating (Qnet) derived from the assumed temperatures and ozone distribution. Qnet defines the residual velocity, and a horizontal diffusion is added to account for 3-D transport by waves that are averaged over in the residual circulation. The modeled Qnet's are qualitatively similar, but differ significantly from each other and from a new reference standard derived from the NMC temperature and SBUV ozone climatologies. Large differences in net heating and circulation cannot be explained by the temperature differences alone.

We have identified a problem with the derivation of global circulations from Qnet: the requirement that Qnet must average to zero globally across a pressure surface (which does not often happen in these calculations) has led to various corrections to the calculated Qnet, e.g., offsetting by a constant. Because the stratosphere below 100 mbar at mid latitudes connects with the pressure surfaces in the tropical troposphere, errors in the 2-D calculation of net heating in the convective troposphere may impact the polar stratosphere when Qnet is corrected. It seems clear that the concept of a residual circulation from Qnet must be re-evaluated for the lower stratosphere.

Since Qnet describes only part of the transport, and the application of diffusion coefficients (K<sub>yy</sub>'s) is often model dependent, we examined the different model circulations with synthetic tracers using prescribed chemical loss frequencies. For synthetic CFC-like tracers, the spread in modeled lifetimes is similar to that reported by the different models for the CFCs and N<sub>2</sub>O. Thus, a large fraction of these difference can be attributed to the different stratospheric transports.

Overall the vertical and latitudinal distribution of O<sub>3</sub>, HNO<sub>3</sub>, CH<sub>4</sub>, and N<sub>2</sub>O from satellite observations were matched by the models, but some patterns in the observed N<sub>2</sub>O and CH<sub>4</sub> global distributions (e.g., semi-annual oscillation in the upper tropical stratosphere) are not paralleled in the models. As a group, the models perform well at mid to high latitudes between 20 and 30 km. Seasonal variations were well represented except near the winter poles, where only a few models achieved only partial success. The clear signal of photochemically aged air (e.g., very low N<sub>2</sub>O) at low altitudes within the winter polar vortex is extremely difficult to simulate with 2-D models unless the horizontal mixing is suppressed. Also, the models cannot reproduce some unique features observed in the tropical lower stratosphere that are likely associated with the circulation: notably the O<sub>3</sub> profiles and the O<sub>3</sub>:NO<sub>y</sub> ratios. In general, model representation of transport through the lower stratosphere and across the tropopause is still uncertain. The new O<sub>3</sub> climatology (SBUV and SAGE combined) provides one of the best tests of tracer gradients across the tropopause.

The modeled tracer correlations between N<sub>2</sub>O, CH<sub>4</sub> and the CFCs were quite successful in simulating the observations. The relative fall-off of these species is primarily a measure of the chemical loss in the lower stratosphere, but depends on rates of transport in the upper stratosphere. The case of a synthetic tracer with a trend in tropospheric abundance has clearly identified a source of curvature in the correlation plot due to the lag in transport time for trace gases. Improved measurements of the N<sub>2</sub>O-CH<sub>4</sub> correlation curve, its scatter, and its deviations

from linearity in different regions of the stratosphere may provide good overall tests of the models.

Based on experiments with transient tracers such as radioisotopes from weapons tests or volcanic clouds, we have found that the atmospheric circulation can vary significantly from year-to-year. Some of this variation can be viewed as fluctuations about a "mean" circulation that the 2-D models should be able to simulate. However, the quasi-biennial oscillation (QBO) in tropical zonal winds leads to two distinctly separate modes in the stratospheric circulation: different phases of the QBO are expected to have different wave forcing and hence horizontal mixing (approximated as diffusion in the 2-D models). Such an isolation of the tropical stratosphere was observed in the simulations of the Mt. Ruiz volcanic cloud here. The bimodal QBO circulation poses a fundamental, new problem for the models in that the QBO is exceedingly difficult to simulate, and further, that assessment calculations would need to be averaged over two or more years since ozone perturbations may depend on the phase of the QBO.

### IMPACT OF ADDITIONAL CHLORINE & BROMINE

How consistent and reliable are the models in predicting the effects of increasing halocarbons? Clearly the inclusion of heterogeneous (sulfate-layer) chemistry makes O<sub>3</sub> loss below 30 km altitude more sensitive to the abundance of chlorine and bromine species, and the impact of PSCs (not readily incorporated in 2-D models) would further enhance ozone depletion near the winter poles.

The cross-correlations of the source gases for these halogens (e.g., the CFCs, halons, CH<sub>3</sub>Br) show that the decomposition of these halocarbons and the release of Cl<sub>y</sub> and Br<sub>y</sub> in the lower stratosphere is reasonably approximated in the models. The largest uncertainties lie in the lower stratosphere, below 20 km, where the absolute distributions of Cl<sub>y</sub> and Br<sub>y</sub> are not yet well determined from measurements and where the calculations of the catalytic cycles are very different among these models. Although we have extensive observations of ClO and BrO below 20 km from the ER-2 campaigns, which are consistent with observed ozone loss, there remain uncertainties in absolute calibration, rates, and global representation. Even when the composition is fixed, the model predictions of key catalytic rates in the mid-latitude stratosphere (e.g., HO<sub>2</sub>+ClO, ClO+O, ClO+BrO) differ by more than a factor of 2 below 20 km. For example, even the relative role of Br<sub>y</sub> to Cl<sub>y</sub> in ozone destruction is not well determined.

A more rigorous analysis of the recent and upcoming ER-2 measurements (especially the ClO and BrO abundances) would provide an excellent test for the chemical partitioning in the lower stratosphere.

### IMPACT OF ADDITIONAL NO<sub>x</sub> and H<sub>2</sub>O

In the stratosphere, if the uncertainties of model circulation and transport are reduced so that we would be able to predict the absolute increase in NO<sub>y</sub> associated with an aircraft source, then there is some confidence that the first-order impact on ozone chemistry would be assessed well by the current models. This confidence comes from the new role of heterogeneous chemistry: the importance of NO<sub>x</sub> chemistry to O<sub>3</sub> loss below 25 km at mid-latitudes is small even at background levels of sulfate aerosols; under volcanic conditions, its role is further reduced. This confidence does not extend to chlorine-catalyzed loss since these cycles may become greatly enhanced by heterogeneous processing.

Current stratospheric models, even those that "calculate" H<sub>2</sub>O, specify H<sub>2</sub>O in some way or another that critically controls the stratospheric abundance. Although these assumptions are

reasonable, they do not adequately represent the physical processes that change H<sub>2</sub>O near the tropopause. Therefore, estimates of relative H<sub>2</sub>O change from stratospheric aircraft injection can be made, but may be in error if the mechanism for removal of H<sub>2</sub>O in the mid-latitude stratosphere is not understood. For example, if the drying-out mechanism fixes the partial pressure at the tropopause, the prediction would be different than if a fixed flux is removed by some other mechanism at specified latitudes. Current measurements do not yet allow us to build a model for the injection and removal of H<sub>2</sub>O from the lower stratosphere.

The combination of increased H<sub>2</sub>O and HNO<sub>3</sub> (from NO<sub>x</sub> injection) may have a small direct impact on the gas-phase photochemistry, but might substantially increase the occurrence of PSCs. A proper assessment must include the changing stratospheric temperatures (due to long-term greenhouse forcing as well as ozone loss), the declining levels of Cl<sub>y</sub> in the stratosphere (reducing the PSC-driven ozone loss), and a validated model for the changes in PSC formation and chemical processing. All of these, except for the declining Cl<sub>y</sub>, have not yet been tested and verified in the stratospheric assessment models.

In the troposphere, the addition of NO<sub>x</sub> from aircraft is expected to enhance tropospheric ozone. In addition aircraft contrails may generate clouds with subsequent climatic impacts. The models in this assessment have not been evaluated for their abilities in simulating tropospheric transport, chemistry, and climate. It is likely that development and "verification" of a new set of 3-D models will be needed for such assessments.

[The page contains extremely faint and illegible text, likely bleed-through from the reverse side of the document. The text is too light to transcribe accurately.]

# **Chapter 1**

## **Workshop Objectives**



## Workshop Objectives

### A. Introduction

#### 1. History

The stated objectives of the HSRP/Atmospheric Effects of Stratospheric Aircraft (AESA) initiative are to support research in the atmospheric sciences that will improve our basic understanding of the circulation and chemistry of the stratosphere, and that will lead to (interim) assessments of the impact of a projected fleet of HSCTs on the stratosphere. The two most recent model comparison workshops were conducted in support of this goal; they occurred in 1987 at Ft. Myers Beach, Florida and in 1988 in Virginia Beach, Virginia [Jackman et al., 1989]. Those workshops were focused on the differences between models used to calculate the atmospheric effects of the proposed aircraft emissions. The Models and Measurements Workshop was designed to test these models against atmospheric measurements, and took place in Satellite Beach (near Cocoa Beach), Florida, on February 3-7, 1992.

#### 2. Goals

The charge to the Models and Measurements (M&M) Committee of AESA was to (1) establish a standard set of atmospheric measurements that could be used to test the reliability of atmospheric chemistry models, (2) develop a method for evaluating model-measurement comparisons, and (3) direct the first major international stratospheric model-measurement comparison.

The first Committee meetings were held in March and May 1991 to discuss the available data sets. A wide range of measurements were considered for this purpose. These data include: ozone column or total ozone; multiple years of ozone, H<sub>2</sub>O, CH<sub>4</sub>, N<sub>2</sub>O, and NO<sub>2</sub> distributions; column estimates of HNO<sub>3</sub>, NO<sub>2</sub>, HCl, and HF; satellite distributions of nitric acid; ATMOS and balloon profiles of various species, radioisotope, and aerosol distributions; and a "climatology" of polar stratospheric cloud (PSC) occurrences. Certain balloon and aircraft campaigns have obtained simultaneous data on many species and radicals, such that one can determine correlations for long-lived trace species, as well as perform checks on fast photochemical processes.

Multiple years of temperature, wind and geopotential height data are available from which one can characterize the state of the stratosphere for different seasons and locations. One can derive certain dynamical quantities from these measurements, and they, in turn, can be used to diagnose the net transport in both the atmosphere and in models. It is expected that the Upper Atmosphere Research Satellite (UARS) will provide even more extensive distributions of trace species, but they may not be publicly archived until late 1993. More importantly, new aircraft measurement campaigns will be conducted at a range of latitudes and altitudes in the lower stratosphere during 1992 through 1994. Those data should become available fairly quickly.

Many of the data sets already resided in an Upper Atmosphere Data Pilot (UADP) computer system at the NASA Langley Research Center. This repository was supplemented with other measurements during 1991 upon the recommendation and assistance of the M&M Committee members. Output from the models were gridded in formats that are compatible with the measurements and then stored in the UADP. They are defined in Section B of this chapter. Species distributions from the models were compared with the data distributions, and the Committee members then assessed the accuracy of those comparisons at the week-long meeting in February 1992.

This three-volume report represents the culmination of a year-long activity for the members of the Committee and, in particular, for each of the modeling groups. In the course of the effort, errors were found and corrected in individual models, and the observational data sets were critically evaluated. The results that are documented in Chapters 2 and 3 and in volumes II and III can be obtained from the UADP data base, and they will be available in CD-ROM format for further study by the wider community not involved in this limited-attendance Workshop.

It is believed that the need for model-measurement intercomparisons will continue after 1992, as new observations become available and models improve. It is expected that the present M&M activity will lead to insight into specific areas of model improvement, and also provide increasing confidence in the models used for HSRP/AESA and other environmental assessments.

## REFERENCES

- Jackman, C. H., R. K. Seals, Jr., and M. J. Prather, *Two-dimensional Intercomparison of Stratospheric Models*, NASA Conf. Publ. 3042, Virginia Beach, VA, 608 pp., 1989.
- Prather, M. J., H. L. Wesoky, R. C. Miake-Lye, A. R. Douglass, R. P. Turco, D. J. Wuebbles, M. K. W. Ko, and A. L. Schmeltekopf, *The Atmospheric Effects of Stratospheric Aircraft: A First Program Report*, NASA Ref. Publ. 1272, 244 pp., January, 1992.

## **B. Experiment Definition**

This subsection contains the chronology of preparations for the Models and Measurements Workshop. First, are a series of letters. The idea to have a Models and Measurements Workshop was introduced in the "Dear Colleague" letter of February 1991 that resulted from the first annual HSRP/AESA Program meeting [Prather et al., 1992]. The March 1991 letter announced the subgroups. The letter dated early September 1991 formally invited participants to the Workshop. In the attached distribution list, members of the M&M organizing committee are denoted by an asterisk.

Details for the conduct of Experiments A through O are supplied in the multipage letter dated September 20, 1991. The correction to C-14 boundary conditions for Experiment I was mailed out on November 22, 1991, and it is attached. The final two pages of this subsection represent new specifications for Experiments K and L that were prepared at the February 1992 Workshop. The findings from those calculations are discussed in Volume III. Subsection C of Chapter 1 is the Workshop Attendance list.



National Aeronautics and  
Space Administration

Washington, D.C.  
20546

Reply to Attn of

SE-44

8 Feb 91

Dear Colleague,

Either Bill Grose or myself has talked to you this past week about participating in an important new project sponsored by the Atmospheric Effects of Stratospheric Aircraft component of NASA's High-Speed Research Program. The stated objectives of HSRP/AESA are to support research in the atmospheric sciences that will improve our basic understanding of the circulation and chemistry of the stratosphere, and that will lead to (interim) assessments of the impact of a projected fleet of high-speed civilian transport aircraft (HSCTs) on the stratosphere. In addition to sponsoring individual research efforts, HSRP/AESA has put together subcommittees or workshops to study specific topics that are critical to the success of the HSRP/AESA goals (e.g., the Ames Workshop on Atmospheric Measurements in October 1990; the Emissions Subcommittee).

The assessment of the impact of aircraft exhaust (from projected supersonic fleets) on stratospheric chemistry, and particularly ozone, will rely on our 2-D and 3-D global atmospheric models. It has been duly noted at several meetings that the community has presented and published numerous model simulations for future scenarios, but that we have no objective (i.e., quasi-standard) criteria for judging which models are "reliable" for today's atmosphere. The great "2-D Intercomparison of Stratospheric Models" (Sep 88, Virginia Beach, Jackman et al) went a long way toward documenting the similarities and differences among the available 2-D and 3-D models in terms of both chemistry, radiation and circulation. This model intercomparison was not immediately followed up by another because, for one, the community was exhausted, and moreover, the limitations of a model-model intercomparison had been pushed to the limit.

We must now take the next major step of a model-measurement comparison. Therefore, I welcome your participation in the 1992 "Stratospheric Models & Measurements: A Critical Comparison"! Ellis Remsberg has kindly consented to chair this committee; its members and assignments are listed below. A schedule is also given, culminating in a January 1992 workshop.

This new intercomparison meeting (Jan 92) will likely include some specific model-model intercomparisons that have not been adequately answered by the 1988 meeting (e.g., photolysis rates), but will focus on a set of measurements and parallel model simulations. The style will be similar to the last comparison, in which one individual (model or data connections) would take one of the prescribed cases (e.g., total ozone) and cross-compare all model simulations as well as all the different measurements and their uncertainties. We will rely on Bob Seals' database as the repository for all observational data and model simulations, and as the source of the comparisons (graphic or tabular).

This effort is an important new initiative in our community; your responses thus far have been willing and even enthusiastic. My charge to this committee is (1) to establish a standard set of atmospheric measurements that can be used to test the reliability of our models and (2) to develop a method for evaluating model-data comparisons. Please note

that innovation is as important here as critical review: e.g., in addition to the "traditional" zonal monthly mean mixing ratios, we should consider family partitioning, species ratios, and meteorological correlations. The atmosphere has changed significantly since Nimbus-7, what periods should we focus on? We must establish standards that can be used to evaluate 3-D as well as 2-D models, climatological as well as assimilated wind fields. I have chosen to call this effort "Models & Measurements Subcommittee" for now, but, obviously, a great prize (or at least public acclamation) will be accorded the originator of a more accurate and catchy title.

#### MODELS & MEASUREMENTS SUBCOMMITTEE

participant	phone [-fax]	responsibility
Ellis Remsberg, Chair	804-864-5823 [-6326]	NO <sub>y</sub> , N <sub>2</sub> O, H <sub>2</sub> O, CH <sub>4</sub>
David Fahey	303-497-5277 [-5373]	aircraft data
Bill Grose	804-864-5830 [-6326]	3-D chemical models
Charley Jackman	301-286-8399 [-2630]	2-D chemical models
Jack Kaye	202-453-1681 [755-2552]	3-D chemical models
Doug Kinnison	415-422-7975 [-5844]	radioisotopes
Michael Kurylo	202-453-1681 [755-2552]	chemical kinetics
Malcolm Ko	617-547-6207 [661-6479]	2-D chemical models
Rich McPeters	301-286-3832 [-3460]	Ozone
Ron Nagatani	301-763-8071 [-8395]	meteorology
Paul Newman	301-286-3806 [-3460]	T-pv-constit. fields
Michael Prather	212-678-5625 [-5552]	3-D chemical models
Curtis Rinsland	804-864-2699 [-7790]	ATMOS & profiles
Bob Seals	804-864-2629 [-7790]	database
Brian Toon	415-604-5971 [-3625]	aerosol models
Glenn Yue	804-864-2678 [-2671]	aerosol data

OTHER STRATOSPHERIC MODELS (INTERNATIONAL, UPPER ATMOSPHERE PROGRAM, HSRP/AESA) WILL INVITED/EXPECTED TO PARTICIPATE IN THE WORKSHOP AND MAY BE REPRESENTED AT THE PLANNING MEETINGS.

Our schedule will be somewhat hurried at the beginning, but if we prepare well by the May meeting, then we can have ample time to get our work done for the January meeting:

March 13-14, 1991 (DC area)

First subcommittee meeting, define types of datasets and model runs.

Decide if we are missing anything.

May 15-16, 1991 (Williamsburg, VA)

Make final decisions on measurement datasets and model simulations.

June-July 1991

Circulate letter defining the formal comparison.

Jan 1992 (4 days, Florida)

Hold the model-data comparison workshop. Must be a small group, no more than 32 participants = above plus other model representatives. Models and Measurements must have data to Bob Seals by December.

Welcome aboard, thank you for the encouragement. PLEASE LET ME OR ELLIS  
KNOW OF CONFLICTS WITH THE MARCH MEETING AS SOON AS POSSIBLE.

Yours,

(fax copy, signed original in mail)

Michael Prather  
Acting Manager  
HSRP/AESA



National Aeronautics and  
Space Administration

Washington, D.C.  
20546

Reply to Attn of:

SE-44

1 March 1991

Dear Colleagues,

The Models & Measurements Committee for HSRP/AESA will hold its first meeting on 13-14 March 1991 (Wed & Thurs) in Washington DC, at NASA HQ. (I am forwarding Ellis Remsberg's instructions re the meeting. )

The Models and Measurements Committee Meeting of HSRP/AESA will address three issues on March 13-14. First, Charley Jackman and Malcolm Ko will each give a brief summary of the approaches used and problems encountered in the 2-D model intercomparison and model assessment studies, respectively. Bob Seals will also describe the data base that is now available for model testing. Then we will have a generic model discussion for 3D, 2D, and microphysics models. Those persons representing models are asked to discuss briefly (15-20 minutes with handouts of important points)--a) model capability (time and space grids, chemical species, and calculation methodology) and their ideas for model validation, and b) what data are needed for that purpose. Are there any concerns about the available data or any conflicts between data sets that you have noticed? Other members representing models will be expected to comment on or add to those presentations.

Second, persons representing types of data should be prepared to give a brief review and show some examples of their parameter/species data sets as well as the various sources of those data. You will not be asked to give a final critical evaluation at this meeting, but you are asked to report and decide on the most appropriate data sets for comparison at the May meeting. We will attempt to define those data sets at this March meeting. Are there innovative ways to use existing data sets for our purposes? At this point we should identify any other individuals that could assist us in this activity and, if necessary, invite them to the May meeting.

Finally, we will attempt to define the appropriate ways to validate and compare models for the AESA study. We will need to specify types of model runs and devise skill tests for quantifying model/data and model/model agreement. It is hoped that we can make progress in identifying and perhaps resolving some of the model/data discrepancies by the time of the May meeting. If there are any questions, please contact either Michael or me.

Best regards, Ellis  
(and Michael)

distribution:

Ellis Remsberg, Chair	804-864-5823 [-6326]	NO <sub>y</sub> , N <sub>2</sub> O, H <sub>2</sub> O, CH <sub>4</sub>
David Fahey	303-497-5277 [-5373]	aircraft data
Bill Grose	804-864-5830 [-6326]	3-D chemical models
Charley Jackman	301-286-8399 [-2630]	2-D chemical models
Jack Kaye	202-453-1681 [755-2552]	3-D chemical models
Doug Kinnison	415-422-7975 [-5844]	radioisotopes
Michael Kurylo	202-453-1681 [755-2552]	chemical kinetics
Malcolm Ko	617-547-6207 [661-6479]	2-D chemical models
Rich McPeters	301-286-3832 [-3460]	ozone
Ron Nagatani	301-763-8071 [-8395]	meteorology
Paul Newman	301-286-3806 [-3460]	T-pv-constit. fields
Michael Prather	212-678-5625 [-5552]	3-D chemical models
Curtis Rinsland	804-864-2699 [-7790]	ATMOS & profiles
Bob Seals	804-864-2696 [-7790]	database
Brian Toon	415-604-5971 [-3625]	aerosol models
Glenn Yue	804-864-2678 [-2671]	aerosol data

Models & Measurements Committee for HSRP/AESA  
Agenda

WEDNESDAY March 13--Federal Building 6, Rm 5026  
(6th and C Streets, across from Holiday Inn)

9:00--Introduction--Prather/Remsberg

9:20--1988 Virginia Beach Model Comparison Workshop--Jackman

9:40--1991 Virginia Beach Model Comparison Workshop--Ko

10:00--Content and Format of Present Data Base--Seals

10:15--Break

10:30--Model Capability and Validation--30 min. each (includes discussion)  
Grose--3D; Jackman--2D; Toon--microphysics and chemistry

12:00--Lunch

1:00--Quality and form of existing data sets by parameter or species  
(McPeters, Remsberg, Kinnison, Rinsland, Fahey--15 min each)  
Discussion of discrepancies among data sets--20 min

2:35--Break

2:50--Quality of data sets (continued)  
(Kurylo, Yue, Nagatani, Newman--15 min each--followed by discussion)

4:10--New data sets and innovative forms of data--All

4:50--Review of day's findings

5:00--Adjourn

THURSDAY March 14--Federal Building 10, Rm 521J  
(NASA Headquarters, 6th St. and Independence Ave.)

8:30--Discussion on how to validate or ways to test models with data  
(transport and/or chemistry)?--All

9:15--Discussion of what model runs are needed?  
Skill tests for model comparisons?--All

10:30--Break

10:45--Discussion of what kinds of data do we want?  
How to resolve discrepancies among those data?--All

11:30--Summary of action items and issues for May meeting--Remsberg

12:00--Adjourn



National Aeronautics and  
Space Administration

Washington, D.C.  
20546

Reply to Attn of: SE-44

9 September 1991

Dear Colleague,

You are invited to participate in "Stratospheric Models & Measurements (M&M)1992: A Critical Comparison", a workshop on stratospheric chemistry and dynamics to be held on 2-7 February 1992 in Satellite Beach, Florida.

Assessment of the impacts of industrial halocarbons or aircraft exhaust on stratospheric ozone will rely increasingly on our 2-D and 3-D global atmospheric models. It has been duly noted at several meetings that the community has presented and published numerous model simulations for future scenarios, but that we have no objective (i.e., quasi-standard) criteria for judging whether these models are "reliable" in describing today's atmosphere. The great "2-D Intercomparison of Stratospheric Models" (September 1988, Virginia Beach, Jackman et al., 1989) went a long way toward documenting the similarities and differences among the available 2-D and 3-D models in terms of both chemistry, radiation and circulation. That model intercomparison was not immediately followed up by another because, for one, the community was exhausted, and moreover, the model-model intercomparison had been pushed to the limit (with some notable exceptions).

We now take the next major step of a model-measurement comparison. The charge to the M&M 1992 workshop is (1) to establish a standard set of atmospheric measurements (with uncertainties noted!) that can be used to test the reliability of stratospheric chemistry models, (2) to develop a method for evaluating model-data comparisons, and (3) to evaluate the ability of our current assessment models to reproduce the present-day stratosphere. Ellis Remsberg has agreed to chair this effort, and the M&M Committee has prepared the agenda for this workshop.

The M&M Workshop will be held at the Ramada Inn on Satellite Beach, Florida (near Cape Canaveral) from Sunday night 2 February 1992 through Friday noon 7 February 1992. Logistics will be handled by the HSRP/AESA Program office, Attn: Kathy Wolfe, Code SE-44, NASA Headquarters, Washington, DC 20546 (fax 202-488-7438). You will receive further information about hotels and transportation from Ms. Wolfe.

The rules of this workshop will be similar to those in 1988: participants will be assigned one specific task. It will be their responsibility to put together the results from all participants (models and measurements) for that specific experiment, to cross-compare all model simulations as well as all the measurements and their uncertainties. This workshop will include some specific model-model intercomparisons that were not adequately answered by the 1988 meeting (e.g., photolysis rates), but will focus on a set of measurements and parallel model simulations. One person from the organizing group has been selected as the primary presenter and organizer of the discussion of each experiment. Everyone attending the workshop has been assigned to one of the experiments. (If you are unhappy with your assignment, you may be able to swap with another attendee.)

The following Table summarizes the topics selected by the organizing committee. Priority was given to those data sets and model simulations that provide a rigorous test of the global

stratospheric models; specifically, those that can be performed with a majority of the current 2-D and 3-D atmospheric chemistry models.

TABLE Workshop Topics and Assignments

---

A''	Temperatures, Net Radiative Heating, & Residual Circulation (Nagatani*, Harwood, Stordal)
B'	Stratospheric H <sub>2</sub> O (Remsburg*, Zvenigorodsky)
C''	Column Ozone (Newman*, Fisher, Tung)
D'''	Ozone Profiles (McPeters*, Rood, Wuebbles)
E''	Large-Scale Structures in N <sub>2</sub> O and CH <sub>4</sub> (Grose*, Boville)
F''	NO <sub>y</sub> Absolute Stratospheric Abundance and Distribution (Zawodny*, Solomon)
G'	Column abundances of HCl, HF, HNO <sub>3</sub> , NO <sub>2</sub> , ClONO <sub>2</sub> , etc. (Rinsland*, Bruehl)
H'''	Correlation of Long-Lived Species in Simultaneous Observations (Kawa*, Isaksen, Plumb, Schmidt)
I'''	Radionuclides as Exotic Tracers: C-14, Sr-90, Pu-238 (Kinnison*, Sasaki, Weisenstein)
J''	Ruiz Cloud Experiment (Yue*, Hitchman, Visconti)
K'''	Model-Model Comparison of Photolysis Rates (ATMOS) (Eckman*, Anderson, Yung)
L''	Model-Model Comparison of Radicals, Rates & Budgets (ATMOS) (Prather*, Douglass, Jadin)
M'''	ATMOS Partitioning of the Chemical Families (Kaye*, Brasseur, Pyle)
N''	Modeled Transport Fluxes of Ozone, NO <sub>y</sub> , N <sub>2</sub> O (Ko*, Cariolle)
O''	Model-Model Comparison of Idealized Tracers X1 & X2 (Jackman*, Garcia, Mahlman)

---

The quote marks on each lettered topic are proportional to the amount of time likely to be needed for presentation.

---

After the results have been digested from all the experiments, it is our desire to have the author(s) of a given model evaluate its overall performance (e.g., with respect to the HSRP/AESA concerns in the lower stratosphere). We will then summarize those atmospheric aspects that most models do well, poorly, or do not attempt, as well as those areas where the data are clearly inadequate. Format of the final report will be similar to that for the 1988 Workshop (NASA Conference Publication 3042--orange book), and the datasets of atmospheric measurements (and possibly model results) will be publicly available (i.e., published) on CD-ROM and/or through the database.

We will rely on the database at Langley (UADP) as the repository for all observational data and model simulations, and as the source of the comparisons (graphic or tabular).

RESULTS FROM THE MODELS must be put into the database before Christmas, preferably NO LATER THAN 14 December 1991. Note that many of the model results may have already been put into UADP as a result of the UNEP assessment. You may update the model used for the UNEP 1992 assessment, but this is not necessary and you should not spend time making last minute improvements. It is important to examine both the standard gas-phase chemistry and a heterogeneous-sulfate-layer chemistry as described below.

The Upper Atmosphere Data Pilot (UADP) at Langley is being operated by Linda Hunt (804-864-5856, hunt@uadp) and Karen Sage (804-864-5857, sage@uadp). Bob Seals has temporarily shifted to NASA HQ, and the scientific supervision is now under Richard Eckman and Mary Ann Smith.

UADP fax: (804-864-7790),  
 @uadp.larc.nasa.gov (128.155.17.10)  
 @uadp1.larc.nasa.gov (128.155.17.45)  
 (Also available on SPAN as UADP or 10.582)

The detailed M&M '92 Workshop agenda and specifications (to be mailed within the week) will be available in digital format from UADP. Remember, everyone is responsible for interpolating their model results to the standard UADP grid for comparison! The observational data sets will be on that format:

$z^* = 16 \times \log_{10}(1000/p)$ , 0 - 60 km, every 2 km [31 levels]  
 90S to 90N, every 5 degrees [37 latitudes]  
 mid-month preferred, otherwise monthly mean [12 months].

ALL MODEL CALCULATIONS should result effectively in the equivalent of fixed mixing ratios as tropospheric boundary conditions (see Table below). Please submit results for the standard gas-phase chemistry ('Gas') and also the heterogeneous (sulfate layer) chemistry used in UNEP and defined again below ('Het'). For gas-phase chemistry use JPL 90-1 kinetics and cross-sections, EXCEPT for  $k[\text{OH} + \text{CH}_4]$  use  $k = 3.9\text{E-}12 \exp(-1885/T)$  (based on Ravishankara's new work, review = IUPAC '91).

TABLE Bulk Tropospheric Mixing Ratios for 'current' Stratosphere Runs

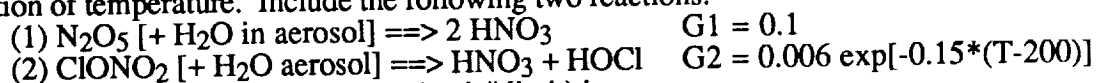
yearSS	F11	F12	F113	F114	F115	1211	1301	H22	CCl4	CH <sub>3</sub> CCl3	CO <sub>2</sub>	N <sub>2</sub> O	CH <sub>4</sub>
1980SS	149	250	11	3	2	0.4	0.4	41	93	85	334	300	1538
1990SS	253	434	44	7	5	2.0	2.6	92	103	145	350	308	1685
	ppt ----->									ppt	ppm	ppb	ppb

also fixed: CH<sub>3</sub>Cl= 600 ppt, CH<sub>3</sub>Br= 15 ppt, N<sub>2</sub>= 78%, O<sub>2</sub>= 21%

These Steady-State scenarios use tropospheric boundary conditions from 2.5 years previous, and are identical to the UNEP scenarios.

Definition of Heterogeneous/Sulfate Chemistry ('Het'): we specify a "background" aerosol for the lower stratosphere in terms of total surface area (cm\*\*2) per unit volume (cm\*\*3), SA (/cm). SA is defined as a function of  $z^*$  (log p), latitude and season. The Table below gives a smoothed/filled recommendations for SA (based on analysis by Poole, Thomason, & Yue) and corresponds to the lower limit used in the UNEP scenarios. The sulfate-layer particles are assumed to be H<sub>2</sub>SO<sub>4</sub> + nH<sub>2</sub>O; the exact composition (i.e., water content) will depend on temperature, but that is not included in this simple parameterization. In the case

where the reaction probability, G2, depends strongly on the H<sub>2</sub>O content, we define it as a function of temperature. Include the following two reactions:



The effective rate coefficient (in the "kinetic" limit) is:

$$K = (\text{mean speed})/4 \times SA \times G \quad (/sec)$$

The average speed is 1.455E4 x SQRT(T/mol.wt.) cm/s, but we will assume a constant value (mol.wt. = 100, T = 210 K) of (mean speed)/4 = 5200 cm/s.

TABLE \*\*\*LOWER LIMIT\*\*\* AEROSOL SURFACE AREA (units = 1E-8 /cm)

(km) z*	Jan-Feb-Mar-Apr-May-Jun				Jul-Aug-Sep-Oct-Nov-Dec					
	60-90N	30-60N	30N-30S	30-60S	60-90S	60-90N	30-60N	30N-30S	30-60S	60-90S
32	0.025	0.025	0.100	0.050	0.025	0.025	0.025	0.10	0.075	0.025
30	0.05	0.075	0.175	0.10	0.050	0.050	0.075	0.175	0.15	0.050
28	0.125	0.175	0.325	0.20	0.125	0.125	0.175	0.325	0.25	0.125
26	0.25	0.25	0.425	0.30	0.25	0.25	0.25	0.425	0.375	0.25
24	0.35	0.375	0.50	0.425	0.35	0.35	0.375	0.50	0.50	0.35
22	0.45	0.50	0.625	0.625	0.50	0.45	0.50	0.625	0.625	0.50
20	0.625	0.625	0.75	0.80	0.75	0.625	0.625	0.75	0.75	0.625
18	0.75	0.75	0.75	1.0	1.0	0.75	0.75	0.75	1.0	1.0
16	0.875	0.875	0.50	1.0	1.125	0.75	0.75	0.50	1.0	1.25
14	1.125	1.125	0.50	1.0	1.25	0.875	0.875	0.50	1.25	1.5
12	1.25	1.25	0.50	1.0	1.25	1.0	1.0	0.50	1.25	1.75

TABLE Summary of Model Calculations for M&M '92

4 'Best Current Atmospheres', Same as Already Done for UNEP:  
*1990SS Atmosphere and (Secondly) 1980SS Atmosphere  
 Gas-phase ('Gas') and Heterogeneous Chemistry ('Het')*

4 Single Profile Calculations:  
*ATMOS Profiles at 31N & 48S Used for Detailed Rates, J-Values,....  
 Use Both 'Gas' and 'Het' Chemistries*

3 Multi-Year Gas Tracer Experiments:  
*Carbon-14  
 Synthetic Tracers X1 and X2*

3 Multi-Year Particle-Gas Tracer Experiments:  
*Strontium-90 and Plutonium-238  
 Ruiz Volcanic Cloud*

Attendance at the M&M '92 workshop is limited by space, and, hence, is by invitation only. The workshop is sponsored primarily by the Atmospheric Effects of Stratospheric Aircraft component of NASA's High-Speed Research Program (HSRP/AESA) with the

support of the Atmospheric Chemistry Modeling and Analysis Program (ACMAP, formerly Upper Atmosphere Theory) and the Upper Atmosphere Research Program (UARP). Participation in this effort is limited to investigators supported by the HSRP, UARP or ACPMAP, as well as to international groups participating in HSRP or UNEP assessments. Attendance at the February 1992 M&M Workshop cannot exceed 50 participants. If you are unable to attend and wish to send a substitute, or if you are not on the workshop list and would like to attend, please contact Ellis Remsberg (fax 804/864-6326, [remsberg@haloe.larc.nasa.gov](mailto:remsberg@haloe.larc.nasa.gov)) or Michael Prather (fax 212/678-5552, [prather@halo.giss.nasa.gov](mailto:prather@halo.giss.nasa.gov)). Expenses for the meeting should be absorbed by existing grants; foreign participants are expected to cover their own costs. In cases where participants are unable to attend without some support, please notify the HSRP/AESA Program office as soon as possible.

We look forward to seeing you in February.

Yours,

Ellis Remsberg  
Chair, M & M Workshop

Michael Prather  
Manager, HSRP/AESA

Distribution: M&M '92 Workshop (\* M&M organizing committee)

Dan Albritton	NOAA Aeronomy
Gail Anderson	AFGL
Byron Boville	NCAR
Guy Brasseur	NCAR
Christoph Bruhl	MPI Mainz, Germany
Daniel Cariolle	CNRM, France
Anne Douglass	NASA Goddard
Richard Eckman*	NASA Langley
Don Fisher	DuPont
Rolando Garcia	NCAR
Bill Grose*	NASA Langley
Robert Harwood	U. Edinburgh, U.K.
Matt Hitchman	U. Wisconsin
Linda Hunt	NASA Langley
Ivar Isaksen	U. Oslo, Norway
Charley Jackman*	NASA Goddard
Evgeny Jadin	CAO, USSR
Randy Kawa*	NOAA Aeronomy
Jack Kaye*	NASA HQ
Doug Kinnison*	LLNL
Malcolm Ko*	AER
Michael Kurylo*	NASA HQ
Jerry Mahlman	GFDL
Rich McPeters*	NASA Goddard
Ron Nagatani*	NMC
Paul Newman*	NASA Goddard
Alan Plumb	M.I.T.
Lamont Poole*	NASA Langley
Michael Prather*	NASA GISS
John Pyle	U. Cambridge, U.K.

Ellis Remsberg*	NASA Langley
Curtis Rinsland*	NASA Langley
Richard Rood	NASA Goddard
Karen Sage*	NASA Langley
Toru Sasaki	MRI, Japan
Ulrich Schmidt	KFA Julich
Bob Seals	NASA Langley
Mary Ann Smith	NASA Langley
Susan Solomon	NOAA Aeronomy
Frode Stordal	NILU, Norway
K.K. Tung	U. Washington
Guido Visconti	U. Aquila
Robert Watson	NASA HQ
Debra Weisenstein	AER
Howard Wesoky*	NASA HQ
Don Wuebbles	LLNL
Glenn Yue*	NASA Langley
Yuk Yung	Cal. Tech.
Joe Zawodny*	NASA Langley
Sergey Zvenigorodsky	CAO, USSR

cc:

Kathy Wolfe  
Randy Soderholm

ARC  
ARC



National Aeronautics and  
Space Administration

Washington, D.C.  
20546

Reply to Attn of: **SE-44**

## **MEMORANDUM**

**To:** Models and Measurements '92 Participants

**From:** High-Speed Research Program/Atmospheric Effects of Stratospheric Aircraft Program Office

**Date:** September 20, 1991

**Subject:** Models and Measurements (M&M) '92 Detailed Agenda and Specifications

By now you should have received a letter inviting you to the M&M '92 Workshop to be held on 2-7 February 1992 in Satellite Beach, Florida. The letter promised that the detailed agenda and specifications would be mailed within the week. On Ellis Rembsberg's behalf, I am enclosing the detailed agenda and specifications for the M&M '92 Workshop. If you have any questions, please contact Ellis Rembsberg at 804/864-5823.

=====  
Models & Measurements '92 Workshop: Detailed Agenda  
=====

=====  
MMW'92==

=====  
MMW'92==

History:

From: prather@halo.giss.nasa.gov Tue 17 Sep 91 16:00  
From: REMSBERG@HALOE.LARC.NASA.GOV Tue Sep 17 15:12:33 1991  
From: REMSBERG@HALOE.LARC.NASA.GOV Sun Sep 15 15:56:56 1991  
From: prather@halo.giss.nasa.gov Wed 28 Aug 91 09:50:41

=====  
MMW'92==

Notes:

This document is available digitally in the UADP (Upper Atmosphere Data Pilot) database at NASA Langley. A menu selection under the heading "Models & Measurements '92 Workshop" will contain this file and all of the scenarios and input data required to perform the experiments. The ASCII format precludes the use of subs/supers so please note carefully the chemical and mathematical expressions; we have tried to be as standard as possible.

The Upper Atmosphere Data Pilot (UADP) at Langley is being operated by Linda Hunt (804-864-5856, hunt@uadp.larc.nasa.gov) and Karen Sage (804-864-5857, sage@uadp.larc.nasa.gov). Bob Seals has temporarily shifted to NASA HQ, and the scientific supervision is now under Richard Eckman (eckman@dobson.larc.nasa.gov) and Mary Ann Smith.

UADP fax: (804-864-7790),  
uadp.larc.nasa.gov (128.155.17.10)  
uadp1.larc.nasa.gov (128.155.17.45)  
Also available on SPAN as UADP or 10.582

If you do not presently have an account on uadp, contact Linda or Karen for access details.

Remember, everyone is responsible for interpolating their model results to the standard UADP grid for comparison! The observational data sets will be on that format:

$z^* = 16 \times \log_{10}(1000/p)$ , 0 - 60 km, every 2 km	31 levels
90S to 90N, every 5 degrees	37 latitudes
mid-month preferred, otherwise monthly mean	12 months.

The UNEP bulletins are also available on-line at UADP. Both the UNEP scenarios for composition and lifetimes and specifications for the heterogeneous chemistry can be selected through the menu.

There is a directory of M & M participants that we hope to expand to HSRP (High-Speed Research Program), UARP (Upper Atmosphere Research Program), and ACPMAP (Atmospheric Chemistry Modeling and Analysis Program) investigators. PLEASE SUBMIT YOUR INTERNET ADDRESS (INCLUDING IP#) ALONG WITH PHONE/FAX NUMBERS TO Linda Hunt (hunt@uadp) or Karen Sage (sage@uadp) as soon as possible. The directory will be kept on-line in the UADP database.

MODELERS: If available, we will use the model data put into UADP for the UNEP "1980 SS" and "1990 SS" atmospheres. Both gas-phase and heterogeneous chemistry calculations will be considered; heterogeneous chemistry refers to the "lower-limit background sulfate layer" scenario in the UNEP bulletins. If you did a PSC model, that can also be considered, but be sure to concisely document the 'different' models that you submit for MMW'92. Please update or submit your model results before Christmas!

The following list of proposed experiments and assignments has been developed for the Models and Measurements '92 Workshop by the organizing committee. Any questions concerning a given experiment should be addressed to the person selected to lead the discussion of that experiment in February (i.e., the first name in the list). If any important clarification or redefinition occurs, please notify Prather and Remsberg immediately, so that all participants can be informed in a timely manner.

**PRIORITIES:** We believe that all of these comparisons are important for understanding and calibrating/evaluating the stratospheric models. But if forced to choose, we would place the comparisons with the current atmosphere as highest priority.

**A. Temperatures and Net Radiative Heating**  
(Nagatani, Harwood, Stordal)

The net radiative heating is the fundamental quantity in 2-D models for determining the residual circulation. In order to compare respective 2-D models, it is necessary to compare the circulations within each model. In this sense, we propose that each modeling group supply their net radiative heating rates, temperature background field, and monthly mean residual circulation (vertical velocity in cm/sec) for each month over an annual cycle. These net radiative heating rates, temperatures, and circulations will be compared to those derived using NMC temperatures and SBUV ozone measurements. Digital tables (UADP format) of  $K_{yy}$ ,  $K_{zz}$ , and  $K_{yz}$  would be helpful in diagnosing model differences for the tracer transport problems.

An 8-year average of stratospheric height and temperature analyses from NMC will cover the period from November 1979 to October 1986 at 8 levels (70, 50, 30, 10, 5, 2, 1, and 0.4 mbar). In addition, the high and low temperature ranges at ten-degree latitude intervals will be archived. All model data should be supplied in the UADP format. (N.B. Under section K we also recommend a comparison of the solar heating and IR net cooling using a specified ATMOS reference profile, in order to sort model differences due to radiative codes. We also need  $T(z^*)$  in order to convert mixing ratios to densities.)

**B. Stratospheric H<sub>2</sub>O**  
(Remsberg, Zvenigorodsky)

The predictive calculation of H<sub>2</sub>O in global stratospheric models is limited, and we choose here to consider water along with temperatures and heating rates as a check of the model inputs. Therefore, we will compare the H<sub>2</sub>O fields from the models (assumed or calculated) with the available near-global datasets. Water vapor mixing ratios will be based on SAGE II (monthly, 10-50 km, 50S-50N with some higher latitudes), LIMS (monthly, 100 mbar to 1 mbar, 64S to 84N), and in situ measurements (AAOE & AASE campaigns are limited to high-latitude, lower stratosphere in winter; STEP covers the tropical tropopause region). Monthly zonal means of stratospheric H<sub>2</sub>O used in the models should be put in UADP.

**C. Column Ozone**  
(Newman, Fisher, Tung)

The column abundance of ozone has been the classic test of stratospheric chemistry models. We will use the observed abundance from TOMS for "1980" (an average of 1979-1980 to eliminate QBO considerations) and also a "1990" ozone distribution. Rather than use actual data, the

"1990" reference will be produced by superimposing the derived TOMS decadal trend versus latitude on the "1980" distribution so that solar cycle and QBO effects need not be included in the model calculations. Comparison will focus on the basic climatology shown in the "Dobson map" (O<sub>3</sub> column vs. latitude by month) and on the decadal trend observed by TOMS (Stolarski et al., GRL, 18, 1015-1018, 1991).

#### D. Ozone Profiles (McPeters, Rood, Wuebbles)

The observed ozone profiles (mixing ratio vs latitude and  $z^*$ ) will be derived from a combination of SBUV and SAGE II. SBUV is global (except for polar night), but cannot resolve the profile below the ozone maximum. SAGE II has excellent vertical resolution, but less complete global sampling (often limited to latitudes between 50S and 50N). Due to the non-uniform monthly sampling of SAGE II, an estimate of the sampling bias will be provided. LIMS ozone is also available from 100 mbar to 0.1 mbar and extends into polar night and poleward of 50N.

A second possible method of testing the modeled ozone will be to examine the amplitudes and phases of the annual and semi-annual cycles. Comparisons in this format will emphasize the seasonal fluctuations about the mean rather than the mean itself. Irrespective of the difference in vertical resolution and systematic offsets between SAGE II and SBUV, both sets of ozone data show very close and detailed agreement when compared in this manner. It would be interesting to use ozonesonde data better to resolve the tropopause, but no one has proposed how usefully to compare the high frequency, single locale sondes with a zonally, monthly averaged model.

#### E. Large-Scale Structures in N<sub>2</sub>O and CH<sub>4</sub> (Grose, Boville)

The large-scale structures seen in the near-global maps of N<sub>2</sub>O and CH<sub>4</sub> from SAMS represent a test of the seasonal transport in the middle stratosphere, plus an estimate of chemical destruction at low and middle latitudes. The equator-to-pole slope of isolines may be related to competition between chemistry and transport. The local slope is likely to be controlled by transport in the lower stratosphere.

Distributions of N<sub>2</sub>O and CH<sub>4</sub> were obtained above 28 km from Nimbus-7 SAMS. The results are available in UADP in a monthly zonal mean format for 3 successive years--1979, 1980, and 1981. Interannual variations for the monthly data can be noted, as well. The monthly patterns in the "present-day" (or "1980 SS" UNEP atmosphere) model calculations should agree with observations to within the precision estimates that have been quoted for those data. Monthly comparisons will be shown as contours (latitude by  $z^*$ ) of model/data ratios with an increment of 0.1. We will also examine latitude/time plots of the annual cycle of N<sub>2</sub>O and CH<sub>4</sub> at selected  $z^*$  levels (10 and 4.2 mbar).

Balloon and ATMOS profiles will augment the SAMS data and point to uncertainties and discrepancies in instrument calibration. The balloon profiles in UADP are grouped by season and latitude (10 degree bins) and will include the recent profiles of Schmidt et al. (GRL, 1991) at 68N as well as the earlier "classic" data from NOAA and KFA. Estimates of variability within a given season will be obtained from the data.

#### F. NO<sub>y</sub> Absolute Stratospheric Abundance and Distribution (Zawodny, Solomon)

The absolute abundance of odd-nitrogen (NO<sub>y</sub>) in the stratosphere is key to calculating the abundance of O<sub>3</sub>, as well as the relative perturbations caused by additions of chlorine or aircraft exhaust. Unfortunately, we have limited global data on total NO<sub>y</sub> that is independent of chemical modeling of the individual species in the family.

The monthly distributions of (NO<sub>2</sub>+HNO<sub>3</sub>) from LIMS will be used as a lower limit estimate of "1980 SS" atmospheric abundance of NO<sub>y</sub> from 40 mbar to 1 mbar, but are limited to only part of the year. Comparisons will be in terms of contours of the NO<sub>y</sub> model/data ratios. A determination of agreement will take into account the accuracy estimates for those two LIMS species. (The variances of LIMS data about their zonal means are also available for an assessment of effects of wave activity in 3-D chemical/transport models.)

ATMOS profiles of most of the NO<sub>y</sub> species (see Table MM1) as well as direct aircraft measurements of NO<sub>y</sub> from the ER-2 (STEP, AAOE, & AASE campaigns) in the lower stratosphere (see section H) provide independent measures of the absolute abundance.

The SAGE II measurements of NO<sub>2</sub> at sunset provide a useful constraint on modeled odd-nitrogen and are provided with similar averaging as the ozone data (50S - 50N, 20-40 km). After the model partitioning of NO<sub>y</sub> has been evaluated using the ATMOS measurements (Section M), a comparison with the SAGE-II NO<sub>2</sub> data should allow for a test of the seasonal distribution of NO<sub>y</sub>, or at least NO<sub>x</sub>.

#### G. Column abundances of HCl, HF, HNO<sub>3</sub>, NO<sub>2</sub>, ClONO<sub>2</sub>. (Rinsland, Bruehl)

The integrated column abundances of certain species such as HCl, HF, HNO<sub>3</sub>, NO<sub>2</sub> and ClONO<sub>2</sub> provide important constraints on stratospheric models. For most of these species, the column is dominated by stratospheric (rather than tropospheric) concentrations and is predominantly weighted towards the lower stratosphere where densities (not necessarily mixing ratios) are greatest. While the seasonal variations in the column at one location are a combination of stratospheric chemistry and changes in the altitude of the tropopause, the latitudinal patterns (by aircraft transects) often reveal striking patterns that are measures of vertical transport (the tropical "V" in HNO<sub>3</sub>) or a combination of unusual chemistry and transport as one approaches the winter poles.

For latitudinal HCl and HF, there have been several published sets of aircraft measurements. For the present work a comparison with the 1978-1982 measurements of Mankin and Coffey is recommended (JGR, 88, 10,776-10784, 1983), which cover 5N to 70N. These results yield a well-defined latitudinal distribution for both gases, and are conveniently centered on 1980. Their measurements were taken at a constant pressure level of 197 mbar, and the model data will be integrated above the  $z^* = 12$  km (178 mbar) level to compute the stratospheric columns. Recent aircraft campaigns have revealed significant differences in the HF and HCl total columns derived by Mankin and Coffey and those obtained by the group at JPL (e.g., see measurements in Fig. 2 of Kaye et al., GRL, 17, 529-532, 1990). However, on a relative basis, the data from the two groups are very consistent. Therefore, it may be useful to normalize the results to the value at the equator.

## H. Correlation of Long-Lived Species in Simultaneous Observations (Kawa, Isaksen, Plumb, Schmidt)

Direct comparison of measured concentrations of individual trace gases at a specific latitude, longitude, and time of year with those computed from a monthly mean, zonally averaged model are not often meaningful. The natural variability of the atmosphere often shows "folded" or highly structured profiles that cannot be reproduced by the coarser resolution or limited structure of the model. Furthermore, no two January's are alike, so even a well measured monthly mean profile will differ from year to year. However, the essence of chemical transformations in the stratosphere is contained in the relative decay or production of these tracers (N<sub>2</sub>O, CH<sub>4</sub>, CFC-11, CFC-12, HCFC-22, CH<sub>3</sub>CCl<sub>3</sub>, CH<sub>3</sub>Cl, CCl<sub>4</sub>, CFC-113, CFC-114, O<sub>3</sub>, NO<sub>y</sub>, Cly, ...).

Recently, studies have shown that potential vorticity or N<sub>2</sub>O concentrations provide a useful coordinate with which to compare concentrations of the species taken at different times and locations. Several studies have made use of correlation plots of N<sub>2</sub>O-NO<sub>y</sub> and N<sub>2</sub>O-O<sub>3</sub> to characterize denitrification and ozone loss. More recent theoretical work has related the tracer correlations to average fluxes and hence lifetimes associated with stratospheric removal.

We will use a combination of aircraft campaign data (STEP, AAOE, AASE), balloon data (KFA-Schmidt), and ATMOS profiles to define a set of observed tracer correlations. Where helpful we will include the spatially/temporally averaged SAMS N<sub>2</sub>O and CH<sub>4</sub>. Modeled correlations will be taken from the "1990 SS" (steady-state) UNEP atmosphere. We shall normalize the observations to account for the increasing tropospheric concentrations of CFCs and CH<sub>4</sub>. We will examine basic correlation plots such as O<sub>3</sub> vs. N<sub>2</sub>O, or CFC-11 vs. N<sub>2</sub>O. Preliminary examination of some model results indicate that the following can be expected: (1) most of the points should lie on a compact curve; (2) points off the compact curves characterize locations where local photochemical removal rate is sufficiently fast that transport no longer controls the distribution; and (3) in the lower stratosphere, the curve should be a straight line with the slope equal to the ratio of the fluxes (hence, lifetimes due to stratospheric removal) of N<sub>2</sub>O and CFC-11.

Composite averages of NO<sub>y</sub>, O<sub>3</sub>, and the simultaneously measured ratio NO<sub>y</sub>/O<sub>3</sub> will be constructed as functions of latitude from the three major ER-2 aircraft campaigns, including ferry and test flights. Data will be averaged over 5 degree latitude intervals at pressures between 50 and 90 mbar. Data from inside the southern polar vortex and poleward of 5 degrees inside the boundary of the northern polar vortex will be excluded because of the denitrification commonly observed at these latitudes. Sample standard deviations of the 10-sec average data points within each latitude interval will also be provided. These data primarily represent the winter season in each hemisphere. Data are included from approximately 30 flights in the lower stratosphere over the latitude range from 65S to 70N. Simple overplots of model NO<sub>y</sub>/O<sub>3</sub> ratios versus averaged data will be shown as line plots (vs. latitude) or contours (latitude by z\*).

We assume that your model results (1990 SS boundary conditions) include latitude by z\* distributions of N<sub>2</sub>O, CH<sub>4</sub>, CFC-11, CFC-12, HCFC-22, CH<sub>3</sub>CCl<sub>3</sub>, CH<sub>3</sub>Cl, CCl<sub>4</sub>, CFC-113, CFC-114, O<sub>3</sub>, NO<sub>y</sub> and Cly (for at least four months: March 15, June 15, September 15 and December 15).

## I. Radionuclides as Exotic Tracers: C-14, Sr-90 (Kinnison, Sasaki, Weisenstein)

The goals of the C-14 scenario and the subsequent radionuclide experiment are to provide fundamental tests of dynamical transport in the models that are independent of chemistry. Further, the injection of these exotic species into the lower stratosphere is somewhat parallel to

the proposed HSCT emissions, and, thus, the time scales for the removal and global dispersion of these radionuclides is a very important test of the models. The C-14 in the stratosphere is in the form of CO<sub>2</sub> and thus acts as a passive gas tracer, whereas the metal Sr-90 will stick to aerosols and their transport must also include a settling velocity.

Initial distributions ( $z^*$  by latitude) of excess C-14 for 15 October 1963 will be in the UADP database. The initial distributions are in units of 10E5 atoms of excess C-14 per gram of dry air. By definition, these units are proportional to mixing ratios and can be modeled as such. Model-derived distributions submitted to the UADP database should be in units of 10E5 atoms of excess C-14 per gram of dry air. Each modeler should integrate C-14 from 15 October 1963 to 15 January 1971 and save C-14 data in  $z^*$  versus latitude form for each month of this time period.

The lower boundary should be specified according to the following equations given in the appendix of the reference by H.S. Johnston ("Evaluation of Excess Carbon-14 and Strontium-90 Data for Suitability to Test Two-Dimensional Stratospheric Models," JGR, 94, 18485-18493, 1989):

$$\text{C-14 (N.Hem.)} = 73.0 - 0.27823 t - 3.45648\text{E-}3 t^{**2} + 4.21159\text{E-}5 t^{**3}$$

$$\text{C-14 (S.Hem.)} = 44.5 + 1.02535 t - 2.13565\text{E-}3 t^{**2} + 8.61853\text{E-}5 t^{**3}$$

where  $t$  = months after October 15, 1963. The upper boundary conditions should be specified as zero flux.

Initial distributions ( $z^*$  versus latitude) for Sr-90 (15 October 1964) will be in the UADP database. The units are particles per cm<sup>3</sup>, but include a conversion to mixing ratio. Since Sr-90 rapidly coalesces on aerosol particles, average settling velocities between 0 and 30 km are available as latitude-by- $z^*$  distributions for this time period. Above 30 km, assume that the aerosols become small enough to act like a gas. The settling velocities will be in the UADP database, and we encourage calculations both with and without the prescribed settling velocities.

Each modeler should integrate Sr-90 from 15 October 1964 to 15 January 1971, saving altitude versus latitude data for each month. The lower boundary values in the model should be fixed with respect to time at the initial distribution concentrations. The upper boundary values should be specified as zero flux. (Pu-238 was dropped due to lack of good data.)

#### J. Ruiz Cloud Experiment (Yue, Hitchman, Visconti)

The evolution of fine dust particles from the eruption of a volcano provides a unique tracer of stratospheric transport. These particles evolve from the SO<sub>2</sub> injected by the volcano, are transported globally, and eventually are removed on time scales of a year by both sedimentation and large-scale transport. Like the exotic radionuclides, they provide a direct test of the transient recovery of the stratosphere to tracer perturbations in the lower stratosphere. Importantly, they also measure the global spread of a locally injected species. The volcano Nevado del Ruiz (5N, 75W) in Colombia erupted on 13 November 1985 and was observed by SAGE II. The observed optical depth associated with Ruiz reached a maximum in February 1986 and three years later decayed into the background levels of aerosols left by El Chichon (1982). Initial distributions ( $z^*$  by latitude) of aerosol size (i.e., mass-weighted mean diameter) will be derived from SAGE II data, as will the aerosol concentrations in terms of number per cc of air. The SAGE II data are used to define the isopleths during the following two years, and to derive an e-folding time for the aerosol mass-loading.

In this study, aerosol particles are treated as one constituent with a single size. Such treatment is oversimplified: stratospheric aerosols have a large range of sizes that continually change due to microphysical processes including coagulation, growth, and sedimentation. This simple

approach to the "chemistry" of stratospheric aerosols allows us to propose a general experiment for all participating 2-D/3-D models. The time-dependent aerosol size will be derived from the SAGE II data set. The effective fallout velocities will then be calculated and will be defined in a file available from the UADP database. The initial aerosol concentrations will also be defined in a file on UADP. The models should transport the aerosols with the mean circulation (advection plus diffusion) along with a settling velocity. Results should be reported as zonal mean concentrations for the 24 months following February 1986.

K. Model-Model: Photolysis Rates, Solar Heating & IR Cooling  
(Eckman, Anderson, Yung)

This section focuses on the gory details of UV-visible radiative transfer in the models. We do not have an obvious "measurement" with which to compare, so we will focus on model-model comparisons. THERE ARE STILL UNRESOLVED DIFFERENCES (factor of 2) FROM THE 1988 INTERCOMPARISON. For O<sub>2</sub> photodissociation, we will compare against the high-resolution Schumann-Runge band model put together at Harvard and AFGL (Gail Anderson, AFGL) which is based on recent lab work (Yoshino, SAO) and is tied to the stratospheric attenuation data (Hall & Anderson, JGR, 96, 12927-12931, 1991).

The standard atmosphere is based on the ATMOS occultation profiles at 31N as given in Table KLM-1. The other assumptions needed for the photolysis calculations are given in Table MM-1, except that we will consider only the case for solar zenith angle (SZA) equal to 0 deg. (Of course, at 31N the SZA is never 0 deg, but it was felt that this would make for a simpler intercomparison.) Please note that photolysis rates should be reported for (1) no scattering AND with a full scattering/albedo model, and (2) as a total J-value AND that due to wavelengths < 200 nm. In order to assess model differences in the net diabatic heating (section A) due to the radiative codes, calculate the instantaneous solar UV heating and IR net cooling, again using the ATMOS data at 31N and the 1990 SS atmosphere.

L. Model-Model: Radicals, Rates & Budgets for ATMOS profiles  
(Prather, Douglass, Jadin)

Use the ATMOS profile and scenario calculated above (use real geometries for 31N and 48S), and report noontime values for certain radicals as well as 24-hour averages of critical rates in the odd-oxygen budget. The main objective would be to compare the basic budgets of O<sub>3</sub> and NO<sub>y</sub> across all models (remembering how well we all fared with the model-measurement just above). Use densities (#/cm<sup>3</sup>) and rates (#/cm<sup>3</sup>/sec), and the same submittal format as for the J-values (see Table MM-1).

- |                            |  |   |                             |
|----------------------------|--|---|-----------------------------|
| (a) noon OH                | (b) avg OH                                 | (c) avg O('D)                                 | (d) noon O                  |
| (e) noon NO                | (f) noon NO <sub>2</sub>                   | (g) avg loss NO <sub>y</sub>                  | (h) avg OH+NO <sub>2</sub>  |
| (i) avg NO <sub>2</sub> +O | (d) avg ClO+O                              | (h) avg HO <sub>2</sub> +O <sub>3</sub>       | (i) avg HO <sub>2</sub> +NO |
| (j) avg ClO+BrO            | (k) avg Cl <sub>2</sub> O <sub>2</sub> +hv | (l) avg NO <sub>3</sub> +hv=NO+O <sub>2</sub> | (m) avg HOCl+hv (n)         |
| noon N                     | (o) avg O                                  | (p) noon O('D)                                |                             |

M. ATMOS Partitioning of the Chemical Families  
(Kaye, Brasseur, Pyle)

This section tests the ability of the models under highly restricted conditions (i.e., independent of transport) to partition the chemical families. It uses simultaneous observations from ATMOS of the NO<sub>y</sub> family and Cl<sub>y</sub> family at sunrise and sunset. (It will clearly use results from sections K & L to diagnose model differences in partitioning.)

Models should calculate the photochemical steady-state (i.e., 24-hour periodic) solution for the radical species from 14 km to 50 km at 48S and 31N, for early May conditions (solar declination = 15 deg). Report calculated concentrations at sunrise, sunset, noon and midnight for the individual species of the NO<sub>y</sub>, Cly, Bry and HO<sub>x</sub> families as defined in Table MM-1. Use the ATMOS atmosphere profiles for O<sub>3</sub>, temperature, CH<sub>4</sub>, H<sub>2</sub>O, NO<sub>y</sub> and Cly (*see* Table MM-1). Define 'sunset' for reporting densities as SZA = 90.0 deg although the stratosphere is not dark at this time; interpolate in local solar time if necessary. A separate calculation using fixed HNO<sub>3</sub> from ATMOS is also recommended using the HNO<sub>3</sub> profiles given in Table KLM-1.

Curtis Rinsland and others are in the final stages of preparing an ATMOS paper on the budgets of chlorine and fluorine at 31N. After accounting for unobserved species (e.g., CH<sub>3</sub>CCl<sub>3</sub> and F-113 below 20 km and ClO, HOCl, and COClF between 20 and 40 km), the ATMOS data indicate a 31N spring 1985 stratospheric total mixing ratio of chlorine equal to 2.61 +/- 0.17 ppbv throughout the stratosphere, which we adopt here. (This value is consistent with tropospheric chlorine loading delayed about 5 years.) The following updated 31N ATMOS profiles of chlorine-containing molecules will be available for the M&M assessment: HCl, CH<sub>3</sub>Cl, ClONO<sub>2</sub>, CCl<sub>4</sub>, CCl<sub>2</sub>F<sub>2</sub>, CCl<sub>3</sub>F, and CHClF<sub>2</sub> (Zander et al., 1991). Both gas phase and heterogeneous cases should be run. Specify sulfate surface area and heterogeneous rates for N<sub>2</sub>O<sub>5</sub> and ClONO<sub>2</sub> as in the UNEP scenarios bulletin.

#### N. Modeled Transport Fluxes of Ozone, NO<sub>y</sub>, N<sub>2</sub>O (Ko, Cariolle)

The local tendency of the continuity equation (i.e., the rate of change of species' concentration) can be separated into terms connected with transport and photochemical production/loss. In order to understand the modeled response of the trace gases to changes in photochemical environment, we need to examine the magnitudes of these terms. For this, we suggest sending to the data base the following diagnostic quantities, all of which have the same units (i.e., mixing ratio/sec):

- local chemistry at each grid point of
  - net chemical production term, (P-L) for O<sub>3</sub>, N<sub>2</sub>O, NO<sub>y</sub>
  - chemical production only
    - for O<sub>3</sub> report sum of rates O<sub>2</sub>+hv, HO<sub>2</sub>+NO, and CH<sub>3</sub>OO+NO
    - for N<sub>2</sub>O skip
    - for NO<sub>y</sub> report 2 x rate O('D)+N<sub>2</sub>O -> NO+NO
  - total photochemical loss for ozone
- net transport (flux divergence) due to
  - vertical advection
  - horizontal advection
  - vertical diffusion
  - horizontal diffusion.

Include results for the 4 months: March 15, June 15, September 15 and December 15. All of these quantities can be plotted as latitude-by-z\* contour maps. We hope to convince groups that have data assimilation capability to perform some calculations for this comparison.

O. Model-Model Comparison of Idealized Tracers X1 & X2  
(Jackman, Garcia, Mahlman)

This simple experiment allows us to calibrate the transport of the different models, isolating the effect of transport on lifetimes. Further, it gives us a simple lead-in to the tracer correlations (section H) and their use in lifetime estimates (e.g., does the X1-X2 scatter plot stay in a straight line, a compact curve?).

Maintain the mixing ratio at 1 ppb everywhere below 500 mbar and set the loss frequency independent of latitude & season:

$$L(p) = \begin{array}{ll} \text{X1} & \text{X2} \\ 0 & 0 & \text{for } p > 100 \text{ mbar} \\ = 3.0\text{E-}6/p^{**2} & 1.5\text{E-}6/p^{**2} \text{ (/sec)} & \text{for } 1 < p < 100 \text{ mbar} \\ = 3.0\text{E-}6 & 1.5\text{E-}6 \text{ (/sec)} & \text{for } p < 1 \text{ mb} \end{array}$$

Calculate a steady-state distribution. (Hint: start with a uniform 1 ppb throughout the stratosphere rather than with none!) Report for both X1 & X2 (a) steady-state lifetimes and (b) latitude-z\* grid of monthly mean mixing ratios.

P. New Frontiers  
(All)

What does the future hold? How can we integrate the high-resolution data and 3-D models into the process of improving our assessment tools? Will we ever be able to 'validate' a model? with what data?

CHEMICAL FAMILIES:

=====

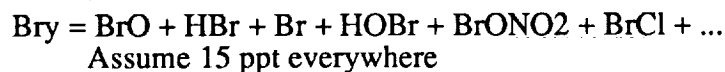
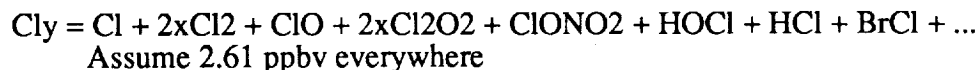
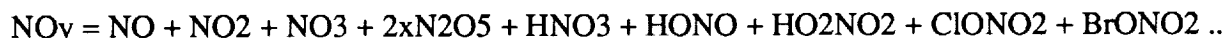


Table MM-1. Photolysis Calculations (Sections K & M)

---

---

Section K: Use ATMOS background atmosphere profile for 31N  
===== Use SZA = 0, instantaneous J-values

Calculate both  
(NS) no Rayleigh or aerosol extinction (scattering plus absorption)  
and no surface albedo  
and (RS) include Rayleigh-phase scattering and surface albedo = 0.30

Calculate both  
(TOT) J-values from all solar wavelengths  
and (200) J-values only from wavelengths less than 200 nm

Section M: Use ATMOS background atmosphere profile for 31N and 48S  
===== Use your 'best' photolysis rate calculation which should include Rayleigh-  
phase scattering and surface albedo, if possible.

Use correct SZA solar declination for early May:

$$\cos(\text{SZA @ 48S}) = \sin(+16) \times \sin(-48) + \cos(+16) \times \cos(-48) \times \cos(15t)$$

$$\text{SZA at local solar noon} = 64 \text{ deg}$$

$$\cos(\text{SZA @ 31N}) = \sin(+16) \times \sin(+31) + \cos(+16) \times \cos(+31) \times \cos(15t)$$

$$\text{SZA at local solar noon} = 15 \text{ deg}$$

where t = hours past local solar noon, and all trig functions are in deg.

Calculate both:  
(LN) local noon instantaneous rates (Solar Zenith Angle = 0 deg)  
and (24) full 24-hour average rates

=====

Calculate the following quantities as a function of z\* (0 - 60 km by 2km):

- |                           |                           |
|---------------------------|---------------------------|
| (a) column of O3 overhead | (b) column of O2 overhead |
| (c) J(O2)                 | (d) J(NO)                 |
| (e) J(O3-->O(3P))         | (f) J(O3-->O(1D))         |
| (g) J(NO2)                | (h) J(HNO3)               |
| (i) J(ClONO2)             | (j) J(N2O)                |
| (k) J(CFC-11)             | (l) J(CFC-12)             |
| (m) J(H2O)                | (n) J(N2O5)               |

Note: If you include anything else in your calculation (e.g., NO2), then show its effect separately!

Note: If your model differs from the above set assumptions, PLEASE DOCUMENT and estimate differences.

It was determined at the February 1992 Workshop that the original specifications of Experiments K and L were confusing to the modelers and that meaningful comparisons were not possible. Consequently the participants developed new specifications at the Workshop; and these instructions are given below. New model calculations were performed and submitted to the data base, and the results were discussed at an M&M work session during the May 1992 HSRP/AESA Annual Meeting in Virginia Beach. These results are found in Sections K and L of this final report.

### Section K Model - Model

Repeat the photolysis calculations as given in original Section K, except:

1. Realistic geometry  
Use the solar zenith angle given for 30N in table MM-1 (i.e., solar dec. = +15°, SZA @ local noon = 15°).
2. In the list of photolysis rates  
Drop (m) J (H<sub>2</sub>O)  
Add J (NO<sub>3</sub>)  $\rightarrow$  NO + O<sub>2</sub>
3. Use ATMOS as high as possible (68 km).  
Report J-values only for 0  $\rightarrow$  60 km.
4. Do 4 cases (RS+TOT, RS<200, NS+TOT, NS<200)  
for noon only (SZA = 15°); Do RS-TOT for 24-hr average.

### Section L

Two cases for 30N

1. Gas phase
2. Heterogeneous reactions as specified in original assignment sheet (lower limit)  
  
Use ATMOS NO<sub>y</sub>, p, T, O<sub>3</sub>, CH<sub>4</sub> H<sub>2</sub>O as given in attached table (6 Feb 92 recommendation)  
  
Use radiation field with scattering and 0.30 ground albedo  
  
Calculate HNO<sub>3</sub>  
  
Use Bry = 15 ppt, constant at all altitudes  
  
Use the Cly profile that is given in the attached table  
  
Calculate your best steady state  
  
Report all quantities between 14 and 52 km  
  
Report the same rates and densities as required in the original section L except

Drop	(n)	noon N
Add	ClO	noon + 24-hr average
	HO <sub>2</sub>	noon + 24-hr average
	OH + O	24-hr average
	O + O <sub>3</sub>	24-hr average

For heterogeneous only

N <sub>2</sub> O <sub>5</sub> + (H <sub>2</sub> O/aerosol)	24-hr average
ClONO <sub>2</sub> + (H <sub>2</sub> O/aerosol)	24-hr average

Report L-NO<sub>y</sub> as the 24-hr average of 2 k [N] [NO]

**Atlantic Research Corporation**

a unit of Sequa Corporation

ARC Professional Services Group  
CI Systems Division  
Suite 700  
600 Maryland Avenue, SW  
Washington, DC 20024  
202 455-8234  
202 455-7438 (fax)

**SEQUA**

22 November 1991

Dear Colleague:

The following change has been made to the Models and Measurements Workshop agenda sent to you in September. The third paragraph under agenda item I (page 6) has been modified. Please note the correction in the equation for the southern hemisphere lower boundary value as a function of time (2.13565E-3 was changed to 2.13565E-2). An additional sentence was added after the equations. The paragraph now reads as follows:

The lower boundary should be specified according to the following equations given in the appendix of the reference by H. S. Johnston ("Evaluation of Excess Carbon-14 and Strontium-90 Data for Suitability to Test Two-Dimensional Stratospheric Models", *JGR*, 94, 18485-18493, 1989):

$$\text{C-14 (N.Hem.)} = 73.0 - 0.27823 t - 3.45648\text{E-}3 t^{**2} + 4.21159\text{E-}5 t^{**3}$$

$$\text{C-14 (S.Hem.)} = 44.5 + 1.02535 t - 2.13565\text{E-}2 t^{**2} + 8.61853\text{E-}5 t^{**3}$$

where t = months after October 15, 1963. For all times after 15 June 1968, set the lower boundary values for the Southern Hemisphere equal to the calculated values from the Northern Hemisphere. The upper boundary conditions should be specified as zero flux.

Linda Hunt and Karen Sage, the UADP database managers, have requested that all participants send telephone and fax numbers as well as a current e-mail Internet address, including numeric IP number (e.g., 128.155.17.45) and name form with computer username (e.g., hunt@uadp1.larc.nasa.gov). Please send this information to hunt@uadp1.larc.nasa.gov or sage@uadp2.larc.nasa.gov. If you are not available via Internet, let them know how best to reach you. If you do not have access to e-mail, use your account on the UADP VAX to send them mail. If you need a UADP computer account, let Linda or Karen know. They can be reached at telephone 804/864-5856 or -5857, or by fax at 804/864-7790.

Sincerely,

*Kathy A. Wolfe*

Kathy A. Wolfe  
Senior Program Coordinator  
High Speed Research Program/  
Atmospheric Effects of Stratospheric Aircraft

### **C. List of Participants**

The following list of participants includes only those who attended the series of meeting leading up to and including the Workshop in February 1992. We have also included those directly involved in developing the measurement data sets. Many others, beyond this limited list, have contributed to the success of the Workshop, and we all thank them.

**HIGH-SPEED RESEARCH PROGRAM  
ATMOSPHERIC EFFECTS OF STRATOSPHERIC AIRCRAFT  
MODELS AND MEASUREMENTS (M&M) WORKSHOP  
LIST OF PARTICIPANTS**

**2-7 February 1992  
Satellite Beach, Florida**

Ms. Gail P. Anderson  
Geophysics Directorate  
PL/GPOS  
Hanscom Air Force Base  
Hanscom Field, MA 01731  
Affiliation: Geophysics Directorate/PL  
Telephone: 617/377-2335  
Fax: 617/377-8780  
E-Mail: afgl::chetwynd (SPAN)

Dr. Christoph Bruhl  
Abtlg. Chemie der Atmosphere  
Max-Planck-Institut fur Chemie  
(Otto-Hahn-Institut)  
Postfach 3060  
D-6500 Mainz  
GERMANY  
Affiliation: Max-Planck-Institut for Chemistry  
Telephone: 011-49-6131 305434  
Fax: 011-49-6131 305436  
E-Mail: chb@ibma.ipp-garching.mpg.de (Internet)  
bruhl@haloe.larc.nasa.gov (Internet)

Dr. Brian J. Connor  
Mail Stop 401B  
Langley Research Center  
National Aeronautics and Space Administration  
Hampton, VA 23665-5225  
Affiliation: NASA/Langley Research Center  
Telephone: 804/864-5698  
Fax:  
E-Mail:

Dr. Anne R. Douglass  
Code 916  
Goddard Space Flight Center  
National Aeronautics and Space Administration  
Greenbelt, MD 20771  
Affiliation: NASA/Goddard Space Flight Center  
Telephone: 301/286-2337  
Fax: 301/286-3460  
E-Mail: douglass@sgccp.gsfc.nasa.gov (Internet)  
pacf::douglass (SPAN)

Dr. Richard S. Eckman  
Mail Stop 401B  
Langley Research Center  
National Aeronautics and Space Administration  
Hampton, VA 23665-5225  
Affiliation: NASA/Langley Research Center  
Telephone: 804/864-5822  
Fax: 804/864-6326  
E-Mail: eckman@dobson.larc.nasa.gov (Internet)  
dobson::eckman or 10592::eckman (SPAN)  
RSECKMAN (NASAmail)

Dr. David W. Fahey  
R/E/AL6  
Aeronomy Laboratory  
National Oceanic and Atmospheric Administration  
325 Broadway  
Boulder, CO 80303-3328  
Affiliation: NOAA/Aeronomy Laboratory  
Telephone: 303/497-5277  
Fax: 303/497-5373  
E-Mail: fahey@aztec.al.bldrdoc.gov (Internet)

Dr. Donald A. Fisher  
E320/290  
Du Pont Experimental Station  
E. I. Du Pont de Nemours, Inc.  
P. O. Box 80320  
Wilmington, DE 19880-0320  
Affiliation: E. I. Du Pont de Nemours, Inc.  
Telephone: 302/695-4276  
Fax: 302/695-9658  
E-Mail: fisherda@esvax.dnet.dupont.com (Internet)

Dr. Ian Folkins  
Atmospheric Chemistry Division  
National Center for Atmospheric Research  
P. O. Box 3000  
1850 Table Mesa Drive  
Boulder, CO 80307  
Affiliation: National Center for Atmospheric Research  
Telephone: 303/497-1865  
Fax: 303/497-1400  
E-Mail: folkins@ncar.ucar.edu (Internet)

Dr. Rolando R. Garcia  
National Center for Atmospheric Research  
P. O. Box 3000  
1850 Table Mesa Drive  
Boulder, CO 80307  
Affiliation: National Center for Atmospheric Research  
Telephone: 303/497-1446  
Fax: 303/497-1400  
E-Mail: rgarcia@ncar.ucar.edu (Internet)

Dr. Claire Granier  
Atmospheric Chemistry Division  
National Center for Atmospheric Research  
P. O. Box 3000  
1850 Table Mesa Drive  
Boulder, CO 80307  
Affiliation: National Center for Atmospheric Research  
Telephone: 303/497-1445  
Fax: 303/497-1400  
E-Mail: granier@acd.ucar.edu (Internet)

Dr. William L. Grose  
Mail Stop 401B  
Langley Research Center  
National Aeronautics and Space Administration  
Hampton, VA 23665-5225  
Affiliation: NASA/Langley Research Center  
Telephone: 804/864-5820, -5691  
Fax: 804/864-6326  
E-Mail: grose@haloe.larc.nasa.gov. (Internet)  
haloe::grose (UARS CDHF)

Dr. Matthew H. Hitchman  
Department of Meteorology  
1225 West Dayton Street  
University of Wisconsin-Madison  
Madison, WI 53706  
Affiliation: University of Wisconsin-Madison  
Telephone: 608/262-4653  
Fax: 608/262-0166  
E-Mail: matt@adams.meteor.wisc.edu (Internet)

Ms. Linda A. Hunt  
Atmospheric Sciences Division, Mail Stop 401A  
Langley Research Center  
National Aeronautics and Space Administration  
Hampton, VA 23665-5225  
Affiliation: Lockheed  
Telephone: 804/864-5856  
Fax: 804/864-7790  
E-Mail: hunt@uadp1.larc.nasa.gov (Internet)

Dr. Charles H. Jackman  
Code 916  
Goddard Space Flight Center  
National Aeronautics and Space Administration  
Greenbelt, MD 20771  
Affiliation: NASA/Goddard Space Flight Center  
Telephone: 301/286-8399  
Fax: 301/286-3460  
E-Mail: jackman@pacf.span.nasa.gov (Internet)  
jackman@twod.gsfc.nasa.gov (Internet)  
pacf::jackman (SPAN)

Dr. S. R. Kawa  
Code 916  
Goddard Space Flight Center  
National Aeronautics and Space Administration  
Greenbelt, MD 20771  
Affiliation: NASA/Goddard Space Flight Center  
Telephone: 301/286-5656  
Fax: 301/286-3460  
E-Mail: kawa@maia.gsfc.nasa.gov (Internet)

Dr. Jack A. Kaye  
Code SED05  
Headquarters  
National Aeronautics and Space Administration  
Washington, DC 20546  
Affiliation: NASA Headquarters  
Telephone: 202/358-0253  
Fax: 202/358-3098  
E-Mail: jkaye@nasamail.nasa.gov (Internet)  
J.KAYE (Omnet)  
PACF::KAYE (SPAN)

Mrs. Rose M. Kendall  
ARC Professional Services Group  
Suite 700  
600 Maryland Avenue, SW  
Washington, DC 20024  
Affiliation: ARC Professional Services Group  
Telephone: 202/488-8234  
Fax: 202/488-7438  
E-Mail: r\_kendall@oactqm.hq.nasa.gov (Internet)

Dr. Jonathan Kinnersley  
Department of Meteorology  
University of Edinburgh  
James Clerk Maxwell Building, King's Buildings  
Mayfield Road  
Edinburgh, EH9 3JZ  
UNITED KINGDOM  
Affiliation: University of Edinburgh  
Telephone: 011-44-31-650 5098  
Fax: 011-44-31-662 4269  
E-Mail: jsk@edinburgh.meteorology.ac.uk (Service specified)

Dr. Douglas E. Kinnison  
Atmospheric and Geophysical Sciences  
Division, L-262  
P. O. Box 808  
Lawrence Livermore National Laboratory  
7000 East Avenue  
Livermore, CA 94550-9900  
Affiliation: Lawrence Livermore National Laboratory  
Telephone: 510/422-7975  
Fax: 510/422-5844  
E-Mail: kinnison1@llnl.gov (Internet)

Dr. Malcolm K. W. Ko  
Atmospheric and Environmental Research, Inc.  
840 Memorial Drive  
Cambridge, MA 02139  
Affiliation: AER, Inc.  
Telephone: 617/547-6207  
Fax: 617/661-6479  
E-Mail: mko@aer.com (Internet)

Dr. Michael J. Kurylo  
Code SEP  
Headquarters  
National Aeronautics and Space Administration  
Washington, DC 20546  
Affiliation: NASA Headquarters  
Telephone: 202/358-0237  
Fax: 202/358-3098  
E-Mail: MKURYLO@nasamail.nasa.gov (Internet)  
MKURYLO (NASAMAIL)

Dr. Richard D. McPeters  
Code 916  
Goddard Space Flight Center  
National Aeronautics and Space Administration  
Greenbelt, MD 20771  
Affiliation: NASA/Goddard Space Flight Center  
Telephone: 301/286-3832  
Fax: 301/286-3460  
E-Mail: mcpeters@sgccp.gsfc.nasa.gov (Internet)  
pacf::mcpeters (SPAN)

Dr. Chester Miller  
E320/240  
Du Pont Experimental Station  
E. I. Du Pont de Nemours, Inc.  
Wilmington, DE 19880-0320  
Affiliation: E. I. Du Pont de Nemours, Inc.  
Telephone: 302/695-4303  
Fax: 302/695-9658  
E-Mail: cmiller@a1@esvax@mcimail (Internet)

Dr. Ronald M. Nagatani  
W/NMC-53  
Climate Analysis Center/NMC  
National Oceanic and Atmospheric Administration  
5200 Auth Road  
Washington, DC 20233  
Affiliation: NOAA/National Meteorological Center  
Telephone: 301/763-8071  
Fax: 301/763-8125  
E-Mail: nagatani@oahu.wwb.noaa.gov (Internet)  
140.90.129.112 (Internet)  
oahu::nagatani (SPAN)

Dr. Paul A. Newman  
Code 916  
Goddard Space Flight Center  
National Aeronautics and Space Administration  
Greenbelt, MD 20771  
Affiliation: NASA/Goddard Space Flight Center  
Telephone: 301/286-3806  
Fax: 301/286-3460  
E-Mail: newman@aeolus.gsfc.nasa.gov (Internet)  
newman@odin1.gsfc.nasa.gov (Internet)  
odin1::NEWMAN (SPAN)

Dr. Giovanni Pitari  
Dipartimento di Fisica  
Universita' degli Studi L'Aquila  
Via Vetoio  
67101 Coppito (L'Aquila)  
ITALY  
Affiliation: Universita' degli Studi L'Aquila  
Telephone: 011-39-862-433074  
Fax: 011-39-862-433033  
E-Mail: VXSCAQ::PITARI (SPAN)  
pitari@vxscq.infn.it (Internet)  
pitari@vxscq.cineca.it (Internet)

Dr. Michael J. Prather  
Department of Geosciences  
211 Physical Sciences Research Facility  
University of California, Irvine  
Irvine, CA 92717  
Affiliation: University of California, Irvine  
Telephone: 714/856-5838  
Fax: 714/725-3256  
E-Mail: mprather@uci.edu (Internet)

Dr. Ellis E. Remsberg  
Mail Stop 401B  
Langley Research Center  
National Aeronautics and Space Administration  
Hampton, VA 23665-5225  
Affiliation: NASA/Langley Research Center  
Telephone: 804/864-5823  
Fax: 804/864-6326  
E-Mail: remsberg@haloe.larc.nasa.gov (Internet)  
HALOE::REMSBERG (UARS CDHF)

Dr. Curtis P. Rinsland  
Mail Stop 401A  
Langley Research Center  
National Aeronautics and Space Administration  
Hampton, VA 23665-5225  
Affiliation: NASA/Langley Research Center  
Telephone: 804/864-2699  
Fax: 804/864-7790  
E-Mail: rinsland@risbox.larc.nasa.gov (Internet)

Dr. Richard B. Rood  
Code 910.3  
Goddard Space Flight Center  
National Aeronautics and Space Administration  
Greenbelt, MD 20771  
Affiliation: NASA/Goddard Space Flight Center  
Telephone: 301/286-8203  
Fax: 301/286-3460  
E-Mail: rood@sgccp.gsfc.nasa.gov (Internet)

Dr. Joan E. Rosenfield  
Code 916  
Goddard Space Flight Center  
National Aeronautics and Space Administration  
Greenbelt, MD 20771  
Affiliation: NASA/Goddard Space Flight Center  
Telephone: 301/286-3817  
Fax: 301/286-3460  
E-Mail: rose@cdc910b21.gsfc.nasa.gov (Internet)  
rose@zephyr.gsfc.nasa.gov (Internet)  
odin1::rose (SPAN)

Ms. Karen H. Sage  
Atmospheric Sciences Division, Mail Stop 401A  
Langley Research Center  
National Aeronautics and Space Administration  
Hampton, VA 23665-5225  
Affiliation: Lockheed  
Telephone: 804/864-5857  
Fax: 804/864-7790  
E-Mail: sage@uadp2.larc.nasa.gov (Internet)

Dr. Toru Sasaki  
Physical Meteorology Research Division  
Meteorology Research Institute  
1-1 Nagamine  
Tsukuba, Ibaraki 305  
JAPAN  
Affiliation: Meteorology Research Institute  
Telephone: 011-81-298-51-7111 x 310 or  
Fax: 011-81-298-55-6936  
E-Mail:

Dr. Ulrich Schmidt  
Institut für Atmosphärische Chemie  
KFA Forschungszentrum Jülich GmbH  
Postfach 1913  
D-5170 Jülich  
FEDERAL REPUBLIC OF GERMANY  
Affiliation: Institut für Atmosphärische Chemie  
Telephone: 011-49 2461 61-6221 or 46-980-72000  
Fax: 011-49 2461 61-5346 or 46 980-21331  
E-Mail:

Dr. Robert K. Seals, Jr.  
Mail Stop 401  
Langley Research Center  
National Aeronautics and Space Administration  
Hampton, VA 23681  
Affiliation: NASA/Langley Research Center  
Telephone: 804/864-5378  
Fax: 804/864-7790  
E-Mail: rkseals@nasamail.nasa.gov (Internet)  
seals@eosdps.larc.nasa.gov (Internet)  
RKSEALS (NASAmail)

Dr. Mary Ann H. Smith  
Atmospheric Sciences Division  
Mail Stop 401A  
Langley Research Center  
National Aeronautics and Space Administration  
Hampton, VA 23665-5225  
Affiliation: NASA Langley Research Center  
Telephone: 804/864-2701  
Fax: 804/864-7790  
E-Mail: mahsmith@uxv.larc.nasa.gov (Internet)

Dr. Richard S. Stolarski  
Code 916  
Goddard Space Flight Center  
National Aeronautics and Space Administration  
Greenbelt, MD 20771  
Affiliation: NASA/Goddard Space Flight Center  
Telephone: 301/286-9111  
Fax: 301/286-3460  
E-Mail: stolarski@sgccp.gsfc.nasa.gov (Internet)  
pacf::stolarski (SPAN)

Professor Ka-Kit Tung  
Department of Applied Mathematics, FS-20  
University of Washington  
Seattle, WA 98195  
Affiliation: University of Washington  
Telephone: 206/685-3794  
Fax: 206/685-1440  
E-Mail: tung@amath.washington.edu (Bitnet)

Ms. Debra Weisenstein  
Atmospheric and Environmental Research, Inc.  
840 Memorial Drive  
Cambridge, MA 02139  
Affiliation: AER, Inc.  
Telephone: 617/547-6207  
Fax: 617/661-6479  
E-Mail: dkweis@aer.com (Internet)  
dweisenstein@aer.com (Internet)

Mr. Howard L. Wesoky  
Code RJH  
Headquarters  
National Aeronautics and Space Administration  
Washington, DC 20546  
Affiliation: NASA Headquarters  
Telephone: 202/453-2823  
Fax: 202/755-5442  
E-Mail: h\_wesoky@oaetqm.hq.nasa.gov (Internet)  
HWESOKY (NASAmail)

Mrs. Kathy A. Wolfe  
ARC Professional Services Group  
Suite 700  
600 Maryland Avenue, SW  
Washington, DC 20024  
Affiliation: ARC Professional Services Group  
Telephone: 202/488-8234  
Fax: 202/488-7438  
E-Mail: k\_wolfe@oaetqm.hq.nasa.gov (Internet)  
KWOLFE (NASAmail)

Dr. Donald J. Wuebbles  
Atmospheric and Geophysical Sciences  
Division, L-262  
P. O. Box 808  
Lawrence Livermore National Laboratory  
7000 East Avenue  
Livermore, CA 94550  
Affiliation: Lawrence Livermore National Laboratory  
Telephone: 510/422-1845  
Fax: 510/422-5844  
E-Mail: wuebbles@llnl.gov (Internet)

Dr. Glenn K. Yue  
Atmospheric Sciences Division, Mail Stop 475  
Langley Research Center  
National Aeronautics and Space Administration  
Hampton, VA 23665-5225  
Affiliation: NASA/Langley Research Center  
Telephone: 804/864-2678  
Fax: 804/864-2671  
E-Mail: yue@arbd1.larc.nasa.gov (Internet)

Dr. Yuk L. Yung  
Mail Code 170-25  
Division of Geological and Planetary Science  
California Institute of Technology  
Pasadena, CA 91125  
Affiliation: California Institute of Technology  
Telephone: 818/356-6940  
Fax: 818/585-1917  
E-Mail: yly@mercu1.gps.caltech.edu (Internet)

Dr. Joseph M. Zawodny  
Mail Stop 475  
Langley Research Center  
National Aeronautics and Space Administration  
Hampton, VA 23665-5225  
Affiliation: NASA/Langley Research Center  
Telephone: 804/864-2681  
Fax: 804/864-2671  
E-Mail: zawodny@arbd0.larc.nasa.gov (Internet)  
arbd0::Zawodny (SPAN)

## **Chapter 2**

### **Summary of Findings**



## SUMMARY OF FINDINGS

Ellis Remsberg, Michael Prather

The confidence assigned to predictions of future scenarios by assessment models will be based on conclusions about what those models can do well. We shall make that judgement from our knowledge of how the models incorporate the known physical and chemical processes in the atmosphere and, finally, how they are able to simulate observations of the current atmosphere. This Workshop focusses primarily on the comparison with observations. A principal byproduct of the Workshop is a determination of where the models and/or the measurements must be improved in order to enhance that confidence.

In this Workshop the overall performance of the models is evaluated in terms of both transport and chemistry. Indeed, when comparing the distribution of trace species in the stratosphere, the influence of transport and chemistry cannot be readily separated. Particular attention is given here to the lower stratosphere, where the aircraft emissions and chlorine-/bromine-induced ozone loss are expected to be most important.

The detailed comparisons with global atmospheric measurements are summarized first (derived from Sections A through G, Volume II). Such comparisons are traditional for the global models, and here we have re-examined and codified a database of stratospheric measurements that provide several independent tests of the models. Results from more specialized diagnostic studies (Sections H through O, Volume III) provide additional, independent tests of model performance. Many of these comparisons are new to this Workshop; some have been used by a few modeling groups but are applied here to all models, and others represent a continuation of unresolved issues from the last stratospheric model intercomparison (Jackman et al., 1989). Included in this summary are some issues of model verification that require further effort. Although many of the concerns raised here are not new, they have been clarified by the systematic and thorough comparisons in this Models and Measurements Workshop.

### A. Comparisons with Global Atmospheric Measurements

#### 1. Approach

Traditionally, the stratospheric modeling community has compared their multi-dimensional model results with "present-day" observed distributions of total (i.e., column) ozone, with profiles of ozone, CH<sub>4</sub>, N<sub>2</sub>O, NO<sub>2</sub> and HNO<sub>3</sub>, and with measurements of HCl and HF columns as a function of latitude and season. These comparisons pointed out some successes of the models and also identified serious flaws. In general there are no simple fixes to the models for many of these discrepancies, and on occasion the fault has been found to lie with the measurements. We continue this tradition here by comparing the global-scale dynamical and chemical structure of the stratosphere in Volume II (Sections A-G).

Typically, the approach has been to validate model transport first. This step has evolved considerably since the 1-D stratospheric models of the 1970s in which the vertical diffusion coefficient was adjusted to fit the long-lived tracer data. There is considerable ambiguity in this approach even with 2-D comparisons since the photochemical model for CH<sub>4</sub> and N<sub>2</sub>O also controls their predicted distributions. We first examine the temperatures and net heating rates predicted/used by the models. These comparisons allow some evaluation of the different circulations in the models, but such measurements

do not uniquely define the stratospheric circulation of trace gases. Special tests of the modeled transport of trace gases that rely on transient phenomena (e.g.,  $^{14}\text{CO}_2$  from nuclear weapons testing) or model-model intercomparison (e.g., synthetic tracers) are examined in Volume III (Sections H-O).

This part contains a summary of the model simulations of the present-day global atmosphere, derived from the findings in Sections A through G. Model results using tropospheric boundary conditions appropriate for 1980 and 1990 have been documented and archived in the UADP as part the 1991 UNEP/WMO Ozone Assessment. In most cases these results have been updated and augmented for this Workshop because of the need for additional diagnostics. Most models reported results for two chemistries: one with gas-phase reactions only ("gas"), and one that also includes heterogeneous reactions of  $\text{N}_2\text{O}_5$  and  $\text{ClONO}_2$  on the background sulfate aerosol layer ("het").

Use of multi-year or 3-D data to test the 2-D models is deceptive. We have not clearly evaluated just what a 2-D, zonally, monthly averaged model should represent in terms of atmospheric variability. We have identified here, however, significant shifts in the circulation of tracers from some years relative to others (i.e., the QBO), which cannot be interpreted simply as a generally random year-to-year variability. The most extensive data sets with multi-year histories are those of ozone and temperature. The 2-D models would need to use these histories in order to derive a multi-year circulation based on heating rates. (The WASH model adopted a diabatic circulation from successive years of NMC temperatures, but no one has yet coupled both ozone and temperature to derive net heating.) Multi-year simulations of  $\text{O}_3$  (with differing circulations) would provide an important test of the year-to-year variability and help to identify particular modes or patterns in the zonal mean ozone distribution, which should be correlated with observations of other tracers such as  $\text{N}_2\text{O}$ .

## 2. Model Transport

How well do the models simulate transport in the stratosphere and how do we know? First, the 2-D residual circulation from the models is compared to a "reference" diabatic circulation derived from calculations of net heating using climatological averages of temperature from National Meteorological Center (NMC) and ozone from solar backscatter ultraviolet (SBUV) (Sections A and B). This comparison is not complete in that the residual advection alone does not completely define the transport of trace gases in the stratosphere; some of the 3-D mixing of tracers must be approximated in 2-D models by a parameterized diffusive transport. Thus, the answer to the opening question must also include an evaluation of model simulations of  $\text{O}_3$ ,  $\text{CH}_4$ ,  $\text{N}_2\text{O}$ ,  $\text{NO}_2$  and  $\text{HNO}_3$  (Sections C through G). More specific diagnostic tests of model transport are also available in Sections H, I, J, N and O; they are summarized in Part B of this chapter. The comparisons with T and  $\text{H}_2\text{O}$  have been included here predominantly as a means of testing the model assumptions, since most models do not yet predict these quantities.

### Temperature (Section A)

The temperature structure adopted by the models is important for both the chemistry and the derived circulation. Almost all of the models specify, rather than calculate, the monthly mean temperature distributions. Those temperatures have been compared with a reference climatology of NMC temperatures. Differences in temperature are substantial among the models and between the models and the NMC temperatures, particularly at high latitudes in the upper stratosphere. Models (few) that calculate temperatures have polar regions that generally are too cold; an exception is the revised NOCAR model (see Garcia et al., p. 12967, 1992).

Temperature differences of 5 to 10 K are not critical for gas-phase chemistry, but may totally change the character of heterogeneous chemistry depending on the water content of the sulfate aerosols or the predicted occurrence of PSCs. The differences between models and the NMC climatology here could have important consequences. NMC temperatures for the lower stratosphere are based on radiosonde observations, and in general there is no reason to question these measurements.

Temperature uncertainties are critical for deriving a diabatic circulation. Issues that remain unanswered include: (1) the accuracy of the several satellite temperature data sets in the upper stratosphere; (2) the importance of zonal variations in temperature relative to the monthly means used in the models; and (3) the importance of year-to-year variations in temperature on both the chemistry and the derived circulations.

### **Heating rates and circulation (Section A)**

There is qualitative agreement regarding the net heating rates and residual circulation, both among the models and with the observations. The details differ significantly. The sense and extent of the so-called Brewer-Dobson circulation (i.e., upward in the tropics and downward at mid and high latitudes) is generally correct, but its strength varies by at least a factor of two among the models. Results from other tests are equally non-definitive: the  $^{14}\text{CO}_2$  tracer simulation (Section I) indicates that the Brewer-Dobson circulation may be too strong in the models; however, other tracer patterns (e.g.,  $^{90}\text{Sr}$ ,  $\text{CH}_4$ ,  $\text{HNO}_3$  column) do not clearly support this premise.

A distinct problem for zonally-averaged models is that the net heating,  $Q_{\text{net}}$ , does not determine the tracer transport alone; eddy transports are coupled with  $Q_{\text{net}}$  (or at least they should be). Models that have eddy transports derived from observed distributions of wave activity or calculated potential vorticity fluxes seem to yield a more representative net transport with altitude and latitude and for each season. The sensitivity of tracers to the model circulations was demonstrated best in Section O through lifetime experiments with synthetic tracers. The roles of mean and diffusive transport were sorted out for several of the models in Section N, and the mean transport is by far the dominant term. Comparisons of vertical profiles in Sections D, E, F, I, and J suggest that diffusion is also too strong in some models. Those with weak diffusion or at least diffusion limited seasonally to specific regions of the stratosphere (where wave transports are believed to be most effective) seem to perform best.

We have also identified a worrisome aspect for the application of residual circulations derived from the diabatic heating. In some instances the monthly mean vertical motions at specific locations are opposite to the calculated local net heating. This occurs because of the assumption of a required conservation of net heating across a pressure level which, in turn, leads to local adjustments in order to achieve this global balance. A consequence of this re-balancing of heating rates is that errors in the tropical troposphere (100 - 200 mbar) may significantly affect the net heating assumed over the winter pole in the lower stratosphere.

From the discussion in this section it is clear that significant uncertainties remain in the transport in zonally-averaged models, such that advancements in our understanding of chemical mechanisms may not necessarily improve many of the model/measurement comparisons in this report. Specific issues that must be addressed more carefully are: (1) the effect of year-to-year variations in temperature (and ozone) on the derived circulations, and (2) the introduction of tropical-wave forcing mechanisms in models. None of the models include an accurate representation of the quasi-biennial oscillation

(QBO), which modulates the upward branch of the net circulation and appears to control the timing of meridional transports into and out of the tropics (see Ruiz simulation, section J). Both the CAMED model and the new NOCAR model have simulated the semi-annual oscillation (SAO) at tropical latitudes. Annually varying diabatic circulations derived from a multi-year time series of observed temperatures will contain some of the effects of changes in wave forcing at all latitudes; however, they will not necessarily describe the complete transport.

### **3. Distributions of Long-Lived Species**

#### **Water vapor (Section B)**

Current stratospheric models, even those that "calculate" H<sub>2</sub>O, specify H<sub>2</sub>O in some way or another that critically controls the stratospheric abundance. While these assumptions are reasonable, they do not adequately represent the physical processes that change H<sub>2</sub>O near the tropopause. Therefore, relative H<sub>2</sub>O change from stratospheric aircraft injection can be estimated, but might be in error if the mechanism for exchange of H<sub>2</sub>O in the mid-latitude lower stratosphere is not understood. For example, if the drying-out mechanism fixes the partial pressure at the tropopause, the prediction would be different than if a fixed flux were removed by some other mechanism.

The available water vapor data sets are most uncertain between about 50 and 300 mb. The SAGE II climatology is favored over LIMS in the region of largest discrepancy because it covers all seasons and it extends into the upper troposphere. There is an obvious difference between the SAGE II and the Oort climatologies for H<sub>2</sub>O in the upper troposphere, but recent evidence favors the SAGE II values. A better climatology needs to be compiled for these altitudes, coupling SAGE II with aircraft data from the various ER-2 and DC-8 missions. Simultaneous measurements of CH<sub>4</sub> and H<sub>2</sub>O would eventually provide a test of the physical processes controlling H<sub>2</sub>O in the lower stratosphere.

#### **Integrated column ozone (Section C)**

Column ozone is controlled by both circulation and chemistry. The test of reproducing observed total ozone must be taken as a non-unique test of a model. The model's integrated ozone columns are in reasonable qualitative agreement with TOMS data. Certain details point to nearly universal problems in the model formulation that show up in other M and M tests. For example, the measurements show steep gradients between 30 N and 50 N, but the models tend to wash out these gradients, mixing the ozone from the tropics to the mid-latitudes. Some of these problems appear in the other column measurements (Section G). Four of the models -- DUPONT, GISS, MRI and OSLO -- substantially underestimate column ozone as well, possibly a sign of the modeled tropopause being too high.

The inclusion of sulfate-layer chemistry is interesting: it has no major affect on the observed column abundance over the period 1980-1992, but it greatly influences the predicted trend. The modeled trends, 1980-1990, are grossly similar to those measured, but the observed seasonality of ozone loss over the northern hemisphere points clearly to some missing processes (i.e., wintertime PSC chemistry) that are not included in most of the models. The NCAR model simulates ozone trends fairly well, but differs from the other models in simulating the chemical partitioning and budgets (see Sections L and M). Some recent work using the ITALY model has demonstrated that the lower stratospheric temperature increase due to volcanic aerosols can alter the net circulation such that downward diabatic descent is increased at high latitudes in winter leading to an increase

in column ozone. This increase partially offsets an ozone decrease due to just the PSC-induced chemistry.

We now have the TOMS decadal trend as well as the "mean" column ozone to provide a critical test of the models. The trend may provide more a measure of the chemical perturbation than of the circulation (with caveats noted above).

### **Ozone profiles (Section D)**

Ozone above 35 km in the sunlit stratosphere is a relatively short-lived gas that is expected to be in photochemical steady state. In the lower stratosphere near the tropopause, however, it is extremely long-lived and generally behaves like a tracer with small photochemical tendencies (e.g.,  $\text{CFCl}_3$  or  $\text{CH}_4$ , but with opposite gradients). In the upper stratosphere (35 - 50 km), comparison of the vertical profiles of ozone provides a fundamental test of the photochemical balance of odd-oxygen budgets over two scale heights. A basic problem remains for the model ozone photochemistry in the upper stratosphere near 40 km: simulated concentrations of ozone are systematically 20 to 40 percent below observations.

We introduce here a new climatology for the  $\text{O}_3$  distribution based on SBUV observations (Version 6). The SAGE II profiles (less frequent, less global coverage) were used to define the relative profile below the ozone maximum, for which SBUV can only detect the total column. This climatology is new and it agrees with an ECC climatology to within 20 percent at 20 km (about the accuracy of both data sets). It may provide one of the best tests of transport in the lower stratosphere.

Generally, the models are able to produce the overall features of the seasonal ozone variation, including the basic latitudinal variation and the seasonal behavior at high latitudes. Models agree with data at mid and high latitudes of the lower stratosphere to within about 20 percent, but they clearly overestimate ozone at low latitudes. For the tropics at 20 km, DUPONT, NCAR and NOCAR did the best. [The CALJPL model ozone profiles were not submitted to the UADP data base.] Coupled with Section H (tracer correlations), the ozone profile comparisons show a clear problem for most models near and above the tropical troposphere.

Profile shape is a concern for many models, particularly at high latitudes, indicating deficiencies in the model circulation in polar regions, especially in winter. ITALY does the best job of matching the observed profiles in polar regions, possibly because that model obtains its ozone distribution from 3-D transport fields. Many models have their peak ozone mixing ratio at too low an altitude, even at mid latitudes in summer.

### **Global distributions of $\text{N}_2\text{O}$ and $\text{CH}_4$ (Section E)**

The "standard" global data set for  $\text{N}_2\text{O}$  and  $\text{CH}_4$  comparisons (i.e., SAMS) has some obvious problems. Below about 30 km the balloon profiles are considered more reliable than the SAMS data for comparison; however, their sampling is so sparse as to make comparisons with the global models difficult. It is important to realize that the SAMS data are accurate only for  $\text{N}_2\text{O}$  values less than about 150 ppbv and for  $\text{CH}_4$  values less than about 1.1 ppm. The strikingly different behavior of the SAMS  $\text{N}_2\text{O}$ - $\text{CH}_4$  correlations between 1979 and 1980 demonstrates an obvious problem with the SAMS measurements (versus a change in transport), since a change in meridional mixing would not so perturb the correlations.

There are some patterns in the observed  $\text{N}_2\text{O}$  and  $\text{CH}_4$  global distributions that are not paralleled in the models. As a group, the models perform well at mid to high latitudes between 20 and 30 km, indicating that the net transport in the models is representative of the atmosphere. Model/measurement profiles agree well at mid latitudes but at high latitudes are less uniform at 30 km than at 20 km. These high latitude results are similar to those from the ozone profile comparisons in Section D. On the other hand, the profile comparisons near 30 N indicate that many models have a net upward transport that is too strong in the lower sub-tropical stratosphere (also argued for in Section I). One should not over-interpret the 30N profiles in terms of vertical motions instead of horizontal transports: these profiles lie on the edge between tropical upwelling and mid-latitude descent, often showing inverted profiles with tropical values at upper altitudes and typical mid-latitude profiles in the lower stratosphere. Comparisons at tropical latitudes, while reasonable, are too few from which to draw firm conclusions about model performance. More data are needed from that region.

Improved measurements of the  $\text{N}_2\text{O}$ - $\text{CH}_4$  correlation curve and its deviations from linearity in different regions of the stratosphere may provide the best test yet of the relative loss rates (photolysis versus OH) for these species. Proper simulation of this relationship is critical for interpreting chemical processing and transport variations. We need to know what part of the observed correlations represents a true geophysical measurement. Obviously, more and better  $\text{N}_2\text{O}$  and  $\text{CH}_4$  profile data are needed between 20 and 35 km.

#### **Abundances and distribution of $\text{NO}_y$ species (Section F)**

The distribution of  $\text{NO}_y$  (the sum of all odd-nitrogen species) is interesting as a second-order derived quantity of the stratospheric models. First-order can be defined as the distribution of  $\text{N}_2\text{O}$  (the primary source of  $\text{NO}_y$ ), and a third-order derived quantity is clearly  $\text{O}_3$  whose concentration depends on the  $\text{NO}_y$  distribution. (Other examples of second-order quantities are  $\text{H}_2\text{O}$  and  $\text{Cl}_y$ , all chlorine release from halocarbons.) The global distribution of  $\text{NO}_y$  is a test of the models' circulation and chemistry. The primary source of  $\text{NO}_y$  depends on the yield of NO from  $\text{N}_2\text{O}$  loss; and a significant fraction of  $\text{NO}_y$  is lost above 40 km through photolysis of NO.

Global data for  $\text{NO}_y$  are not without problems--we must either employ a pseudo- $\text{NO}_y$  (a sum of some of the  $\text{NO}_y$  species), or be restricted to the lower stratospheric in situ data (Section H), or be limited to ATMOS profiles. Measurements of an  $\text{NO}_y$  climatology need to be made over several years to account for known year-to-year variations in the circulation as diagnosed from other tracers. In the lower stratosphere, however, we prefer to compare correlations of  $\text{NO}_y$  with  $\text{O}_3$  and  $\text{N}_2\text{O}$  (see Section H) because difficulties in registering the height of the tropopause are overcome. Differences among the models remain for the predicted  $\text{NO}_y$  distributions, and can be attributed in part to the circulation and in part to  $\text{NO}_y$  chemistry.

The seasonality of stratospheric  $\text{NO}_2$  concentrations (at sunset from SAGE II) shows a clear indication of chemical processing of  $\text{NO}_x$  ( $=\text{NO}+\text{NO}_2$ ) into  $\text{HNO}_3$  or other reservoirs around winter in the lower mid-latitude stratosphere, presumably due to the heterogeneous reaction of  $\text{N}_2\text{O}_5$  on sulfate aerosols. Models using only gas phase reactions did not reproduce the large winter-summer difference in  $\text{NO}_2$ , as seen by SAGE II between 20 and 26 km in the mid latitudes (30 to 50 degrees latitude) of both hemispheres. Further, the LIMS  $\text{HNO}_3$  measurements support this inclusion of heterogeneous chemical processes. For example, the summer-autumn  $\text{HNO}_3$  observations are modeled reasonably by either gas phase or heterogeneous models, but

the winter-spring observations are only predicted well in the same models by including the  $\text{N}_2\text{O}_5$ -sulfate reaction.

Systematic errors for LIMS  $\text{NO}_2$  are rather large in the lower stratosphere, which may account for its apparent differences with the SAGE II  $\text{NO}_2$  and with model  $\text{NO}_2$ . The precision of the LIMS data, however, is very good, such that its relative variations with latitude, longitude, and time are considered trustworthy. Therefore, the observed variability in LIMS  $\text{NO}_2$  is an appropriate test of variability for species in multi-dimensional models. Further, it is difficult to make comparisons directly with the global  $\text{NO}_2$  climatology from SAGE II (or ATMOS) unless the models are able to report "sunset" or "sunrise" values for  $\text{NO}_2$  (i.e., solar zenith angle of 90 degrees corresponding to direct sun in the stratosphere). In view of the importance of this comparison, the models should consider such diagnostics as standard.

### **Column abundances of HF, HCl, $\text{HNO}_3$ , $\text{ClONO}_2$ , and $\text{NO}_2$ (Section G)**

Comparison with the observed column abundances provides an integrated check on the models. Nitric acid, chlorine nitrate, and nitrogen dioxide columns are a measure of the partitioning of the  $\text{NO}_y$  family. HCl is one of the principal reservoir gases for the chlorine released from halocarbons, and HF provides a measure of the decomposition of chlorofluorocarbons. It must be recognized that columns are only integrative measures of the distribution and emphasize the lower altitude portion of a stratospheric profile.

The latitudinal gradient in column  $\text{HNO}_3$  shows a clear preference for the heterogeneous-chemistry versions of the models. However, more observations are needed, e.g., chlorine nitrate columns may provide an excellent calibration/test of heterogeneous chemistry in the models, and we should make an effort to acquire a seasonal climatology at least at one or two mid latitude points.

All models underestimate column  $\text{NO}_2$  compared with LIMS, but this finding may be explained by systematic errors for LIMS  $\text{NO}_2$ . (The appearance that the gas-phase models are closer than the heterogeneous models must not be taken seriously here.) The latitudinal and seasonal variations in LIMS  $\text{NO}_2$  (precision about 5 percent) are followed well by the models. In general, the comparisons of both  $\text{HNO}_3$  and  $\text{NO}_2$  in the low-to-mid stratosphere across all seasons and latitudes indicate that model simulations of transport and  $\text{NO}_y$  chemistry (i.e.,  $\text{NO}_x$ - $\text{HNO}_3$  partitioning) in the lower stratosphere are reproducing the major features of the observations.

There are significant differences between the JPL and NCAR observations of the HCl column (40 percent) and the HF column (70 percent). More reliance is placed on the observed latitudinal and seasonal variations of these gases. The NCAR (Mankin and Coffey, 1983) measurements exhibit high-to-low latitude ratios that are nearly equivalent (about a factor of 3) for HCl and HF. Latitudinal variations of the HCl and HF columns are not equally matched in the models: those that do well for HF may do poorly for HCl. This points to problems with the model HF/HCl ratios.

## **B. Special Diagnostic Studies**

### **1. Introduction**

Some specific experiments were developed to test aspects of model transport and chemistry. For example, Section H describes tracer correlations using primarily a large volume of data from several ER-2 aircraft campaigns to diagnose model transport near 20 km. Sections I ( $^{14}\text{CO}_2$  and  $^{90}\text{Sr}$  from weapons tests) and J (volcanic cloud from Mt.

Ruiz) document the ability of models to simulate the observed dispersion of time-dependent tracers that were released directly into the lower stratosphere. Additionally, model calculations were conducted and compared with each other for photodissociation processes (Section K) and specific chemical production and loss rates (Section L). Species profiles at sunset were compared directly with the 30N measurements from the 1985 flight of ATMOS (Section M). Section N represents model-model comparisons of the role of advective versus diffusive transport for  $N_2O$  and  $O_3$ , and Section O looks at the atmospheric lifetimes predicted for idealized tracers with specified stratospheric loss rates (i.e., identical "chemistries" across all models). These model-model comparisons are an essential, but secondary component of the M & M workshop; they allow us to evaluate the individual components of the models in a way not possible for atmospheric chemical tracers.

## 2. Transport Diagnostics

### Simultaneous observations of long-lived species (Section H)

Section H focuses on the observed correlations of long-lived trace gases measured relative to  $N_2O$  from several ER-2 aircraft campaigns (16 to 20 km). This data set is extended with some altitude profiles (balloons and ATMOS) and the global  $N_2O$ - $CH_4$  maps from SAMS. The modeled slopes of the correlation diagrams for various tracers are in basically good agreement with the observations, although for some species (e.g.,  $CHF_2Cl$ ,  $CCl_4$ ,  $CH_3Cl$  and  $CH_3CCl_3$ ) the measurement errors are too great to constrain the models.

We conclude that the relative rate of stratospheric destruction for many species (e.g.,  $N_2O$ ,  $CH_4$ ,  $CF_2Cl_2$ , and  $CFCl_3$ ) is verified. Loss of  $CH_4$  is primarily due to OH and that of  $N_2O$  and the CFCs is due to ultraviolet photolysis (180 to 230 nm); therefore, the credibility for modeling these two independent processes is greatly enhanced by this success. Further, the stratospheric lifetimes of these gases are reasonably determined on a relative scale based on the theory of Plumb and Ko (1992).

The  $NO_y/O_3$  ratios show clear problems with the models that cannot be argued away as an altitude offset of the tropopause (which could be done when only vertical profiles are examined). These discrepancies occur throughout the lower stratosphere, but the cause in the tropics is likely to be different than that at high latitudes. Most models underestimate  $NO_y$  at 20 km in low latitudes, perhaps because their vertical advection is too strong (see also Sections E and I). Models generally also predict too little  $NO_y$  at high latitudes. The models generally fail to simulate the steep  $NO_y/O_3$  gradient between the tropics and mid latitudes. The ITALY model does meet this test, consistent with its weaker horizontal diffusion. More  $NO_y/O_3$  measurements are needed at low latitudes, especially above 20 km.

Some specific model anomalies, good and bad, show up with regard to species correlations: NCAR shows some loss of HCFC-22 and  $CH_4$  without a corresponding loss of  $N_2O$  in the tropical lower stratosphere; CAMED shows different patterns for  $CHF_2Cl$  and  $CH_4$  (both are driven by OH). The AER model is able to simulate the expected level of curvature in the correlations due to the rapid growth in tropospheric  $CHF_2Cl$ . All in all, there is a wealth of model/data comparisons in this Section, and they have been presented in an innovative way that was not available for previous validation efforts. Such correlation analysis techniques should be standard for future studies.

## **Radionuclides as exotic tracers (Section I)**

The observed decay of excess atmospheric carbon-14 ( $^{14}\text{CO}_2$  from weapons tests) from 1963 to 1970 provides useful, but limited profile data (only at 31N) for testing the circulation of the lower stratosphere. The observations of stratospheric strontium-90 ( $^{90}\text{Sr}$ , also from weapons tests) from 1964 to 1967 also provide a test of the removal of a transient tracer injected into the lower stratosphere at northern mid latitudes. The  $^{90}\text{Sr}$  has more complete profile data available at four widely spaced latitudes (70N, 31N, 9N, 42S), but it attaches to aerosols and is therefore not just a tracer of air motions as is  $^{14}\text{CO}_2$ .

The use of bomb- $^{90}\text{Sr}$  as a paired simulation with  $^{14}\text{CO}_2$  greatly enhances this test of model transport. The  $^{90}\text{Sr}$  observations are more extensive, and there is a critical difference between these two tracers:  $^{90}\text{Sr}$  on aerosols has an additional "settling velocity" relative to mean flow. The CAMED, WASH and LLNL models simulate the trends in  $^{90}\text{Sr}$  very well, whereas the ITALY and DUPONT models do the best job for  $^{14}\text{CO}_2$ .

The  $^{14}\text{CO}_2$  experiment shows clear problems with the tropopause as determined by dynamical mixing; this is similar to problems noted with ozone profiles in Section D. The large scatter in concentrations predicted in the middle stratosphere is a problem caused by differing model transports as shown also by results for the synthetic tracers in Section O. At 31N the models show a more-rapid-than-observed decline in  $^{14}\text{CO}_2$  at 20 km, with an over prediction at higher altitudes, in agreement with findings for  $\text{CH}_4$  and  $\text{N}_2\text{O}$  in Section E. With multi-dimensional models the obvious "solution" (i.e., cut down the vertical transport) may not apply since we do not have measurements of  $^{14}\text{CO}_2$  above 20 km at other latitudes, and thus, cannot say anything about latitudinal transport above 20 km. However, the inescapable failure of the models is obvious: they predict too rapid a decrease in the 16-20 km range from 70N to 42S.

In 1970 the observed excess  $^{14}\text{CO}_2$  shows an interesting profile with a relative maximum in the lower stratosphere that could not be reproduced by any model under the assumptions of a single  $^{14}\text{CO}_2$  injection in 1963. It is likely that something is wrong with the experiment as posed here (e.g., errors in measurement of residual bomb- $^{14}\text{CO}_2$ , importance of sources after 1963, tropospheric injection, etc.). Models that do well in the  $^{90}\text{Sr}$  test and the early  $^{14}\text{CO}_2$  simulation still have problems with the 31N profile of  $^{14}\text{CO}_2$  in 1970.

## **Mt. Ruiz volcanic cloud (Section J)**

The volcano Nevado del Ruiz (5N, 75W) in Colombia erupted on 13 November 1985 and aerosols from it were observed by the SAGE II satellite experiment. This was the strongest volcanic eruption observed by SAGE II prior to the Pinatubo eruption of 1991. Initial distributions of the aerosol layer, centered near 20 km, were provided to the models from the SAGE II data of 1 February 1986. The Ruiz cloud (like the bomb- $^{90}\text{Sr}$  simulation in Section I) opened a new era in model comparison by including the sulfate-layer aerosols. We account for stratospheric aerosols not being transported identically as gases by including a settling velocity (albeit a single one here) for the downward motion of aerosols relative to air.

The models in general show a propensity to mix the volcanic aerosols rapidly beyond the tropics and to wash out the sharp peak in particle concentration (through either vertical or horizontal mixing); both results are contradictory to SAGE II observations. Many models, however, are able to follow in general the observed removal of the aerosol over

the twelve months following the initialization. This is consistent with the success of the 90Sr simulation.

The observed containment of volcanic aerosols within the tropics points to the possible importance of the quasi-biennial oscillation in producing contained circulations during certain phases and more mixed transport at other times. The comparisons with 2-D model circulations that are based on an "average" circulation are clearly inadequate.

### **3. Photolysis and Chemistry Diagnostics**

Sections K, L, and M have a common theme in that we adopted a mean atmospheric profile based on the ATMOS solar occultation measurements made at sunset, 30N, May 1985, giving us a framework with which to compare the basic photochemistry of the models independent of their transport. Because of ambiguities and misinterpretations of the experiment at the February workshop, these sections were revised and reviewed again by the participants at the May 1992 HSRP/AESA meeting. Only these more recent findings are presented in this report. In Section K photolysis rates are examined, and in Section L the model chemistry of rates and radicals is compared; these Sections are basically model intercomparisons. Section M is a true model and measurement comparison: the models simulated the sunset profiles of  $\text{NO}_y$  and  $\text{Cl}_y$  species to match the ATMOS profiles.

#### **Photodissociation rates (Section K)**

The section on photolysis rates continues a long-standing, unresolved problem of model intercomparison since the 1-D model assessments of the 1970s. The 1988 intercomparison demonstrated clear differences among the models, even though we made certain we were all doing the "same calculation." For this Workshop, we again specified the atmosphere (based on a mean ATMOS profile at 30N, likewise for Sections L and M), but we required some additional diagnostics.

New this time, we have a reference standard for transmission in the  $\text{O}_2$  Schumann-Runge bands from the AFGL-Harvard work. The existence of a reference for  $\text{O}_2$  has greatly improved our perspective in comparing the models, but the spread in values is still large, about a factor of 1.5. When we include the Herzberg continuum ( $> 200$  nm), the agreement among models for  $\text{O}_2$  photolysis is better than 15 percent above 30 km. This consistency in the Herzberg continuum is likely to be the reason that the models calculate such similar ozone profiles for the mid stratosphere.

Unfortunately we have no such reference for photodissociation of NO. The differences in modeled NO photolysis rates are larger than for  $\text{O}_2$  photolysis because only wavelengths in the Schumann-Runge bands, specifically less than 192 nm, contribute. The value of  $J(\text{NO})$  determines the fall-off of  $\text{NO}_y$  mixing ratios in the upper stratosphere and will therefore affect the absolute value of the slope of the  $\text{NO}_y$ - $\text{N}_2\text{O}$  correlation in the lower stratosphere.

The discrepancy in photolysis rates for CFC-11, CFC-12, and  $\text{N}_2\text{O}$  is also large, ranging over a factor of 1.4 in the region of most important loss for these species (20-30 km). It probably reflects the divergent values in transmission of solar flux shortward of 200 nm.

The calculated photolysis rates for  $\text{NO}_2$  agree to within 25 percent if scattering is not included. The treatment of scattering is so diverse among the models as to introduce substantially larger differences in the photolysis rates, as compared with calculations

using only O<sub>2</sub> and O<sub>3</sub> absorption. We need to establish a reference scattering model for these UV-visible calculations (290-700 nm).

### **Photochemistry of radicals and rates (Section L)**

This Section is a model-to-model intercomparison designed to answer the question: "Do we all calculate the same photochemical budgets for ozone given a prescribed atmosphere?" Both noon-time and 24-hour species profiles were calculated. Gas phase and heterogeneous chemistry calculations were conducted in separate runs. Eight models participated in this activity.

There is very good agreement above 30 km among the models for the noontime and 24-hour-average densities of O, O(1D), OH, HO<sub>2</sub>, NO<sub>2</sub>, and NO. Some important differences appear at 20 km. There is a spread of O(1D) values in the lower stratosphere that is related directly to the model disagreements in the J-values (Section K). The models are consistent in calculating the diurnal average of chemical rates with the exception of two models that approximate the diurnal cycle with averaging factors. The predicted NO<sub>y</sub> loss still varies by a wide range throughout the stratosphere. The OH densities vary considerably in the lower stratosphere between models. Model/measurement comparisons of NO<sub>y</sub> and HO<sub>x</sub> species should be considered again, perhaps using new measurements from SPADE and ATMOS.

The impact of heterogeneous chemistry is fairly consistent among the models for profiles of radicals and the ozone-destroying reactions. Model results differ by about a factor of 2. Overall, the results from Section L are encouraging, but still not adequate: even where there is basic agreement in the chemical processes included in the models, inexplicable differences remain.

### **Species comparisons with ATMOS at sunset (Section M)**

This section examined the chemical partitioning of the NO<sub>y</sub> and Cl<sub>y</sub> families against the ATMOS species profiles at sunset. The total family abundances for NO<sub>y</sub> (from ATMOS), Cl<sub>y</sub> (from empirical correlations with NO<sub>y</sub>), and Br<sub>y</sub> (fixed at 15 pptv) are given in a Table at the beginning of Section K. Five models took part in this calculation (AER, CALJPL, GISS, GSFC, and LLNL).

Model/measurement profile comparisons agree very well for species in the NO<sub>y</sub> family (NO, NO<sub>2</sub>, HNO<sub>3</sub>, and HO<sub>2</sub>NO<sub>2</sub>), even at 20 km! There is more spread among the model N<sub>2</sub>O<sub>5</sub> values, but at 30N in May this species is only a few percent of total NO<sub>y</sub> at sunset. A sunrise comparison would be a better test for N<sub>2</sub>O<sub>5</sub>. In general the gas phase NO<sub>x</sub> chemistry is being modeled well, at least at 30N in spring. Effects of HO<sub>x</sub> radicals on ozone in the lower stratosphere must be understood better, but based on these findings it appears that the HO<sub>x</sub> uncertainties demonstrated in Section L may not affect NO<sub>y</sub> partitioning at the level shown here. A much greater effort should be directed at observations below 20 km where the divergence among models is greatest.

The HCl comparisons were reasonable above 30 km, but not so good at 20 km. This is disturbing, because HCl should be most of the Cl<sub>y</sub> (based on the ATMOS simultaneous measurements of ClONO<sub>2</sub>). Perhaps the specified Cl<sub>y</sub> profile is not correct there. CALJPL matches the 20 km observations better than the other models (but with a different Cl<sub>y</sub>). The ClO and ClONO<sub>2</sub> comparisons are generally acceptable, but the GSFC Cl<sub>y</sub> partitioning was different from the ATMOS observations and the other models.

Partitioning of Br<sub>y</sub> into BrO, HBr, and BrONO<sub>2</sub> is more variable among the models, even though the Br<sub>y</sub> profile was specified. Br<sub>y</sub> species data should be compiled for any future comparison. The HF/HCl ratio can also be part of any future model/data comparison once the HALOE data from UARS are available.

#### 4. Model-Model Comparisons of Transport

##### Transport fluxes (Section N)

This section on modeled fluxes required special diagnostics, and five models contributed (AER, CAMED, GSFC, ITALY, and LLNL). The local tendency of the continuity equations for N<sub>2</sub>O and O<sub>3</sub> have been separated into terms representing transport processes (i.e., flux divergences) and photochemical production/loss. Transport was further broken down into both advection and diffusion in the horizontal and vertical directions. Generally, advection in the 2-D models plays a more dominant role than the parameterized diffusion in the lower stratosphere. However, if the Brewer-Dobson circulation is too strong in some models (as suggested in some other Sections of this report), then this conclusion may need to be revised.

These diagnostics clearly show the dominant factors controlling O<sub>3</sub> in the lower stratosphere. Ozone in the lower stratosphere responds to changes in the circulation at all latitudes. Ozone in the tropical lower stratosphere is dominated by local production and is relatively unaffected by perturbations to chemical reactions that destroy ozone. At high latitudes the reverse is true: production is unimportant, and O<sub>3</sub> responds to changes in photochemical loss.

##### Model-model comparison of idealized tracers, X1 and X2 (Section O)

The use of synthetic tracers with prescribed chemistry is very important in documenting those differences in lifetime and tracer cross-correlations that are due strictly to the model circulation rather than the chemistry. A tracer experiment was designed to approximate the atmospheric behavior of CFC/N<sub>2</sub>O-like species. We prescribed constant tropospheric concentrations and stratospheric loss rates (varying only with pressure) for two tracers X1 and X2 (twice the loss frequency of X1). In general, we found a spread in predicted lifetimes for X1 and X2 across the models that is similar to that for CFCs and N<sub>2</sub>O. This comparison does not mean that differences in the chemical models do not contribute to this variation in calculated lifetimes for CFCs and N<sub>2</sub>O, but that the different tracer circulations can explain most of the range in calculated CFC lifetimes.

Ten models participated in this experiment. The relative tracer lifetimes for X1 are categorized as follows: (1) shortest--NOCAR, GSFC, CALJPL, and NCAR; (2) medium--LLNL, ITALY, and CAMED; and (3) longest--AER, DUPONT, and WASH. Generally, models that compute the shortest lifetimes for X1 tend to predict the shortest residence times for the 14CO<sub>2</sub> tracer and vice versa. Those models that do best in matching the ozone profiles at high latitudes in winter, also show a unique seasonal feature in their tracer X profiles.

Tracer correlations are becoming a valuable tool for diagnosing the stratosphere. These set experiments help us interpret the basic correlations between long-lived tracers, e.g., the degree of curvature and the dispersion in the (X1, X2) scatter plot. Cross-correlations of tracers X1 and X2 show large ranges in the tightness of the curve, depending apparently on the rate of horizontal mixing. The correlation of X with a transient tracer W (i.e., a tracer like X with a tropospheric trend in concentration) shows that some additional curvature is introduced into the correlation.

## REFERENCES

Garcia, R. R., F. Stordal, S. Solomon, and J. T. Kiehl, A new numerical model of the middle atmosphere. I. Dynamics and transport of tropospheric source gases, *J. Geophys. Res.*, 97, 12967-12992, 1992.

Jackman, C. H., R. K. Seals, Jr., and M. J. Prather, eds., *Two-dimensional Intercomparison of Stratospheric Models*, NASA Conference Publication 3042, NASA, Washington, D.C., 1989, 595 pp.

Mankin, W. G., and M. T. Coffey, Latitudinal distribution and temporal changes of stratospheric HCl and HF, *J. Geophys. Res.*, 88, 10776-10784, 1983.

Plumb, R. A., and M. K. W. Ko, Interrelationships between mixing ratios of long-lived stratospheric constituents, *J. Geophys. Res.*, 95, 10145-10156, 1992.

1. The first part of the document discusses the importance of maintaining accurate records of all transactions. It emphasizes that proper record-keeping is essential for the integrity of the financial system and for the ability to detect and prevent fraud.

2. The second part of the document outlines the specific requirements for record-keeping, including the need to maintain original documents and to keep copies of all transactions. It also discusses the importance of regular audits and the need to report any discrepancies immediately.

3. The third part of the document discusses the consequences of failing to maintain accurate records, including the potential for fines and penalties. It also discusses the importance of training staff on proper record-keeping procedures and the need to establish a strong internal control system.

## Chapter 3

# Upper Atmosphere Data Base and Model Submission

PRECEDING PAGE BLANK NOT FILMED

54  
~~INTENTIONALLY BLANK~~

114  
115  
116  
117  
118  
119  
120  
121  
122  
123  
124  
125  
126  
127  
128  
129  
130  
131  
132  
133  
134  
135  
136  
137  
138  
139  
140  
141  
142  
143  
144  
145  
146  
147  
148  
149  
150  
151  
152  
153  
154  
155  
156  
157  
158  
159  
160  
161  
162  
163  
164  
165  
166  
167  
168  
169  
170  
171  
172  
173  
174  
175  
176  
177  
178  
179  
180  
181  
182  
183  
184  
185  
186  
187  
188  
189  
190  
191  
192  
193  
194  
195  
196  
197  
198  
199  
200  
201  
202  
203  
204  
205  
206  
207  
208  
209  
210  
211  
212  
213  
214  
215  
216  
217  
218  
219  
220  
221  
222  
223  
224  
225  
226  
227  
228  
229  
230  
231  
232  
233  
234  
235  
236  
237  
238  
239  
240  
241  
242  
243  
244  
245  
246  
247  
248  
249  
250  
251  
252  
253  
254  
255  
256  
257  
258  
259  
260  
261  
262  
263  
264  
265  
266  
267  
268  
269  
270  
271  
272  
273  
274  
275  
276  
277  
278  
279  
280  
281  
282  
283  
284  
285  
286  
287  
288  
289  
290  
291  
292  
293  
294  
295  
296  
297  
298  
299  
300  
301  
302  
303  
304  
305  
306  
307  
308  
309  
310  
311  
312  
313  
314  
315  
316  
317  
318  
319  
320  
321  
322  
323  
324  
325  
326  
327  
328  
329  
330  
331  
332  
333  
334  
335  
336  
337  
338  
339  
340  
341  
342  
343  
344  
345  
346  
347  
348  
349  
350  
351  
352  
353  
354  
355  
356  
357  
358  
359  
360  
361  
362  
363  
364  
365  
366  
367  
368  
369  
370  
371  
372  
373  
374  
375  
376  
377  
378  
379  
380  
381  
382  
383  
384  
385  
386  
387  
388  
389  
390  
391  
392  
393  
394  
395  
396  
397  
398  
399  
400  
401  
402  
403  
404  
405  
406  
407  
408  
409  
410  
411  
412  
413  
414  
415  
416  
417  
418  
419  
420  
421  
422  
423  
424  
425  
426  
427  
428  
429  
430  
431  
432  
433  
434  
435  
436  
437  
438  
439  
440  
441  
442  
443  
444  
445  
446  
447  
448  
449  
450  
451  
452  
453  
454  
455  
456  
457  
458  
459  
460  
461  
462  
463  
464  
465  
466  
467  
468  
469  
470  
471  
472  
473  
474  
475  
476  
477  
478  
479  
480  
481  
482  
483  
484  
485  
486  
487  
488  
489  
490  
491  
492  
493  
494  
495  
496  
497  
498  
499  
500  
501  
502  
503  
504  
505  
506  
507  
508  
509  
510  
511  
512  
513  
514  
515  
516  
517  
518  
519  
520  
521  
522  
523  
524  
525  
526  
527  
528  
529  
530  
531  
532  
533  
534  
535  
536  
537  
538  
539  
540  
541  
542  
543  
544  
545  
546  
547  
548  
549  
550  
551  
552  
553  
554  
555  
556  
557  
558  
559  
560  
561  
562  
563  
564  
565  
566  
567  
568  
569  
570  
571  
572  
573  
574  
575  
576  
577  
578  
579  
580  
581  
582  
583  
584  
585  
586  
587  
588  
589  
590  
591  
592  
593  
594  
595  
596  
597  
598  
599  
600  
601  
602  
603  
604  
605  
606  
607  
608  
609  
610  
611  
612  
613  
614  
615  
616  
617  
618  
619  
620  
621  
622  
623  
624  
625  
626  
627  
628  
629  
630  
631  
632  
633  
634  
635  
636  
637  
638  
639  
640  
641  
642  
643  
644  
645  
646  
647  
648  
649  
650  
651  
652  
653  
654  
655  
656  
657  
658  
659  
660  
661  
662  
663  
664  
665  
666  
667  
668  
669  
670  
671  
672  
673  
674  
675  
676  
677  
678  
679  
680  
681  
682  
683  
684  
685  
686  
687  
688  
689  
690  
691  
692  
693  
694  
695  
696  
697  
698  
699  
700  
701  
702  
703  
704  
705  
706  
707  
708  
709  
710  
711  
712  
713  
714  
715  
716  
717  
718  
719  
720  
721  
722  
723  
724  
725  
726  
727  
728  
729  
730  
731  
732  
733  
734  
735  
736  
737  
738  
739  
740  
741  
742  
743  
744  
745  
746  
747  
748  
749  
750  
751  
752  
753  
754  
755  
756  
757  
758  
759  
760  
761  
762  
763  
764  
765  
766  
767  
768  
769  
770  
771  
772  
773  
774  
775  
776  
777  
778  
779  
780  
781  
782  
783  
784  
785  
786  
787  
788  
789  
790  
791  
792  
793  
794  
795  
796  
797  
798  
799  
800  
801  
802  
803  
804  
805  
806  
807  
808  
809  
810  
811  
812  
813  
814  
815  
816  
817  
818  
819  
820  
821  
822  
823  
824  
825  
826  
827  
828  
829  
830  
831  
832  
833  
834  
835  
836  
837  
838  
839  
840  
841  
842  
843  
844  
845  
846  
847  
848  
849  
850  
851  
852  
853  
854  
855  
856  
857  
858  
859  
860  
861  
862  
863  
864  
865  
866  
867  
868  
869  
870  
871  
872  
873  
874  
875  
876  
877  
878  
879  
880  
881  
882  
883  
884  
885  
886  
887  
888  
889  
890  
891  
892  
893  
894  
895  
896  
897  
898  
899  
900  
901  
902  
903  
904  
905  
906  
907  
908  
909  
910  
911  
912  
913  
914  
915  
916  
917  
918  
919  
920  
921  
922  
923  
924  
925  
926  
927  
928  
929  
930  
931  
932  
933  
934  
935  
936  
937  
938  
939  
940  
941  
942  
943  
944  
945  
946  
947  
948  
949  
950  
951  
952  
953  
954  
955  
956  
957  
958  
959  
960  
961  
962  
963  
964  
965  
966  
967  
968  
969  
970  
971  
972  
973  
974  
975  
976  
977  
978  
979  
980  
981  
982  
983  
984  
985  
986  
987  
988  
989  
990  
991  
992  
993  
994  
995  
996  
997  
998  
999  
1000

## Upper Atmosphere Data Base and Model Submission

The Upper Atmosphere Data Program (UADP) at NASA Langley Research Center has been established to serve as a working data base for information on stratospheric trace gases and related parameters. It includes data from both measurements and model calculations. The UADP data base presently includes measurement data from satellite instruments such as Limb Infrared Monitor of the Stratosphere (LIMS), Stratospheric Aerosol Gas Experiment (SAGE2), Stratospheric and Mesospheric Sounder (SAMS), Solar Backscatter Ultraviolet (SBUV), Total Ozone Mapping Spectrometer (TOMS), and Atmospheric Trace Molecule Spectroscopy (ATMOS) and a compilation of stratospheric balloon measurements. The recent focus, however, has been on assembling two-dimensional results from atmospheric model calculations, principally for use in intercomparison activities. The data assembled for the Models and Measurements Workshop are available on CD ROM.\*

The UADP served as the focal point for assembly of data for the Models and Measurements Workshop discussed in this report. A substantial amount of work was required, which involved the handling of data from the various model groups, incorporation of the desired data into the UADP data base, data manipulation to derive sums and ratios, and display of the data in graphical form. The work was done using UADP software on workstations prior to the workshop at Langley and at the workshop itself. Subsequent to the workshop revised data sets were entered in the data base.

The principal area of work in dealing with the model data sets was decoding from the wide variety of formats used by the model groups that submitted data. While some model groups scrupulously followed the standard data format for data transmittal, most did not. Data were submitted on a common grid with each model group being responsible for converting their data to that grid. For the two-dimensional data set addressed here the desired standard intercomparison grid was

Horizontal: 90S to 90N in latitude at increments of 5 degrees

Vertical:  $z^* = 0$  to 60 km in increments of 2 km where  $z^* = 16 \log_{10}$  of  $(1000/P)$  and P is the pressure in mbar.

The data presented represents results from fourteen model groups. The groups are designated by the following abbreviations and the principal investigators are listed:

AER            M. Ko, D. Weisenstein, J. Rodriguez, N.D. Sze  
                  Atmospheric and Environmental Research, Inc.  
                  840 Memorial Dr.  
                  Cambridge, MA 02139

CALJPL        Y.L. Yung  
                  California Institute of Technology  
                  Pasadena, CA 91125

D. Crisp  
Jet Propulsion Laboratory  
4800 Oak Grove Dr.  
Pasadena, CA 91109-8099

---

\* Additional information about the UADP and how to obtain the CD can be obtained from Linda Hunt/Karen Sage; MS 401A; NASA Langley Research Center; Hampton, VA 23681; Telephone 804-864-5856 or 804-864-5857.

CAMED-θ	R. S. Harwood, J. Kinnersley Department of Meteorology University of Edinburgh King's Buildings Mayfield Rd. Edinburgh EH9 3JZ, UK	J. A. Pyle Dept. of Physical Chemistry University of Cambridge Lensfield R. Cambridge CB2 1EP UK
DUPONT	C. Miller, D. Fisher E32/240 DuPont Experimental Station E.I. DuPont De Nemours, Inc. Wilmington, DE 19880-0320	
GISS	M. Prather Dept. of Geosciences University of California, Irvine Irvine, CA 92717	
GSFC	C. H. Jackman, A. R. Douglass Code 916 NASA/Goddard Space Flight Center Greenbelt, MD 20771	
ITALY	G. Pitari, E. Mancini, G. Visconti Dipartimento di Fisica Universita' degli Studi L'Aquila Via Vetoio 67101 Coppito (L'Aquila), Italy	
LLNL (or LLNLND)	D. Wuebbles, P. Connell, K. Grant, D. Kinnison, D. Rotman Atmos. and Geophys. Sciences Div., L-262 P. O. Box 808 Lawrence Livermore National Laboratory 7000 East Ave. Livermore, CA 94550	
MPI	C. Bruhl, P.J. Crutzen Max Planck Institute for Chemistry D-6500 Mainz, Germany	
MRI	T. Sasaki Physical Meteorology Research Institute 1-1 Nagamine Tsukuba, Ibaraki 305, Japan	

NCAR	<p>C. Granier, G. Brasseur, I. Folkins, S. Walters National Center for Atmospheric Research Boulder, CO 80307</p> <p>M. Hitchman University of Wisconsin Madison, WI 53706</p> <p>Anne Smith University of Michigan Ann Arbor, MI</p>
NOCAR	<p>R. Garcia National Center for Atmospheric Research Boulder, CO 80307</p> <p>S. Solomon R/E/AL6 Aeronomy Lab NOAA 325 Broadway Boulder, CO 80303</p>
OSLO	<p>I. Isaksen, F. Stordal Institute of Geophysics University of Oslo P. O. Box 1022 Blindern 0315 Oslo 3, Norway</p>
WASH	<p>K.K. Tung, H. Yang, E.P. Olaguer University of Washington Seattle, WA 98195</p>

Table 1 indicates which model groups participated in each experiment.

**Table 1: Model Data Summary**

	A	B	C	D	E	F	G	H	I	J	K	L	M	N	O
AER	x	x	x	x	x	x	x	x	x	x	x	x	x	x	x
CALJPL	x	x	-	-	x	-	-	-	x	x	x	x	x	-	x
CAMED	x	x	x	x	x	x	x	x	x	x	x	x	-	x	x
DUPONT	x	x	x	x	x	x	x	x	x	-	x	-	-	-	x
GISS	-	-	x	x	x	-	-	-	x	-	x	x	x	-	-
GSFC	x	x	x	x	x	x	x	x	x	x	x	x	x	x	x
ITALY	x	x	x	x	x	x	x	x	x	x	x	x	-	x	x
LLNL	x	x	x	x	x	x	x	x	x	x	x	x	x	x	x
LLNLND	-	-	x	x	x	-	-	-	x	-	-	-	-	-	-
MPI	-	x	x	x	-	-	x	-	x	-	x	-	-	-	-
MRI	-	x	x	x	x	x	x	x	-	-	-	-	-	-	-
NCAR	x	x	x	x	x	x	x	x	x	x	x	x	x	-	x
NOCAR	x	x	-	x	x	x	x	x	-	-	-	-	-	-	x
OSLO	-	-	x	-	-	-	-	-	-	-	-	-	-	-	-
WASH	x	x	x	x	x	x	x	x	x	x	x	x	x	-	x

## **Chapter 4**

### **Update of Model Descriptions**



## AER Two-Dimensional Photochemical Transport Model

Malcolm Ko, Debra Weisenstein, Jose Rodriguez, and N.D. Sze  
Atmospheric and Environmental Research, Inc.

The AER two-dimensional model domain extends from the south pole to the north pole and from approximately the ground to 55 km. Latitude and log-pressure are used as coordinates, with horizontal resolution of 9.5 degrees and vertical resolution of 0.5 in units of  $\ln(1000/p(\text{mb}))$ , equivalent to approximately 3.5 km.

The dynamical transport occurs through the zonal-mean diabatic circulation, by quasi-horizontal diffusion along isentropic surfaces and by vertical diffusion in the troposphere and upper stratosphere. The diabatic circulation used was based on the calculated heating rates of Murgatroyd and Singleton (1961) for the upper stratosphere and Dopplick (1979) for the lower stratosphere, and resembles that derived by Rosenfield et al. (1987) in both structure and magnitude. Temperatures are taken from a climatology obtained from W.-C. Wang (personal communication) and are nearly identical to an 8-year average of National Meteorological Center (NMC) temperatures in the troposphere and middle to lower stratosphere. However, the upper stratosphere in the polar regions is significantly colder than indicated by NMC temperatures.

The horizontal eddy diffusion coefficient,  $K_{yy}$ , is a function of latitude, altitude, and season. Its value is  $1.5 \times 10^{10} \text{ cm}^2 \text{ s}^{-1}$  in the troposphere; in the stratosphere below 25 km it varies from  $3 \times 10^9 \text{ cm}^2 \text{ s}^{-1}$  in the tropics to  $6 \times 10^9 \text{ cm}^2 \text{ s}^{-1}$  in the middle latitudes in winter and  $1 \times 10^{10} \text{ cm}^2 \text{ s}^{-1}$  in the middle latitudes in summer. These values yield a good fit to observed ozone profiles in the lower stratosphere and are close to the magnitudes derived by Newman et al. (1986). The value of  $K_{yy}$  in the stratosphere above 25 km is  $3 \times 10^9 \text{ cm}^2 \text{ s}^{-1}$  for all latitudes and seasons and is based on the work of Kida (1983) and Tung (1984). The calculation of  $K_{yz}$  is based on a translation of the horizontal diffusion, which is assumed to be acting along isentropic surfaces, to the model's log-pressure grid.

The vertical diffusion coefficient,  $K_{zz}$ , is  $1 \times 10^5 \text{ cm}^2 \text{ s}^{-1}$  in the troposphere,  $1 \times 10^3 \text{ cm}^2 \text{ s}^{-1}$  in the stratosphere below 40 km, and  $1 \times 10^4 \text{ cm}^2 \text{ s}^{-1}$  above 40 km. The relatively large vertical diffusion coefficient in the troposphere simulates convective overturning and synoptic scale eddies. Stratospheric vertical diffusion was estimated by Kida (1983) to be  $1 \times 10^3 \text{ cm}^2 \text{ s}^{-1}$ . Enhanced vertical mixing above 40 km is based on Garcia and Solomon's (1985) work in gravity wave breaking. The tropopause height is 100 mb in the tropics and decreases gradually to 450 mb at high latitudes. There is a small latitudinal shift of tropopause heights with season.

The model contains 62 chemical species, including complete diurnal chemistry for the  $\text{NO}_y$ ,  $\text{Cl}_x$ ,  $\text{Br}_x$ ,  $\text{F}_x$ ,  $\text{HO}_x$ ,  $\text{O}_x$ , and methyl and ethyl families. Source gases include  $\text{N}_2\text{O}$ ,  $\text{CH}_4$ ,  $\text{C}_2\text{H}_6$ ,  $\text{H}_2$ ,  $\text{CO}$ ,  $\text{CCl}_4$ , CFC-11, CFC-12, CFC-113, HCFC-22,  $\text{CH}_3\text{Cl}$ ,  $\text{CH}_3\text{CCl}_3$ , Halon-1211, Halon-1301, and  $\text{CH}_3\text{Br}$ . The water vapor concentration is not calculated but is parameterized in the stratosphere based on a fit to the Nimbus-7 observations of Remsberg et al. (1984). Stratospheric water vapor does not vary with season, but does change annually based on the difference between calculated  $\text{CH}_4$  and a 1985  $\text{CH}_4$  profile. The tropospheric values of  $\text{H}_2\text{O}$  vary seasonally depending on the parameterized value of relative humidity and the assigned temperature.

The kinetic reaction rates and absorption cross sections are taken from JPL (1990) except for the reactions between HCFCs, OH, and OH+CH<sub>4</sub> which are taken from JPL (1992). These are the reaction rates specified for the 1991 UNEP assessment. The solar fluxes are from WMO (1982). The spectral resolution is 5 nm over the wavelength range from 170 nm to 405 nm. The solar zenith angle is a function of altitude. The Strobel (1978) parameterization is used for multiple scattering.

Washout and rainout provide removal of H<sub>2</sub>O<sub>2</sub>, CH<sub>3</sub>OOH, CH<sub>2</sub>O, NO<sub>y</sub>, Cl<sub>x</sub>, Br<sub>x</sub>, and F<sub>x</sub> in the troposphere below 10 km with lifetimes of 5 days, 10 days, and 40 days for levels 1, 2, and 3, respectively.

The family chemistry approach is used for the transport of NO<sub>y</sub>, Cl<sub>x</sub>, Br<sub>x</sub>, and O<sub>x</sub>, but HNO<sub>3</sub> is transported separately from other members of the NO<sub>y</sub> family. When the lifetime of HNO<sub>3</sub> becomes short it is solved using chemical equilibrium, and then the total NO<sub>y</sub> family is transported together. Explicit diurnal calculations are performed for the short-lived species every 10 days of model simulation. An iterative Newton scheme is used to solve for all the short-lived species simultaneously, using 12 intervals for the daylight hours and five intervals for the nighttime hours.

Production and loss terms for the long-lived species are updated every 10 days and are calculated as diurnal averages of the product of the rate and the species density over the 17 diurnal time intervals. Lightning is included as a source of NO<sub>y</sub> in the tropical troposphere, with a source strength of 2 MT/yr. Concentrations of long-lived atmospheric species are integrated forward in time using the iterative upstream scheme of Smolarkiewicz (1984). The scheme is positive definite with small implicit diffusion. The advective time step is 12 hours.

## REFERENCES

- Dopplick, T. G., Radiative heating of the global atmosphere: Corrigendum, *J. Atmos. Sci.*, **36**, 1812-1817, 1979.
- Garcia, R. R., and S. Solomon, The effect of breaking gravity waves on the dynamics and chemical composition of the mesosphere and lower thermosphere, *J. Geophys. Res.*, **90**, 3850, 1985.
- Jet Propulsion Laboratory, *Chemical Kinetics and Photochemical Data for Use in Stratospheric Modeling, Evaluation Number 9*, JPL Publication 90-1, NASA/JPL, Pasadena, CA, 1990.
- Jet Propulsion Laboratory, *Chemical Kinetics and Photochemical Data for Use in Stratospheric Modeling, Evaluation No. 10*, JPL Publication 92-20, NASA/JPL, Pasadena, CA, 1992.
- Kida, H. General circulation of air parcels and transport characteristics derived from a hemispheric GCM, Part 1, A determination of advective mass flow in the lower stratosphere, *J. Meteorol. Soc. Japan*, **61**, 171-185, 1983.
- Murgatroyd, R. J., and F. Singleton, Possible meridional circulation in the stratosphere and mesosphere, *Quart. J. Royal Meteor. Soc.*, **87**, 125-135, 1961.

- Newman, P. A., M. R. Schoeberl, and R. A. Plumb, Horizontal mixing coefficients for two-dimensional chemical models calculated from National Meteorological Center data, *J. Geophys. Res.*, *91*, 7919-7924, 1986.
- Remsberg, E. E., J. M. Russell III, L. L. Gordley, J. C. Gille, and P. L. Bailey, Implications of the stratospheric water vapor distribution as determined from the Nimbus-7 LIMS experiment, *J. Atmos. Sci.*, *41*, 2934-2945, 1984.
- Rosenfield, J. E., M. R. Schoeberl, and M. A. Geller, A computation of the stratospheric diabatic residual circulation using an accurate radiative transfer model, *J. Atmos. Sci.*, *44*, 859-876, 1987.
- Smolarkiewicz, P. K. A simple positive definite advection scheme with small implicit diffusion, *Mon. Weather Rev.*, 479-487, 1984.
- Strobel, D. F., Parameterization of the atmospheric heating rate from 15 to 120 km due to O<sub>2</sub> and O<sub>3</sub> absorption of solar radiation, *J. Geophys. Res.*, *83*, 6225-6230, 1978.
- Tung, K. K. Modeling of tracer transport in the middle atmosphere, in Dynamics of the Middle Atmosphere, J. R. Holton and T. Matsuno (eds.), pp. 412-444, Terra Scientific Publishing, Tokyo, Japan, 1984.
- World Meteorological Organization (WMO), *The Stratosphere 1981: Theory and Measurements*, WMO Global Ozone Monitoring Project, Report No. 11, WMO, Geneva 1982.

#### REFERENCES TO AER 2-D MODEL

- Ko, M. K. W., N. D. Sze, M. Livshits, M. B. McElroy, and J. A. Pyle, The seasonal and latitudinal behaviour of trace gases and O<sub>3</sub> as simulated by a two-dimensional model of the atmosphere, *J. Atmos. Sci.*, *41*, 2381-2408, 1984
- Ko, M. K. W., K. K. Tung, D. K. Weisenstein, and N. D. Sze, A zonal mean model of stratospheric tracer transport in isentropic co-ordinates: Numerical simulations for nitrous oxide and nitric acid, *J. Geophys. Res.*, *90*, 2313-2329, 1985
- Ko, M. K. W., M. B. McElroy, D. K. Weisenstein, and N. D. Sze, Lightning: A possible source of stratospheric odd nitrogen, *J. Geophys. Res.*, *91*, 5395-5404, 1986.
- Ko, M. K. W., N. D. Sze, and D. K. Weisenstein, The roles of dynamical and chemical processes in determining the stratospheric concentration of ozone in one-dimensional and two-dimensional models, *J. Geophys. Res.*, *94*, 9889-9896, 1989.
- Ko, M. K. W., N. D. Sze, and D. K. Weisenstein, Use of satellite data to constrain the model-calculated atmospheric lifetime for N<sub>2</sub>O: Implications for other trace gases, *J. Geophys. Res.*, *96*, 7547-7552, 1991.
- Rodriguez, J. M., M. K. W. Ko, and N. D. Sze, Role of heterogeneous conversion of N<sub>2</sub>O<sub>5</sub> on sulfate aerosols in global ozone losses, *Nature*, *352*, 134-137, 1991.

Weisenstein, D. K., M. K. W. Ko, J. M. Rodriguez, and N. D. Sze, Impact of heterogeneous chemistry on model-calculated ozone change due to high speed civil transport aircraft, *Geophys. Res. Lett.*, 1991-1994, 1991.

## CALJPL Two-Dimensional Model

Yuk L. Yung, Mark Allen, Dave Crisp, and Rich Zurek  
Caltech/Jet Propulsion Laboratory

### DOMAIN AND GRID

The model is from pole to pole in 10 degree steps. The y coordinate is  $a*\theta$ , where  $a$  is the planetary radius and  $\theta$  is the latitude angle. The vertical coordinate is  $z = H*\ln(p_0/p)$ , where  $H = 7$  km,  $p_0 = 1000$  mb. There are 40 layers from  $z = 0$  ( $p = 1000$  mb) to  $z = 80$  km ( $p$  about  $1.e-2$  mb).

### TRANSPORT

The transport coefficients consist of the stream function for residual mean circulation and eddy diffusivities,  $K_{yy}$  and  $K_{zz}$ , respectively. Since the model is in modular form these coefficients can either be computed from our radiation code or taken from other sources. Currently we use the coefficients from Yang et al. (1991). The advection algorithm is the Prather method (Prather, 1986; Shia et al., 1990). The time step is 1 day.

### CHEMISTRY

The chemistry is based on the CALJPL one-dimensional model (Froidevaux et al., 1985) with updates according to JPL-90-1 (JPL, 1990). The numerical method for solving chemistry is the implicit Newtonian method developed for the one-dimensional model.  $H_2O$  in the troposphere is set to climatological values and is computed in the stratosphere with the  $CH_4$  source. Rainout of soluble species in the troposphere is included.

### PHOTODISSOCIATION RATE CALCULATION

The altitude-dependent actinic flux used in the photodissociation rate coefficient calculations is the sum of the attenuated, direct solar beam and a diffuse flux. The method used in the radiation field computation is described in Michelangeli (1992).

The attenuation of the direct solar beam is calculated at all zenith angles assuming a spherical atmosphere. For solar zenith angle  $\chi > 90$  degrees, there is a time-varying shadow zone in the lower atmosphere. These computations are carried out for 112 wavelength intervals covering the range 950 Å to 8050 Å. Below 1225 Å the intervals vary in width. There is a 1-Å interval centered at solar Lyman alpha, 1215.7 Å. Between 1225 Å and 4050 Å the intervals are 50-Å wide, and longward of 4050 Å they are 100-Å wide.

The diffuse flux is determined by a 16-stream calculation assuming a plane-parallel atmosphere. The computation is done at 14 zenith angles between 0 and 90 degrees and for 43 wavelengths between 1750 Å and 8000 Å. Since the values of the diffuse flux/direct solar beam ratio vary smoothly, the values for the diffuse flux at any arbitrary combination of zenith angle and wavelength were found by interpolation.

The atmospheric opacity results from molecular absorption by  $O_2$  and  $O_3$ , conservative Rayleigh scattering, and nonconservative scattering at the lower boundary (i.e., surface; reflectivity of 0.3 adopted). The  $O_2$  absorption cross section between 1754 Å and 2058 Å follow the methodology in Allen and Frederick (1982), with a small

adjustment for the new Herzberg continuum cross sections tabulated in WMO (1986). At longer wavelengths the room temperature cross sections of Yoshino et al. (1988) and Ditchburn and Young (1962) are used, the latter to extend to 2500 Å. For these opacity calculations the room temperature cross sections for O<sub>3</sub> (WMO, 1986; JPL, 1987) and Rayleigh scattering (WMO, 1986) are adopted.

Optical depths are calculated by integrating down from the top level to the surface. Species column densities above the top level are calculated from the abundance at the top level and the scale height of the species above the top level (assumed equal to the scale height of the species between the top two levels). For  $\chi > 0$  degrees the distance between levels at which concentrations are specified is calculated by the law of cosines.

The photodissociation rate coefficients are summations over the wavelength of the product of actinic flux and species photodissociation cross sections. All cross sections have been updated in accordance with JPL Publication 90-1 (1990) and references therein; in particular, the given temperature dependencies have been accounted for in the rate coefficient computations. One exception is the long wavelength O<sub>2</sub> cross sections as discussed above. Also, the absorption cross sections for NO vary with altitude following Allen and Frederick (1982).

## REFERENCES

- Allen, M., and J. E. Frederick, Effective photodissociation cross sections for molecular oxygen and nitric oxide in the Schumann-Runge bands, *J. Atmos. Sci.*, 39, 2066-2075, 1982.
- Ditchburn, R. W., and P. A. Young, The absorption of molecular oxygen between 1850 and 2500 Å, *J. Atmos. Terr. Phys.*, 24, 127-139, 1962.
- Froidevaux, L., M. Allen, and Y. L. Yung, A critical analysis of ClO and O<sub>3</sub> in the mid-latitude stratosphere, *J. Geophys. Res.*, 90, 12999-13029, 1985.
- Jet Propulsion Laboratory, Chemical Kinetics and Photochemical Data for Use in Stratospheric Modeling, *JPL Publication 87-91*, JPL, Pasadena, CA, 1987.
- Jet Propulsion Laboratory, Chemical Kinetics and Photochemical Data for Use in Stratospheric Modeling, *JPL Publication 90-1*, JPL, Pasadena, CA, 1990.
- Michelangeli, D. V., M. Allen, Y. L. Yung, R.-L. Shia, D. Crisp, and J. Elusziewicz, Enhancement of atmospheric radiation by an aerosol layer, *J. Geophys. Res.*, 97, 865-874, 1992.
- Prather, M. J., Numerical advection by conservation of second-order moments, *J. Geophys. Res.*, 91, 6671-6681, 1986.
- Shia, R. L., Y. L. Ha, J. S. Wen, and Y. L. Yung, Two-dimensional atmospheric transport and chemistry model: numerical experiments with a new advection algorithm, *J. Geophys. Res.*, 95, 7467-7483, 1990.
- World Meteorological Organization, Atmospheric Ozone 1985, Global Ozone Research and Monitoring Project, Report No. 16, WMO, Geneva, 1986.

- Yang, H., E. Olaguer, and K. K. Tung, Simulation of the present-day atmospheric ozone, odd-nitrogen, chlorine and other species using coupled two-dimensional model in isentropic co-ordinates, *J. Atmos. Sci.*, 48, 442-471, 1991.
- Yoshino, K., A. S.-C. Cheung, J. R. Esmond, W. H. Parkinson, D. E. Freeman, S. L. Guberman, A. Jenouvier, B. Coquart, and M. F. Merienne, Improved absorption cross-sections of oxygen in the wavelength region 205-240 nm of the Herzberg Continuum, *Planet. Space Sci.*, 36, 1469-1475, 1988.

## CAMED-theta Two-Dimensional Model

R.S. Harwood and J. Kinnersley  
University of Edinburgh

J.A. Pyle  
University of Cambridge

### MODEL DOMAIN

Pole-to-pole

Chemistry - 0 to about 60 km; Dynamics - 0 to about 100 km

DY =  $\pi/19$ ; DZ about 3.5 km

Isentropic vertical coordinate used (sigma coordinates in the troposphere)

DT = 4 hours (diurnally averaged) Adams-Bashforth explicit time step

### DYNAMICS

The model solves the momentum, continuity, and thermodynamic equations in isentropic coordinates while maintaining thermal wind balance. The dynamical forcing in the stratosphere is from radiative heating and the eddy flux of PV (Ertel's potential vorticity, which is the isentropic coordinate's equivalent of the EP flux divergence). The heating is calculated from the modeled temperature, ozone, and water vapor fields. The vertical velocity used to advect chemicals is directly proportional to the calculated diabatic heating (since isentropic coordinates are used).

The PV flux is parameterized by modeling the lowest three wave-number components of Ertel's potential vorticity from the tropopause upwards. At the tropopause the eddy Montgomery potential (similar to geopotential in isobaric coordinates) is specified using a year's satellite data. The only tuneable parameter is the rate of dissipation of eddy PV (which is nevertheless constrained by estimates of dissipation of temperature anomalies in the middle stratosphere). The propagation of the planetary waves depends on the modeled  $u$  and  $T$ . The breaking of planetary waves is simulated in a way similar to that of Garcia (1991), and the  $K_{yy}$  resulting from the breaking waves is used to diffuse all tracers and chemicals except ozone. A second  $K_{yy}$  is derived from the PV flux and the meridional gradient of the zonal-mean PV, and this  $K_{yy}$  is used to diffuse ozone. The assumption behind the use of different  $K_{yy}$ s is that ozone anomalies have the same lifetime as PV anomalies, whereas zonal anomalies of tracers and all other chemicals have an infinite lifetime unless the waves are breaking.  $K_{yy}$  should ideally depend on the lifetime of each chemical (chemical eddy theory). In the troposphere the  $K_{yy}$ s of Luther (1973) are used for all chemicals and tracers.

$K_{zz}$  is  $5 \text{ m}^2 \text{ s}^{-1}$  in the troposphere and  $0.3 \text{ m}^2 \text{ s}^{-1}$  in the stratosphere and is used to parameterize the vertical fluxes of chemicals, heat, and momentum.

There is zero flux of chemicals through the 60 km boundary, though locally a flux is allowed – the mixing ratio above the 60 km boundary being chosen so that the downward

flux will balance the upward flux (which is determined from the circulation and mixing ratio below 60 km).

Rayleigh friction is used to parameterize gravity wave drag in the mesosphere. In the troposphere, the radiative cooling is specified while surface heat flux and latent heating is parameterized using a convective-type scheme, which produces the greatest heating in the tropics. The forcing of  $u$  is parameterized as Rayleigh friction. The surface temperature is specified from observations.

A full description of the dynamical formula is in Kinnersley and Harwood (1993).

## PHOTOCHEMISTRY

The following chemicals are modeled (family grouping is indicated by square brackets): [ O, O(1D), O<sub>3</sub> ], [ H, OH, HO<sub>2</sub> ], [ N, NO, NO<sub>2</sub>, NO<sub>3</sub>, ClONO<sub>2</sub> ], [ Cl, ClO, ClONO<sub>2</sub>, Cl<sub>2</sub>O<sub>2</sub>, OClO, HCl, HOCl ], [ Br, BrO, HBr, HOBr, BrONO<sub>2</sub> ], [ CH<sub>4</sub>, CH<sub>3</sub>, CH<sub>3</sub>OOH, CH<sub>3</sub>O<sub>2</sub>, CH<sub>3</sub>O, CH<sub>2</sub>O, HCO ], HNO<sub>4</sub>, HNO<sub>3</sub>, N<sub>2</sub>O<sub>5</sub>, N<sub>2</sub>O, H<sub>2</sub>O<sub>2</sub>, H<sub>2</sub>O, CO, CH<sub>3</sub>Br, CCl<sub>4</sub>, CH<sub>3</sub>Cl, CH<sub>3</sub>CCl<sub>3</sub>, CFCl<sub>3</sub>, CF<sub>2</sub>Cl<sub>2</sub>, CHClF<sub>2</sub>, C<sub>2</sub>Cl<sub>3</sub>F<sub>3</sub>, CBrClF<sub>2</sub>, CBrF<sub>3</sub>.

The model calculates the diurnal average of the family mixing ratios in the following way. First, every 10 days, the daytime average photolysis rates are estimated using a 5-point Gaussian integral over longitude. These photolysis rates are used to partition the families, so a nominal daytime mixing ratio is determined for each member of the family. The 24-hour average rate of change of a family mixing ratio is the weighted sum of a daytime rate and a nighttime rate. The daytime rates are found using the daytime mixing ratios of family members. Most of the nighttime rates are taken to be zero assuming that the following species are negligible at night:- O(1D), O, OH, H, HO<sub>2</sub>, NO, N, CH<sub>3</sub>, CH<sub>3</sub>O, CHO, Cl and ClO. Non-zero nighttime rates come either from rain-out or from reactions involving species that are assumed to have little diurnal variation.

Tropospheric rain-out occurs for HNO<sub>3</sub>, HCl, HBr, HNO<sub>4</sub>, H<sub>2</sub>O<sub>2</sub>, CH<sub>2</sub>O and CH<sub>3</sub>OOH.

Photolysis rates are calculated using the solar flux data from WMO (1986) and the cross sections from DeMore et al. (1990). The O<sub>2</sub> and O<sub>3</sub> cross sections from WMO (1986) are used. The NO<sub>2</sub> cross section is taken from Allen and Frederick (1982).

Photolysis rates take into account the variation with height of the number of daylight hours per day at a certain latitude and the illumination of regions above the surface polar night.

## RADIATION

Heating due to absorption of solar UV radiation is calculated using the O<sub>2</sub>, O<sub>3</sub> and NO<sub>2</sub> cross sections mentioned above. The scheme described in Haigh (1984) is used to calculate the heating due to absorption of solar energy in the near infrared by H<sub>2</sub>O, CO<sub>2</sub>, O<sub>2</sub>, CH<sub>4</sub> and N<sub>2</sub>O. Haigh's scheme for long-wave cooling due to H<sub>2</sub>O, CO<sub>2</sub> and O<sub>3</sub> is also used. The Ramanathan (1976) parameterization of CO<sub>2</sub> and O<sub>3</sub> absorptance is known to overestimate the cooling through its treatment of Doppler broadening. Modeled mixing ratios are used for all the above calculations, which are performed everywhere above the tropopause.

As with photochemistry, the variation of daylight with height and the illumination of regions above the surface polar night are taken into account in the heating rates.

## REFERENCES

- Allen, M. and J. E. Frederick, Effective photodissociation cross-sections for molecular oxygen and nitric oxide in the Schumann-Runge bands, *J. Atmos. Sci.*, **39**, 2066-2075, 1982.
- DeMore, W. B., J. J. Margitan, M. J. Molina, R. T. Watson, D. M. Golden, R. F. Hampson, M. J. Kurylo, C. J. Howard, and A. R. Ravishankara, Chemical kinetics and photochemical data for use in stratospheric modelling, *Evaluation No. 9*, JPL Publication 90-1, Jet Propulsion Laboratory, Pasadena, CA, 1990.
- Garcia, R. R., Parameterization of planetary wave breaking in the middle atmosphere, *J. Atmos. Sci.*, **48**, 1405-1419, 1991.
- Haigh, J. D., Radiative heating in the lower stratosphere and the distribution of ozone in a two-dimensional model, *Quart. J. Royal Met. Soc.*, **110**, 167-185, 1984.
- Kinnersley, J. S. and R.S. Harwood, An isentropic 2D model with an interactive parametrisation of dynamical and chemical planetary wave fluxes, *Quart. J. Royal Met. Soc.*, 1993.
- Luther, M. M., Monthly mean values of eddy diffusion coefficients in the lower stratosphere, AIAA paper 73-498, AIAA/AMS conference, Denver, CO, 1973.
- Ramanathan, V., Radiative transfer within the earth's troposphere and stratosphere: A simplified radiative-convective model, *J. Atmos. Sci.*, **33**, 1330-1346, 1976.
- World Meteorological Organization, Atmospheric ozone: Assessment of our understanding of the processes controlling its present distribution and change, Ozone Research and Monitoring Project, WMO Report 16, 1986.

## DUPONT Two-Dimensional Model

**D. A. Fisher, C. Miller, C. H. Hales,  
R. W. Nopper, Jr., and D. L. Filkin  
Du Pont Experimental Station**

Substantial revisions have been made to the DuPont two-dimensional model since the two-dimensional Intercomparison Workshop in 1988. We have converted to straight latitudinal coordinates (from sine of latitude), and modified the latitudinal resolution to better represent behavior near the poles. We have modernized the parameterization of mean meridional transport by replacing the approximation of Murgatroyd and Singleton (1961) by a state-of-the-art diabatic circulation based on detailed calculation of net heating rates, using contemporary spectral parameters in a random band model of the thermal IR. Magnitudes of the eddy diffusion coefficients in the stratosphere have been substantially reduced to reflect current understanding of stratospheric dynamics. Finally, we have modified our spatial discretization scheme and time integration procedures to effectively deal with the complexities of advection-dominated transport.

### DOMAIN AND RESOLUTION

Latitude range (pole-to-pole):

- 25 grid boxes (7.2 degrees equally spaced latitude resolution)

Altitude range (0-60 km):

- 20 grid boxes (3-km resolution - log pressure)

### CHEMISTRY

Approximately 125 chemical and photochemical reactions.

Approximately 35 active chemical species.

All species transported independently (no families), except:

- O<sub>x</sub> family
- Photochemical equilibrium of N and H

Diurnal Effects:

- "Two-tank" approximation (Miller et al., 1979)
- Seasonally and latitudinally varying tank sizes
- Daytime and nighttime average mixing ratios calculated
- 17 diurnally active shorter-lived species
- Remaining species: 24-hour averages

### PHOTOLYSIS

126 spectral intervals from 175.4 to 735 nm.

Multiple scattering:

- Rayleigh phase function (Miller et al., 1978)

Schumann-Runge:

- Penetration: Nicolet and Peetermans (1980)
- O<sub>2</sub> Photolysis: Nicolet and Peetermans (1980)
- NO Photolysis: Frederick and Hudson (1979)

Daytime averaging of J's: 4-point Gaussian quadrature.

## MEAN TRANSPORT

Based on calculated diabatic circulation, but reduced somewhat below 25 km to better match long-lived chemical tracers such as  $N_2O$ ,  $CH_4$ , and  $O_3$

## NET HEATING RATES

Based on SBUV ozone

Solar UV & visible: analogous to photolysis rate calculations

Solar Near-IR: neglected (thus, results valid in stratosphere only)

Thermal IR:

- Random Band model ( $CO_2$ ,  $O_3$ , and  $H_2O$ )
- 39 spectral intervals
- Band parameters (Kuhn, 1978)
- Curtis-Godson averaging
- Fels (1979) Voigt shape approximation
- Analytic differentiation of flux equation

Latent Heat of Condensation: neglected (thus, results valid in stratosphere only)

## EDDY TRANSPORT

In the current version,  $K_{yy}$  and  $K_{zz}$  do not vary temporally.

	<u>Stratosphere</u>	<u>Troposphere</u>
$K_{yy}$ ( $cm^2 s^{-1}$ )	$3 \times 10^9$	$7.5 \times 10^9$
$K_{zz}$ ( $cm^2 s^{-1}$ )	$1 \times 10^3$	$1 \times 10^5$

## NUMERICAL SOLUTION OF SPECIES TRANSPORT EQUATIONS

Spatial discretization:

- Second-order upwinding in log of mixing ratio for mean transport
- Second-order central differencing for eddy transport
- Diurnal average mixing ratio transported

Temporal integration: time-splitting algorithm

- Backward Euler chemistry time step
- Explicit transport time step

Time step: 1 day maximum

## DATA BASE

- Temperature: NMC 4-year monthly average
- Solar Flux: WMO (1986)
- Cross Sections: WMO (1986) and JPL (1990)
- Water Vapor below 15 km: RH specified vs  $y$  &  $z$
- Rainout of soluble species below 10 km: 5-day lifetime

## REFERENCES

- Fels, S. B., Simple strategies for inclusion of Voigt effects in infrared cooling rate calculations, *Applied Optics*, 18, 2634-2637, 1979.
- Frederick J. E., and R. D. Hudson, Predissociation of nitric oxide in the mesosphere and stratosphere, *J. Atmos. Sci.*, 36, 737-745, 1979.
- Jet Propulsion Laboratory, *Chemical Kinetics and Photochemical Data for Use in Stratospheric Modeling*, JPL Publication 90-1, NASA/JPL, Pasadena, CA, 1990.
- Kuhn, W., The effects of cloud height, thickness, and overlap on tropospheric terrestrial radiation, *J. Geophys. Res.*, 83(C3), 1337-1346, 1978.
- Miller, C., P. Meakin, R. G. E. Franks, and J. P. Jesson, The fluorocarbon-ozone theory -- V. One-dimensional modeling of the atmosphere: The base case, *Atmos. Environ.*, 12, 2481-2500, 1978.
- Miller, C., D. L. Filkin, and J. P. Jesson, The fluorocarbon-ozone theory -- VI. Atmospheric modeling: Calculation of the diurnal steady state, *Atmos. Environ.*, 13, 381-394, 1979.
- Murgatroyd, R. J., and F. Singleton, Possible meridional circulations in the stratosphere and mesosphere, *Quart. J. Roy. Meteor. Soc.*, 87, 125-135, 1961.
- Nicolet M., and W. Peetermans, Atmospheric absorption in the O<sub>2</sub> Schumann-Runge band spectral region and photodissociation in the stratosphere and mesosphere, *Planet. Space Sci.*, 28, 85-103, 1980.
- World Meteorological Organization, *Atmospheric Ozone 1985: Assessment of Our Understanding of the Processes Controlling its Present Distribution and Change*, Global Ozone Research and Monitoring Project Report No. 16, WMO, Geneva, 1986.

## I. GISS Photochemical Model

Michael Prather  
University of California, Irvine

The GISS/UCI/Harvard photochemical model has evolved since 1978 (Logan et al., 1978) from a global one-dimensional vertical diffusion model used in early ozone assessments to a high-resolution box model for use in the three-dimensional chemical parameterizations and other evaluations of stratospheric and tropospheric chemistry (see model references). I have attempted to document the unique features of this model, especially (1) the calculation of Rayleigh scattering, which should be a nearly "exact" solution, and (2) the spherical approximation to the solar extinction, which has been used for a decade in terms of Chapman-like function of the total overhead columns of O<sub>2</sub> and O<sub>3</sub>, but now includes full ray-tracing back to the sun allowing for pressure and temperature dependences of the absorbing molecules.

This paper documents the wavelengths and cross sections, the numerical methods of the chemical package, the monochromatic scattering calculation, and the spherical approximation for solar radiation.

### WAVELENGTHS AND CROSS SECTIONS

The wavelength quadrature in current use is based on the Harvard model (pre-1978), and a summary of the wavelengths, solar fluxes, and major cross sections are given in Table 1. Although every effort is made to ensure equivalence of this wavelength structure with NASA/JPL-90, lack of a standard wavelength quadrature precludes this (probably a good thing too!).

A notable, intentional difference between these calculations and the recommendations occurs for wavelengths less than 200 nm in the Schumann-Runge bands. This difference affects most notably our calculation of photolysis rates for O<sub>2</sub>, NO, CF<sub>2</sub>Cl<sub>2</sub>, and N<sub>2</sub>O. We use the opacity distribution functions for each of the S-R bands developed by Fang et al. (1974). The original formulation (Logan et al., 1978) has been updated to correct for errors in band strengths, and most recently to allow for a linear dependence of the opacity distribution function on local temperature. The cross section per average air molecule for Rayleigh scattering,  $\sigma_{\text{Ray}}$ , is derived from the index of refraction for air at 1 bar, 15°C,

$$n = 1 + 10^{-6} [64.328 + 29498.1/(146 - l^2) + 255.4/(41 - l^2)],$$

$$\sigma_{\text{Ray}} = 5.4 \times 10^{-21} (n-1)^2 l^{-4} \text{ cm}^2 \text{ molecule}^{-1}$$

with  $l$  the wavelength in microns ( $10^{-6}$  m).

### CHEMICAL CONTINUITY EQUATIONS

The chemical kinetics package is a fairly standard implementation of NASA/JPL-90. The model includes a complete CH<sub>4</sub> oxidation scheme, but no higher hydrocarbons. Chlorine and bromine chemistry are included, but no fluorine chemistry. The numerical method of solution is inverse-Euler: a first-order, fully implicit scheme that is solved at a fixed set of grid points (i.e., times) during the day,

$$dn_j / dt |_{t_i} = [n_j(t_i) - n_j(t_{i-1})] / [t_i - t_{i-1}] = [P-L]_j(n(t_i))$$

where  $[P-L]_j$  is the net chemical production of species  $j$  at time  $t_i$ , which depends on the radiation field as well as on the densities of other species at the forward time step. The initial conditions,  $n_j(t_{i-1})$ , are given along with a guess for  $n_j(t_i)$ . This guess is used to evaluate  $[P-L]_j$  and the Jacobian matrix  $\partial[P-L]_j/\partial n_k$ . The guess is iteratively corrected (Newton-Raphson) until the equation is solved to an accuracy of 1 part in  $10^{10}$  or the successive corrections are less than 1 part in  $10^6$ .

The quadrature points used to integrate over 24 hours are given in Table 2 for the examples of high accuracy simulations ( $N = 30$ , used in the M&M work) and coarse temporal resolution ( $N = 15$ , used for quick calculations). The coarse grid is accurate to better than about 3% in terms of average rates. Note that the time steps are chosen to be symmetrical about local solar noon, and thus the photolysis rates calculated for a point in the afternoon can be used also for the conjugate point in the morning. The inverse Euler method leads to an averaging of the time points for a quantity  $J$  (photolysis, reaction rate, density, etc.) in the form

$$\langle J \rangle_{24hr} = \sum_{i=2}^N J_i \Delta t_i / 86400 .$$

A diurnal photochemical steady state is defined here as a repeating 24-hour cycle of species densities, i.e.,  $n_j(t_1) = n_j(t_N)$ , which by definition means that  $\langle [P-L]_j \rangle_{24hr} = 0$ . The solution for this steady state is not trivial; a second level of Newton-Raphson linearization (on top of each daily integration) is used to iterate on the initial species concentrations,  $n_j(t_i)$ , so that the above condition is met to 1 part in  $10^4$ .

## MONOCHROMATIC SCATTERING ATMOSPHERE

The optical properties of a plane-parallel scattering atmosphere are defined completely in terms of extinction optical depth  $t$ , cross sections for absorption  $\sigma^{abs}$  and scattering  $\sigma^{scat}$  (e.g.,  $\text{cm}^2 \text{ molecule}^{-1}$ ), and a scattering phase function  $P$ . By convention  $\tau = 0$  at the top of the atmosphere and  $t = t_N$  at the bottom. For an atmosphere defined in terms of altitude  $z$  (e.g., cm), total number density  $N$  (e.g.,  $\text{molecules cm}^{-3}$ ), and mixing ratio by molecular species  $i$  of  $f_i$ , the optical depth is defined as

$$dt = - \left[ \sum_i (\sigma_i^{abs} + \sigma_i^{scat}) f_i(z) \right] N(z) dz = - \left[ \sum_i \sigma_i^{ext} f_i(z) \right] N(z) dz$$

and the single scattering albedo, a local quantity, as

$$\bar{\omega}(z) = \frac{\sum_i \sigma_i^{scat} f_i(z)}{\sum_i (\sigma_i^{abs} + \sigma_i^{scat}) f_i(z)} .$$

The  $\sigma$  can also be functions of the local conditions such as temperature and pressure. The phase function must be similarly weighted if different types of scattering occur within the atmosphere (e.g., isotropic, Rayleigh, Mie).

The equation of radiative transfer for a plane-parallel, scattering atmosphere with an incident flux of 1 photon  $\text{cm}^{-2} \text{s}^{-1}$  at zenith angle of  $\cos^{-1}(-\mu_0)$  with azimuth angle  $\phi_0$  is

$$\mu \frac{dI}{dt}(t, \mu, \phi) = I(t, \mu, \phi) - \frac{\bar{\omega}(t)}{4\pi} \int_{-1}^{+1} d\mu' \int_0^{2\pi} d\phi' P(t, \mu, \phi; \mu', \phi') I(t, \mu', \phi') - \frac{\bar{\omega}(t)}{4\pi} P(t, \mu, \phi; -\mu_0, \phi_0) e^{-t/\mu_0}$$

where  $I$  is the specific intensity (photons  $\text{cm}^{-2} \text{s}^{-1} \text{steradian}^{-1}$ ),  $\mu$  is the cosine angle relative to the zenith (+1 pointing upward), and  $\phi$  is the azimuthal angle relative to the sun at  $\phi_0$ . Both the single scattering albedo  $\bar{\omega}$  and the scattering phase function ( $P$ ) may vary throughout the atmosphere as functions of  $t$ .

Photolysis rates are proportional to the mean intensity,  $\langle I \rangle$ , which can be derived from the average specific intensity and the incident solar beam when the upper boundary condition does not explicitly include the solar term,

$$\langle I(t) \rangle = 4\pi \bar{I}(t) + e^{-t/\mu_0}$$

The mean intensity  $\bar{I}$  can be derived from the zeroth-order moment of the specific intensity expanded in terms of the azimuthal angle according to Chandrasekhar (1960),

$$\bar{I}(t) = \frac{1}{4\pi} \int_{-1}^{+1} d\mu \int_0^{2\pi} d\phi I(t, \mu, \phi) = \frac{1}{2} \int_{-1}^{+1} d\mu I^0(t, \mu)$$

where

$$I(t, \mu, \phi) = \sum_{m=0}^{\infty} I^m(t, \mu) \cos[m(\phi - \phi_0)]$$

$$P(t, \mu, \phi; \mu', \phi') = \sum_{m=0}^{\infty} P^m(t, \mu; \mu') \cos[m(\phi - \phi')] .$$

The specific intensity should be treated as a vector including the four Stokes parameters (i.e.,  $I, Q, U, V$ , see Chandrasekhar, 1960) which describe the intensity, polarization, plane of polarization, and ellipticity of the light field. Similarly, the scattering phase function  $P$  is a matrix coupling the Stokes parameters (e.g., Chandrasekhar, 1960, pp. 35ff; Prather, 1974). However, we adopt a Rayleigh phase function,  $3/4 (1 + \cos^2 \Theta)$ , effectively assuming that all light, including scattered, is natural. [N.B. Depolarization by air would change this phase function to  $3/4 (1.02 + 0.94 \cos^2 \Theta)$ , but is not included here.] In our coordinate system the scattering angle  $\Theta$  is decomposed as

$$\cos \Theta = \mu\mu' + (1-\mu^2)^{1/2}(1-\mu'^2)^{1/2} \cos(\phi - \phi') .$$

The zeroth-order Rayleigh phase function is then

$$P^0(\mu; \mu') = \frac{3}{8} [3 - \mu^2 - \mu'^2 + 3\mu^2 \mu'^2]$$

and the equation of radiative transfer for the zeroth moment  $I^0$  is now expressed as,

$$\mu \frac{dI^0}{dt}(t, \mu) = I^0(t, \mu) - \frac{\bar{\omega}(t)}{2} \int_{-1}^{+1} d\mu' P^0(\mu; \mu') I(t, \mu') - \frac{\bar{\omega}(t)}{4\pi} P^0(\mu; \mu_0) e^{-t/\mu_0}$$

where we assume that all scattering throughout the atmosphere is Rayleigh phase and hence  $P^0$  is independent of  $t$ .

In general, we note that the scattering phase function can be broken into even and odd components,  $P^0 = P^{even} + P^{odd}$ , such that

$$P^{even}(\mu, \mu') = P^{even}(-\mu, \mu') = P^{even}(\mu, -\mu') = P^{even}(-\mu, -\mu')$$

$$P^{odd}(\mu, \mu') = -P^{odd}(-\mu, \mu') = -P^{odd}(\mu, -\mu') = +P^{odd}(-\mu, -\mu')$$

It is useful to reformulate the equation of radiative transfer by defining

$$J(t, \mu) \equiv \frac{1}{2} [I^0(t, +\mu) + I^0(t, -\mu)]$$

$$h(t, \mu) \equiv \frac{1}{2} [I^0(t, +\mu) - I^0(t, -\mu)] \text{ for } 0 \leq \mu \leq 1.$$

The equation for  $I^0$  can be split into even and odd terms

$$\mu \frac{dj}{dt}(t, \mu) = h(t, \mu) - \bar{\omega}(t) \int_0^{+1} d\mu' P^{odd}(\mu; \mu') h(t, \mu') + \frac{\bar{\omega}(t)}{4\pi} P^{odd}(\mu; \mu_0) e^{-t/\mu_0}$$

$$\mu \frac{dh}{dt}(t, \mu) = j(t, \mu) - \bar{\omega}(t) \int_0^{+1} d\mu' P^{even}(\mu; \mu') j(t, \mu') - \frac{\bar{\omega}(t)}{4\pi} P^{even}(\mu; \mu_0) e^{-t/\mu_0}.$$

The integration over angle  $\mu$  is approximated by a set of Gaussian quadrature points and weights over the interval  $[0, 1]$ . In general, we would need  $M$  Gauss points to represent accurately the scattering phase function expressed as a polynomial of order  $2M-1$ , but for Rayleigh phase (second-order polynomial) we choose  $M = 3$ :

$$\mu_i = \{0.1127016654, 0.5000000000, 0.8872983346\}$$

and weights

$$a_i = \{0.2777777778, 0.4444444444, 0.2777777778\}.$$

The integro-differential equations above become coupled differential equations for  $I(t, \mu_k)$ , and the integrals are replaced by sums, e.g.,

$$\int_0^{+1} d\mu I(t, \mu) = \sum_{k=1}^M I(t, \mu_k) a_k .$$

At each level  $t$  the scattering couples all angles. This form of coupled first-order equations is solved in the general scattering case (i.e., Mie) by a coupled finite difference formulation (i.e., spatial leap frog) with  $j(t_i, \mu_k)$  and  $dh/dt$  being defined at odd points along the  $t$ -grid and  $h(t_i, \mu)$  and  $dj/dt$ , at even grid points (*see* Jacob et al., 1989).

Because the Rayleigh scattering phase function is even in  $\mu$ ,  $P^0 = P^{\text{even}}$ , we can combine the two first-order differential equations for  $j(t, \mu)$  and  $h(t, \mu)$  into one second-order differential equation for  $j(t, \mu)$

$$\mu^2 \frac{d^2 j}{dt^2}(t, \mu) = j(t, \mu) - \bar{\omega}(t) \int_0^{+1} d\mu' P^0(\mu; \mu') j(t, \mu') - \frac{\bar{\omega}(t)}{4\pi} P^0(\mu; -\mu_0) e^{-t/\mu_0}$$

where

$$j(t, \mu) \equiv \frac{1}{2} [I^0(t, +\mu) + I^0(t, -\mu)] \text{ for } 0 \leq \mu \leq 1 .$$

The upper boundary condition assumes no incident light except for the solar beam,

$$\mu \frac{dj}{dt} \Big|_{t=0} = j(t=0, \mu)$$

and the lower boundary condition assumes that a fraction of the incident flux is reflected isotropically (i.e., Lambert surface with reflectivity  $L$ ),

$$\mu \frac{dj}{dt} \Big|_{t=t_N} = \frac{1}{2} I^+ - j(t=t_N, \mu)$$

where the reflected intensity  $I^+$  is

$$I^+ = \frac{L}{L+1} [\mu_0 e^{-t/\mu_0} + 4\pi \int_0^1 j(t=t_N, \mu) \mu d\mu] .$$

Once reduced to a single second-order differential equation, we can solve it as a second-order finite difference equation for each  $j(t_i, \mu_k)$ ; we no longer solve for  $h(t, \mu)$ . At each level  $t_i$  there is an  $M \times M$  matrix equation relating  $j(t_{i-1}, \mu_k)$ ,  $j(t_i, \mu_k)$ , and  $j(t_{i+1}, \mu_k)$ , for  $k = 1$  to  $M$ . This set of equations plus the two boundary conditions define a block tridiagonal system of  $N \times M$  variables. The solution (P. Feautrier, 1964) is exact, non-iterative and computational costs scale as  $NM^3$ .

## SPHERICAL SOLAR RAY PATH

The path from a given altitude  $z_k$  (defined relative to the surface radius  $R$ ) back to the sun is computed in a spherical atmosphere, but without any refraction or bending of the path. *[N.B. The index  $k$  is used here to denote a standard level in the atmosphere rather than an angle quadrature point as in the previous section!]* Let  $\mu_0(k) > 0$  be the cosine of the solar zenith angle at level  $k$ , then the cosine of the solar zenith angle at the next level  $k+1$  is given by

$$(1 - \mu_0^2(k))(R + z_k)^2 = (1 - \mu_0^2(k+1))(R + z_{k+1})^2,$$

and the path length between the two levels is

$$x_{k \rightarrow k+1} = (R + z_{k+1})\mu_0(k+1) - (R + z_k)\mu_0(k).$$

This path is apportioned equally to levels  $k$  and  $k+1$ , and thus each standard level  $j > k$  has a length (i.e., weight) associated with it that is a function of the geometry and the cosine of the solar zenith angle at level  $k$  (i.e., time of day).

$$Z_j^k = 1/2 (x_{j \rightarrow j+1} + x_{j \rightarrow j+1}) \quad j > k$$

$$Z_k^k = 1/2 x_{k \rightarrow k+1},$$

while at the uppermost point  $L$ ,

$$Z_L^k = 1/2 x_{L-1 \rightarrow L} + H/\mu_0(L)$$

where  $H$  is the scale height of absorber at the top of the atmosphere (assumed to be 5 km here) and  $\mu_0(L)$  is the cosine of the solar zenith angle at level  $L$  for the ray traced from level  $k$  with cosine angle  $\mu_0(k)$ .

These path lengths define the extinction of the solar beam along a spherical ray path back to the sun and allow for the cross sections to vary as a function of the local temperature  $T$  and density  $N$ . The solar term in the equations above is replaced,

$$\exp[-t_k/\mu_0] \Rightarrow \exp[-\sum_{j=k}^L Z_j^k N(z_j) [\sum_i \sigma_i^{\text{ext}}(N_j, T_j) f_i(z_j)]]$$

and the local solar angle,  $\mu_0(k)$ , is used in the phase function,  $P^0(\mu, -\mu_0(k))$ , for the scattering source term at level  $k$ .

For solar zenith angles greater than  $90^\circ$  [ $\mu_0(k) < 0$ ], this formulation is extended to levels below  $k$  by integrating the path from  $z_k$  to the terminator altitude  $z_t$ , defined where  $\mu_0(t) = 0$

$$z_t = (1 - \mu_0^2(k))^{1/2}(R + z_k) - R$$

and doubling these weights (i.e., folding the path about the terminator where  $\text{SZ} = 90^\circ$ ). We stop all photolysis when local solar zenith angles exceed  $97^\circ$ , corresponding to altitudes 46 km and below being in shadow.

**Table 1. Wavelengths, Solar Fluxes, and Selected Cross Sections**

#	Wavelength (nm)		Cross Sections ( $10^{-21}$ cm <sup>2</sup> molec <sup>-1</sup> )				O(1D) 230K	Yield 300K
			Solar Flux phot cm <sup>-2</sup> s <sup>-1</sup>	O <sub>2</sub>	O <sub>3</sub>			
	mid	interval			230K	%/100K		
1	122		5.60E+11	10.0				
2	170	168 - 173	3.92E+11	880.0	835	0	0.9	0.9
3	175	173 - 178	5.89E+11	270.0	808	0	0.9	0.9
4	180	178 - 183	8.18E+11	S-R	773	0	0.9	0.9
5	185	183 - 188	1.00E+12	S-R	660	0	0.9	0.9
6	190	188 - 193	1.61E+12	S-R	516	0	0.9	0.9
7	195	193 - 198	2.42E+12	S-R	388	0	0.9	0.9
8	200	198 - 203	3.52E+12	S-R	322	0	0.9	0.9
9	205	203 - 208	5.22E+12	0.00750	370	0	0.9	0.9
10	210	208 - 213	1.18E+13	0.00700	586	0	0.9	0.9
11	215	213 - 218	1.81E+13	0.00570	1050	0	0.9	0.9
12	220	218 - 223	2.41E+13	0.00440	1820	0	0.9	0.9
13	225	223 - 228	2.86E+13	0.00350	2970	0	0.9	0.9
14	230	228 - 233	2.81E+13	0.00260	4430	0	0.9	0.9
15	235	233 - 238	2.70E+13	0.00140	6250	0	0.9	0.9
16	240	238 - 243	2.93E+13	0.00090	8150	0	0.9	0.9
17	245	243 - 248	3.43E+13	0.00060	9810	0	0.9	0.9
18	250	248 - 253	3.10E+13	0.00025	11100	0	0.9	0.9
19	255	253 - 256	3.24E+13	0.00010	11400	0	0.9	0.9
20	258	256 - 260	5.43E+13		11300	0	0.9	0.9
21	263	260 - 265	9.64E+13		10300	0	0.9	0.9
22	268	265 - 270	1.62E+14		8760	+0	0.9	0.9
23	273	270 - 275	1.47E+14		6720	+1	0.9	0.9
24	278	275 - 280	1.23E+14		4850	+2	0.9	0.9
25	283	280 - 285	1.61E+14		3000	+4	0.9	0.9
26	288	285 - 290	2.50E+14		1820	+6	0.9	0.9
27	293	290 - 295	4.09E+14		971	+9	0.9	0.9
28	298	295 - 300	3.78E+14		515	+13	0.900	0.900
29	303	300 - 305	3.95E+14		251	+17	0.890	0.900
30	308	305 - 310	4.80E+14		126	+22	0.580	0.760
31	313	310 - 315	5.30E+14		61.8	+27	0.070	0.300
32	318	315 - 320	5.68E+14		31.7	+33	0.000	0.035
33	323	320 - 325	6.44E+14		14.9	+40	0.000	0.000
34	328	325 - 330	7.55E+14		7.07	+47	0.0	0.0
35	333	330 - 335	7.98E+14		3.44	+54		
36	338	335 - 340	8.08E+14		1.41	+63		
37	343	340 - 345	8.24E+14		0.61	+72		
38	348	345 - 350	8.34E+14		0.275	+81		
39	353	350 - 355	8.85E+14		0.112	+92		
40	358	355 - 360	8.78E+14					
41	363	360 - 365	9.39E+14					
42	368	365 - 370	1.07E+15					
43	373	370 - 375	1.04E+15					
44	378	375 - 380	1.05E+15					
45	383	380 - 385	1.01E+15					
46	388	385 - 390	1.01E+15					
47	393	390 - 395	1.03E+15					
48	398	395 - 400	1.30E+15					
49	403	400 - 405	1.69E+15					
50	600:	Integrated O <sub>3</sub> photolysis over Chappuis band = 3.44E-4 s <sup>-1</sup>						

**Table 1 (continued) Wavelengths, Solar Fluxes, and Selected Cross Sections**

Schumann-Runge Bands band	interval (nm)	Cross Sections ( $10^{-21}$ cm <sup>2</sup> molec <sup>-1</sup> ) by %-ile at 190 K					
		0-5%	5-25%	25-50%	50-75%	75-95%	95-100%
(14,0)	177.5 - 178.3	4.330	4.880	6.630	16.000	71.800	1260.00
(13,0)	178.3 - 179.3	2.100	2.320	3.020	6.300	34.500	631.00
(12,0)	179.3 - 180.4	0.5950	0.9750	2.530	7.570	73.500	713.00
(11,0)	180.4 - 181.6	0.3330	1.0200	4.090	16.200	87.700	373.00
(10,0)#	181.6 - 183.1	0.5000	0.5000	2.000	5.000	60.000	900.00
(9,0)	183.1 - 184.6	0.3500	0.4020	0.6660	2.210	17.100	234.00
(8,0)	184.6 - 186.3	0.0835	0.1280	0.4800	2.380	17.000	114.00
(7,0)	186.3 - 188.2	0.0367	0.0481	0.1350	1.180	12.100	78.000
(6,0)	188.2 - 190.2	0.0208	0.0255	0.0506	0.2720	1.820	18.100
(5,0)##	190.2 - 192.5	0.0164	0.0186	0.0326	0.1660	1.630	14.100
(4,0)	192.5 - 194.7	0.0150	0.0157	0.0198	0.0616	0.5780	3.990
(3,0)	194.7 - 197.2	0.0100	0.0100	0.0103	0.0161	0.1090	1.410
(2,0)	197.2 - 198.5	0.0090	0.0091	0.0091	0.0147	0.0463	0.4350
(1,0)	198.5 - 200.0	0.0080	0.0080	0.0080	0.0080	0.0080	0.0204
(0,0)	200.0 - 202.5	0.0080	0.0080	0.0080	0.0080	0.0080	0.0159

Schumann-Runge Bands band	interval (nm)	Cross Sections ( $10^{-21}$ cm <sup>2</sup> molec <sup>-1</sup> ) by %-ile at 270 K					
		0-5%	5-25%	25-50%	50-75%	75-95%	95-100%
(14,0)	177.5 - 178.3	5.780	7.160	10.300	25.100	97.900	1250.00
(13,0)	178.3 - 179.3	2.860	3.260	4.320	9.100	47.100	676.00
(12,0)	179.3 - 180.4	1.190	1.800	3.750	9.340	85.400	653.00
(11,0)	180.4 - 181.6	0.651	1.970	6.750	21.800	97.300	326.00
(10,0)#	181.6 - 183.1	0.6500	0.6500	3.000	8.000	60.000	900.00
(9,0)	183.1 - 184.6	0.3900	0.4900	0.9490	3.330	21.300	219.00
(8,0)	184.6 - 186.3	0.1290	0.2180	0.8280	3.460	19.300	103.00
(7,0)	186.3 - 188.2	0.0626	0.0780	0.2620	1.830	12.500	67.300
(6,0)	188.2 - 190.2	0.0274	0.0358	0.0864	0.4030	2.130	17.400
(5,0)##	190.2 - 192.5	0.0195	0.0244	0.0489	0.2870	1.950	12.700
(4,0)	192.5 - 194.7	0.0150	0.0177	0.0292	0.1030	0.6860	3.550
(3,0)	194.7 - 197.2	0.0100	0.0101	0.0111	0.0215	0.1390	1.360
(2,0)	197.2 - 198.5	0.0090	0.0091	0.0096	0.0154	0.0490	0.4840
(1,0)	198.5 - 200.0	0.0080	0.0080	0.0080	0.0080	0.0080	0.0285
(0,0)	200.0 - 202.5	0.0080	0.0080	0.0080	0.0080	0.0080	0.0182

# NO delta-(1,0) dissociation: effective cross section = 1.31E-17

## NO delta-(0,0) dissociation: effective cross section = 3.50E-18

**Table 1 (continued) Wavelengths, Solar Fluxes, and Selected Cross Sections**

		Cross Sections ( $10^{-21}$ cm <sup>2</sup> molec <sup>-1</sup> )									
#	wave	N <sub>2</sub> O	NO <sub>2</sub>	N <sub>2</sub> O <sub>5</sub>	HNO <sub>3</sub>	ClONO <sub>2</sub>	Cl <sub>2</sub> O <sub>2</sub>	CF <sub>2</sub> Cl <sub>2</sub>	CFCl <sub>3</sub>	CCl <sub>4</sub>	CH <sub>3</sub> CCl <sub>3</sub>
1	122	2600	7500								
2	170	70	15000								
3	175	119	11000								
4	180	135	6300								
5	185	128	260								
6	190	99	293	10000	15600	5550		1240	3160	10000	3800
7	195	62	242	10000	11500	3580		1770	3130	10000	3940
8	200	31.8	250	9200	6600	2930		1730	3080	7720	3780
9	205	13.6	375	8200	2930	2930		1200	2460	3870	2650
10	210	4.9	385	5600	1050	3300		553	1780	144	1920
11	215	1.51	402	3700	356	3620		205	1070	730	1300
12	220	0.43	396	2200	151	3480	1800	62.0	600	648	810
13	225	0.116	324	1440	86.7	2820	2000	18.0	300	580	440
14	230	0.0324	243	990	56.5	2060	3400	4.41	119	466	210
15	235	0.0101	148	770	37.2	1410	4600	1.23	42.0	303	80.0
16	240	.00376	67	620	25.7	985	5800	0.300	14.0	170	32.0
17	245	.00170	43.5	520	21.0	706	6200	0.086	4.80	86.0	11.0
18	250	.00094	28.3	400	19.1	526	6000	0.020	1.80	40.7	4.00
19	255	.00063	14.5	320	19.0	398	5600	0.005	0.640	18.8	1.20
20	258	0	16.7	290	18.9	350	5000	0	0.237	7.84	0.36
21	263		19.7	230	17.9	275	4000		0.094	3.72	0
22	268		25.9	180	16.5	210	3100		0.050	1.83	
23	273		35.7	145	14.7	160	2300		0.030	0.660	
24	278		47.8	124	12.2	123	1900		0.022	0.450	
25	283		62.7	90	9.97	90.0	1650		0.012	0.200	
26	288		72.3	64.6	7.30	64.0	1350		0.0077	0.100	
27	293		82.8	44.2	5.10	46.0	1150		0.0055	0	
28	298		102	30.2	3.25	31.0	1050		0		
29	303		139	20.6	1.93	22.0	925				
30	308		172	14.1	1.08	15.5	775				
31	313		200	9.60	0.560	10.8	625				
32	318		232	6.60	0.220	7.60	475				
33	323		254	4.50	0.080	5.50	370				
34	328		278	3.10	0.035	4.10	310				
35	333		309	2.10	0.010	3.20	250				
36	338		339	1.44	0	2.60	190				
37	343		361	0.980		2.30	128				
38	348		363	0.670		2.00	111				
39	353		412	0.460		1.90	94				
40	358		441	0.314		1.75	77				
41	363		481	0.214		1.62	60				
42	368		526	0.146		1.48	52				
43	373		506	0.100		1.35	44				
44	378		544	0.068		1.20	36				
45	383		575	0.047		1.05	27				
46	388		560	0		0.94	25				
47	393		549			0.80	22				
48	398		510			0.63	19				
49	403		550*			2.60*	44*				

\* Adjusted for cross section beyond 400 nm

**Table 2. Solar Zenith Angle and Time Steps for 30N, +15° Solar Declination**

High Resolution			Low Resolution		
j	sec(0=noon)	cos(SZA)	j	sec(0=noon)	cos(SZA)
1	0.	0.966	1	0.	0.966
2	3864.	0.933	2	86400.	0.876
3	7729.	0.837	3	12882.	0.625
4	11593.	0.686	4	19322.	0.267
5	15458.	0.491	5	24475.	-0.044
6	18034.	0.344	6	27051.	-0.194*
7	20611.	0.190	7	30281.	-0.364*
8	22672.	0.064	8	36741.	-0.616*
9	23702.	0.002	9	46430.	-0.684*
10	25248.	-0.090	10	59349.	-0.194*
11	26021.	-0.135*	11	61925.	-0.044
12	27051.	-0.194*	12	67078.	0.267
13	28666.	-0.282*	13	73518.	0.625
14	30281.	-0.364*	14	79959.	0.876
15	36741.	-0.616*	15	86400.	0.966
16	43200.	-0.707*			
17	49659.	-0.616*			
18	56119.	-0.364*			
19	59349.	-0.194*			
20	60379.	-0.135*			
21	61152.	-0.090			
22	62698.	0.002			
23	63728.	0.064			
24	65789.	0.190			
25	68366.	0.344			
26	70942.	0.491			
27	74807.	0.686			
28	78671.	0.837			
29	82536.	0.933			
30	86400.	0.966			

\* The atmosphere is totally dark for cos(SZA) < -0.12.

## II. GISS Three-Dimensional Stratospheric Tracer Model

Michael Prather  
University of California, Irvine

The GISS three-dimensional Stratospheric General Circulation Model has been analyzed as a dynamical model by Rind and co-workers at GISS [see references]. A single year of model winds from the 23-layer version has been archived for use in the Chemical Transport Model (CTM). This annual cycle of winds is repeated, and for steady-state calculations about six sequential model-year simulations are needed. The stratospheric CTM has been applied to meteoric infall, ozone, nitrous oxide, and (for the M&M Workshop)  $^{14}\text{CO}_2$  (see references). A table describing the model is given below. Although the vertical resolution is extremely coarse (and may lead to errors in the GCM), the CTM uses a second-order moments scheme for the tracer, which is numerically accurate and capable of maintaining large ( $\times 10$ ) gradients between adjacent grid boxes.

The ozone calculations for M&M use a linearized chemistry for  $\text{O}_3$  that depends only on the local ozone mixing ratio. A full table of chemical coefficients was calculated, using the photochemical model described here, for 18 latitudes and 12 months at all model levels in the stratosphere (above 200 mb). The photochemical calculations were based on monthly zonal-mean climatologies derived by McPeters & Jackman (private communication). N.B. The  $\text{O}_3$  chemistry does not respond to changes in temperature or overhead column. The  $\text{N}_2\text{O}$  calculations used similar look-up tables for the loss frequency (photolysis and  $\text{O}(1\text{D})$ ) for the 18x12 standard atmospheres. In the M&M simulations,  $^{14}\text{CO}_2$  is treated as a trace gas; the settling velocities needed for the  $^{90}\text{Sr}$  experiment have not yet been implemented.

**Table 1. GISS Three-Dimensional, 21-layer, "8°×10°" Chemical Transport Model**

J=	latitude	L=	pressure
----	S. Pole	----	984*
1		1	
----	-86.1	----	960*
2		2	
----	-78.3	----	929*
3		3	
----	-70.4	----	884*
4		4	
----	-62.6	----	797*
5		5	
----	-54.8	----	664*
6		6	
----	-47.0	----	507*
7		7	
----	-39.1	----	346*
8		8	
----	-31.3	----	203*
9		9	
----	-23.5	----	100.
10		10	
----	-15.7	----	46.4
11		11	
----	-7.8	----	21.5
12		12	
----	Equator	----	10.0
13		13	
----	7.8	----	4.64
14		14	
----	15.7	----	2.16
15		15	
----	23.5	----	1.00
16		16	
----	31.3	----	0.464
17		17	
----	39.1	----	0.216
18		18	
----	47.0	----	0.100
19		19	
----	54.8	----	0.0466
20		20	
----	62.6	----	0.0215
21		21	
----	70.4	----	0.0022
22			
----	78.3		
23			
----	86.1		
24			
----	N. Pole		

LONGITUDE GRID: 10° FROM 175W  
 OPERATOR-SPLIT TIME STEP: 4-HR  
 TRACER: SECOND-ORDER MOMENTS

\* SCALES WITH SURFACE PRESSURE

## REFERENCES

### Chemical Model

- Chandrasekhar, S., Radiative Transfer, Dover, New York, 393, 1960.
- Fang, T., S.C. Wofsy, and A. Dalgarno, Opacity distribution functions and absorption in Schumann-Runge bands of molecular oxygen, *Planet. Space Sci.*, 22, 413, 1974.
- P. Feautrier, Sur la r'esolution num'erique de l'equation de transfert, *Comp. Rend.*, 258, 3189, 1964.
- Jacob, D. J., E. W. Gottlieb, and M. J. Prather, Chemistry of a polluted cloudy boundary layer, *J. Geophys. Res.*, 94, 12975-13002, 1989.
- Logan, J. A., M. J. Prather, S. C. Wofsy and M. B. McElroy, Atmospheric chemistry: response to human influence, *Phil. Trans. Roy. Soc.*, A290, 187-, 1978.
- Logan, J. A., M. J. Prather, S. C. Wofsy, and M. B. McElroy, Tropospheric chemistry: a global perspective, *J. Geophys. Res.*, 86, 7210-, 1981.
- Prather, M. J., Solution of the inhomogeneous Rayleigh scattering atmosphere, *Astrophys. J.* 192, 787, 1974.
- Prather, M. J., M. B. McElroy, S.C. Wofsy and J.A. Logan, Stratospheric chemistry: multiple solutions, *Geophys. Res. Lett.*, 6, 163-164, 1979.
- Prather, M. J., M. B. McElroy, and S. C. Wofsy, Reductions in ozone at high concentrations of stratospheric halogens, *Nature*, 312, 227-231, 1984.
- Prather, M. J. and A. Jaffe, Global impact of the Antarctic ozone hole: chemical propagation, *J. Geophys. Res.*, 95, 3473-3492, 1990.
- Prather, M. J., More rapid polar ozone depletion through reaction of HOCl with HCl on polar stratospheric clouds, *Nature*, 355, 534-537, 1992.
- Spivakovsky, C. M., S. C. Wofsy and M. J. Prather, A numerical method for parameterization of atmospheric photochemistry: computation of tropospheric OH, *J. Geophys. Res.*, 95, 18,433-18,439, 1990.

### Three-Dimensional Stratospheric Tracer Model

- Rind, D., R. Suozzo, N. K. Balachandran, and M. J. Prather, Climate change and the middle atmosphere, part 1, the doubled CO<sub>2</sub> climate, *J. Atmos. Sci.*, 47, 475-494, 1990 (and references therein for history of stratospheric GCM).
- Prather, M. J., Numerical advection by conservation of second-order moments, *J. Geophys. Res.*, 91, 6671-6681, 1986.
- Prather, M., M. McElroy, S. Wofsy, G. Russell, and D. Rind, Chemistry of the global troposphere: fluorocarbons as tracers of air motion, *J. Geophys. Res.*, 92, 6579-6613, 1987.
- Prather, M. J. and J. M. Rodriguez, Antarctic ozone: meteoric control of HNO<sub>3</sub>, *Geophys. Res. Lett.*, 15, 1-4, 1988.

Prather, M., M. M. Garcia, R. Suozzo and D. Rind, Global impact of the Antarctic ozone hole: dynamical dilution with a three-dimensional chemical transport model, *J. Geophys. Res.*, 95, 3449-3471, 1990.

Prather, M. J., M. M. Garcia, A. R. Douglass, C. H. Jackman, M. K. W. Ko and N. D. Sze, The Space Shuttle's impact on the stratosphere, *J. Geophys. Res.*, 95, 18,583-18,590, 1990.

## GSFC Fast Two-Dimensional Model

Charles H. Jackman and Anne R. Douglass  
Goddard Space Flight Center

### GENERAL INFORMATION

The GSFC two-dimensional fixed transport model has a latitude domain from 85S to 85N with 10-degree latitude bands. The original altitude extended from the ground to 0.23 mb (0 to about 60 km) and was described in Douglass et al. (1989) and Jackman et al. (1989). The altitude levels are equally spaced in log pressure and are approximately 2 km apart. Since these data were published certain applications of the model have required a higher upper boundary, and Jackman et al. (1990) describe our extended model which goes from the ground up to 0.0024 mb (0 to about 90 km). Both versions of the model have been and are being used depending on the requirements of the investigation.

Twenty eight species or families are transported in the model (defined below) including  $O_x$ ,  $NO_z$ ,  $Cl_z$ ,  $Br_y$ ,  $HNO_3$ ,  $N_2O_5$ ,  $ClONO_2$ ,  $HCl$ ,  $N_2O$ ,  $CH_4$ ,  $H_2$ ,  $CO$ ,  $CH_3OOH$ ,  $CFCl_3$ ,  $CF_2Cl_2$ ,  $CH_3Cl$ ,  $CCl_4$ ,  $CHClF_2$ ,  $C_2Cl_3F_3$ ,  $C_2Cl_2F_4$ ,  $C_2ClF_5$ ,  $CH_3CCl_3$ ,  $CBrClF_2$ ,  $CBrF_3$ ,  $CH_3Br$ ,  $HF$ ,  $CClFO$ , and  $CF_2O$ .  $H_2O$  is fixed to LIMS measurements and climatology using a scheme described in Jackman et al. (1987). The typical model time step for most simulations is one day; however, the model time step has been reduced to 1.5 hours for some applications involving tracers.

### CHEMICAL REACTION RATES AND PHOTOLYSIS CROSS SECTIONS

There are 103 binary and tertiary gas-phase-only reactions in our model. Most reaction rates are taken from JPL (1990). We do use the reaction rate of  $3.9 \times 10^{-12} \exp(-1885/T)$  for the  $OH + CH_4$  reaction recommended for assessment runs shown in chapter 8 of the latest UNEP report (WMO, 1992).

There are 39 wavelength intervals included in our radiative transfer scheme (Douglass et al., 1989). Multiple scattering (see below) is applied, and 37 photolysis rates are computed every 10 days of model time, primarily using JPL (1990) cross sections. Solar irradiance values at the top of the atmosphere are taken from Table 7-4 of WMO (1986). Cross sections used in the Schumann-Runge band photolysis of  $O_2$  and the delta bands photolysis of  $NO$  are taken from Allen and Frederick (1982). Cross sections used in the Herzberg continuum photolysis for  $O_2$  are taken from Table 7-4 of WMO (1986). Temperature-dependent absorption cross sections for  $C_2F_3Cl_3$ ,  $C_2F_4Cl_2$ , and  $C_2F_5Cl$  are taken from Simon et al. (1988). Temperature-dependent absorption cross sections for  $CFCl_3$ ,  $CF_2ClBr$ , and  $CF_3Br$  come from a communication dated January 30, 1992, with enclosures by M. K. W. Ko (AER, Inc.), which are recommended kinetic data compiled by Stan Sander to be included in the upcoming NASA Report on "Concentrations, Lifetimes, and Trends of Chlorofluorocarbons, Halons, and Related Molecules in the Atmosphere" (in preparation, 1992).

### FAMILY CHEMISTRY

Well-known family chemistry approximations are used to reduce the number of transported species in the model. These approximations presume that dissociations and reactions that produce interchanges among family members are rapid compared with dissociations and reactions that are sources or sinks for the family. The transported families

and included constituents consist of  $O_x$  ( $O_3$ ,  $O(^3P)$ , and  $O(^1D)$ ),  $NO_x$  ( $N$ ,  $NO$ ,  $NO_2$ ,  $NO_3$ ,  $HO_2NO_2$ ),  $Cl_x$  ( $Cl$ ,  $ClO$ , and  $HOCl$ ),  $Br_y$  ( $Br$ ,  $BrO$ ,  $HBr$ , and  $BrONO_2$ ). Other constituents, which are computed from photochemical equilibrium approximations, include  $H$ ,  $OH$ ,  $HO_2$ ,  $H_2O_2$ ,  $CH_2O$ ,  $CH_3$ ,  $CH_3O$ ,  $CH_3O_2$ , and  $CHO$ . Further explanation of this family chemistry approach and our handling of constituents at night is included in Douglass et al. (1989).

## HETEROGENEOUS CHEMISTRY

Two heterogeneous processes are included that are thought to be important reactions on the lower stratospheric sulfate aerosol layer. Reactions  $N_2O_5 [+H_2O \text{ in aerosol}] \rightarrow 2 HNO_3$  (Reaction probability  $G_1 = 0.1$ ) and  $ClONO_2 [+H_2O \text{ in aerosol}] \rightarrow HNO_3 + HOCl$  (Reaction probability  $G_2 = 0.006 \exp[-0.15(T-200)]$ ) are taken from Table 8-8 of WMO (1992) and are included in our heterogeneous model computations. The aerosol surface areas, as functions of month, altitude, and latitude, are also taken from Table 8-8 (WMO, 1992). The baseline (lower limit) aerosol amount is simulated by dividing all surface areas in the table by 4 because of an error when the table was originally formulated. The reaction rates for the two heterogeneous reactions are represented by the relation

$$k_i = 5200 \text{ cm s}^{-1} * G_i * \text{Surface-Area } (/cm),$$

where  $5200 \text{ cm s}^{-1}$  is an effective collision velocity.

Some heterogeneous chemistry effects on our model simulations are discussed in Considine et al. (1992). Current versions of the model do not include a detailed representation of polar stratospheric clouds and the chemical reactions they catalyze.

## MULTIPLE-SCATTERING DESCRIPTION

We have recently improved our multiple-scattering computation (MSC) and now rely on a two-stream formulation that was developed by Richard S. Stolarski (GSFC) for a trajectory model. This MSC relies on a solution method discussed in Chandrasekhar (1960; Eq. [3] on page 56 and Table III on page 62). A system of two linear equations are set up to describe the upward and downward radiances for each grid point. The upward and downward radiances depend on both the direct beam of radiation, attenuated through the use of Beer's law, and the diffuse or scattered contribution. Isotropic scattering is assumed.

The computational methodology is to use the two-stream Gaussian quadrature solution for each level. Analytic solutions for the scattered radiance at the upper and lower boundaries of each level are used to derive a set of algebraic equations. In each grid box we assume that the absorption cross sections for  $O_2$  and  $O_3$  and the Rayleigh cross section are constant throughout the grid box. The Rayleigh cross section is taken from Eq. (4.34) of Brasseur and Solomon (1984). The result for each latitude is a  $2n \times 2n$  matrix, which is inverted to solve for the  $2n$  coefficients of the analytic solutions in the "n" boxes (here "n" is 46, the number of levels in our extended model). The boundary conditions are zero scattered radiance at the upper boundary and an albedo at the lower boundary, which is set to 0.3 for all wavelengths. This new multiple-scattering method is currently being tested more thoroughly.

## CIRCULATION AND DIFFUSION

The approach of Dunkerton (1978) is used, which assumes that a residual mean circulation can be derived from the diabatic heating and temperature field if the zonal mean wind does not change very rapidly. We take our heating rates from two sources: 1) for pressures from 100 mb to the ground, the heating rates of Doplick (1974, 1979) are used; and 2) for pressures above 100 mb, the heating rates of Rosenfield et al. (1987) are used. The temperature field is a 4-year average (1979-1982) of National Meteorological Center (NMC) data (Rosenfield et al., 1987). The advection field is changed monthly with the heating rates and temperature distributions.

The mean vertical velocity wind field is solved using the heating rates and temperatures. The vertical velocity field is adjusted at each pressure level to ensure no net global upward or downward motion across a pressure level. This "conserved" vertical velocity field is used to compute the mean meridional velocity wind field through the continuity equation.

The horizontal diffusion coefficient  $K_{yy}$  is consistent with the residual circulation calculated monthly from the temperature and heating rates mentioned above. The algorithm for this calculation was developed by David B. Considine (NRC Resident Research Associate at GSFC) and Mark R. Schoeberl (GSFC). The meridional and vertical velocities are obtained from the heating rates in Dunkerton (1978), using the thermodynamic and continuity equations with appropriate approximations. The thermal wind equation is used to calculate the zonal mean wind from the temperature field, and this is then used to calculate the meridional potential vorticity gradient, as in Matsuno (1970). We then assume that the only source of momentum in the stratosphere is due to potential vorticity flux and that the flux is proportional to the meridional gradient of potential vorticity (Newman et al., 1988). We can then obtain an equation for  $K_{yy}$  using only quantities derived from the temperature field and heating rates, using the zonal mean momentum equation.

In a few places this procedure results in negative  $K_{yy}$ . We consider these  $K_{yy}$  values to be nonphysical and replace them with a small positive value equal to  $1 \times 10^{+8}$   $\text{cm}^2 \text{s}^{-1}$  to avoid computational difficulties. In the troposphere,  $K_{yy}$  changes with decreasing altitude from the stratospheric value at the tropopause to  $2 \times 10^{+10}$   $\text{cm}^2 \text{s}^{-1}$  at the ground. The off-diagonal diffusion coefficients  $K_{yz}$  and  $K_{zy}$  are calculated using the potential temperature gradient and the  $K_{yy}$  distribution (Jackman et al., 1988).

The vertical diffusion coefficient  $K_{zz}$  values are fixed in the stratosphere at  $2 \times 10^{+3}$   $\text{cm}^2 \text{s}^{-1}$ . In the troposphere  $K_{zz}$  increases with decreasing altitude from the stratospheric value at the tropopause to  $1 \times 10^{+5}$   $\text{cm}^2 \text{s}^{-1}$  at the ground.

## TRANSPORT SCHEME

The transport scheme follows Prather (1986) with appropriate modifications for the coordinate system and for the density variation with height. This scheme conserves the zero-, first-, and second-order moments of the spatial distribution of a tracer during advection, and is accurate and nondiffusive. Our transport scheme is discussed in Douglass et al. (1989).

## PROCESS SPLITTING

The species continuity equations are solved by process splitting; that is, by assuming that the continuity equation may be factored into a product of difference operators (McRae et

al., 1982). First the advection field is applied to the constituent distributions; then both the diffusion and chemistry operators are implemented. This methodology is explained further in Douglass et al. (1989).

## OFF-LINE DIURNAL MODEL

The GSFC two-dimensional model calculates the evolution of transported species using diurnally averaged photochemical production and loss. These quantities are calculated using daytime average values of many radical species, and the usual output of our model simulations are daytime average values for constituents.

Daytime average quantities, in general, are not directly comparable to measurements that may be appropriate for a particular time of day or for sunrise or sunset. We have developed a diurnal mode of calculation which will allow us to calculate the full diurnal cycle for any day of a model run. The long-lived species and families are held fixed. The model is used in an iterative mode until the radical species reach a repeating diurnal cycle.

This off-line diurnal mode model has not been thoroughly tested and is still undergoing development. Its first uses have been to simulate the diurnal cycle for certain fixed atmospheric conditions constrained by ATMOS data as part of this model and measurement intercomparison.

## REFERENCES

- Allen, M., and J. E. Frederick, Effective photodissociation cross sections for molecular oxygen and nitric oxide in the Schumann-Runge bands, *J. Atmos. Sci.*, 39, 2066-2075, 1982.
- Brasseur, G., and S. Solomon, *Aeronomy of the Middle Atmosphere*, D. Reidel, Boston, 1984.
- Chandrasekhar, S., *Radiative Transfer*, Dover Publications, Inc., New York, 1960.
- Considine, D. B., A. R. Douglass, and R. S. Stolarski, Heterogeneous conversion of  $N_2O_5$  to  $HNO_3$  on background stratospheric aerosols: Comparisons of model results with data, *Geophys. Res. Lett.*, 19, 397-400, 1992.
- Dopplick, T. G., The heat budget, in *The General Circulation of the Tropical Atmosphere and Interactions with Extratropical Latitudes*, vol. 2 (R.E. Newell, J.W. Kidson, D.G. Vincent, and C.J. Boer, eds.), pp. 27-94, MIT Press, Cambridge, MA, 1974.
- Dopplick, T. G., Radiative heating of the global atmosphere: Corrigendum, *J. Atmos. Sci.*, 36, 1812-1817, 1979.
- Douglass, A. R., C. H. Jackman, and R. S. Stolarski, Comparison of model results transporting the odd nitrogen family with results transporting separate odd nitrogen species, *J. Geophys. Res.*, 94, 9862-9872, 1989.
- Dunkerton, T., On the mean meridional mass motions of the stratosphere and mesosphere, *J. Atmos. Sci.*, 35, 2325-2333, 1978.
- Jackman, C. H., P. D. Guthrie, and J. A. Kaye, An intercomparison of nitrogen-containing species in Nimbus-7 LIMS and SAMS data, *J. Geophys. Res.*, 92, 995-1008, 1987.

- Jackman, C. H., P. A. Newman, P. D. Guthrie, and M. R. Schoeberl, Effect of computed horizontal diffusion coefficients on two-dimensional N<sub>2</sub>O model distributions, *J. Geophys. Res.*, 93, 5213-5219, 1988.
- Jackman, C. H., R. K. Seals, Jr., and M. J. Prather, *Two-Dimensional Intercomparison of Stratospheric Models*, NASA Conference Publication 3042, NASA, Washington, D.C., 1989.
- Jackman, C. H., A. R. Douglass, R. B. Rood, R. D. McPeters, and P. E. Meade, Effect of solar proton events on the middle atmosphere during the past two solar cycles as computed using a two-dimensional model, *J. Geophys. Res.*, 95, 7417-7428, 1990.
- Jet Propulsion Laboratory, *Chemical Kinetics and Photochemical Data for Use in Stratospheric Modeling*, JPL Publication 90-1, NASA/JPL, Pasadena, CA, 1990.
- Matsuno, T., Vertical propagation of stationary planetary waves in the winter northern hemisphere, *J. Atmos. Sci.*, 27, 871-883, 1970.
- McRae, G. J., W. R. Goodin, and J. H. Seinfeld, Numerical solution of the atmospheric diffusion equation for chemically reacting flows, *J. Comput. Phys.*, 45, 1-42, 1982.
- Newman, P. A., M. R. Schoeberl, R. A. Plumb, and J. Rosenfield, Mixing rates calculated from potential vorticity, *J. Geophys. Res.*, 93, 5221-5240, 1988.
- Prather, M. J., Numerical advection by conservation of second-order moments, *J. Geophys. Res.*, 91, 6671-6681, 1986.
- Rosenfield, J.E., M.R. Schoeberl, and M.A. Geller, A computation of the stratospheric diabatic residual circulation using an accurate radiative transfer model, *J. Atmos. Sci.*, 44, 859-876, 1987.
- Simon, P. C., D. Gillotay, N. Vanlaethem-Meuree, and J. Wisemberg, Temperature dependence of ultraviolet absorption cross-sections of chlorofluoro-ethanes, *Aeronomica Acta*, issn 0065-3713, A - No. 325, Institut D'Aeronomie Spatiale de Belgique, Brussels, 1988.
- World Meteorological Organization, *Atmospheric Ozone, 1985*, Global Ozone Research and Monitoring Project Report No. 16, WMO, Geneva, 1986
- World Meteorological Organization, *Scientific Assessment of Ozone Depletion, 1991*, Global Ozone Research and Monitoring Project Report No. 25, WMO, Geneva, 1992.

## ITALY Two-Dimensional Model

G. Pitari, G. Visconti, and E. Mancini  
Universita' degli Studi L'Aquila

The two-dimensional model developed at the University of L'Aquila (Italy) is a pure transport model: temperature and diabatic circulation are taken offline monthly from the output of a spectral quasi-geostrophic three-dimensional model (Pitari et al., 1992a) where  $O_3$  mixing ratio is predicted along with vorticity and temperature. The advantage of this approach is that the calculated diabatic circulation is consistent with temperature and ozone, which in turn are needed for longwave and solar heating calculation. In particular, longwave heating is a function of the predicted temperature and then a perfect balance is achieved between solar UV and planetary IR heating rates. This means that no corrections have to be made on the calculated diabatic vertical velocity to ensure mass conservation.

Longwave heating calculation is based on the methods given by Ramanathan (1976) for  $O_3$  and  $CO_2$  and by Sasamori (1968) for  $H_2O$ . Solar heating calculation uses the methods of Lacis and Hansen (1974) for  $H_2O$  and Vardavas and Carver (1984) for  $CO_2$ . The  $O_3$  solar heating is calculated in detail starting from absorption coefficients and solar fluxes on small wavelength intervals covering the whole spectrum; a diurnal average is then performed through a Gaussian quadrature on two zenith angles, this providing a 5% accuracy.

The eddy terms for vorticity and vertical velocity are taken from the same output of the three-dimensional model to calculate the eddy diffusion coefficients. The method outlined by Tung (1984) was used, which consisted of an estimate of parcel displacements from the analysis of seasonal time series of  $v'$  and  $w'$ .  $K_{yy}$  shows typical values of  $1-5 \times 10^8 \text{ cm}^2 \text{ s}^{-1}$  in the tropical stratosphere and values of  $3-8 \times 10^9 \text{ cm}^2 \text{ s}^{-1}$  poleward of 30 degrees latitude. Above 1 mbar  $K_{yy}$  increases, reaching values ranging from  $3-5 \times 10^9 \text{ cm}^2 \text{ s}^{-1}$  in the tropics and  $5-10 \times 10^9 \text{ cm}^2 \text{ s}^{-1}$  at middle to high latitudes. The largest values are observed during winter and spring in the northern hemisphere with a peak of  $2 \times 10^{10} \text{ cm}^2 \text{ s}^{-1}$  in the springtime upper stratosphere and lower mesosphere at 60 degrees latitude.  $K_{zz}$  shows very low values in the stratosphere ( $< 5 \times 10^2 \text{ cm}^2 \text{ s}^{-1}$ ) except poleward of 30 degrees latitude in the northern hemisphere winter and spring.  $K_{zz} = 10^5 \text{ cm}^2 \text{ s}^{-1}$  is used in the troposphere and  $K_{zz} = 10^4 \text{ cm}^2 \text{ s}^{-1}$  is adopted above 1 mb to simulate for gravity wave breaking.

The two-dimensional model has a latitudinal resolution of 10 degrees from pole to pole and a vertical resolution of about 2.8 km from the ground to about 71 km altitude (a log-pressure coordinate is adopted). The model chemistry includes  $O_x$ ,  $HO_x$ ,  $NO_y$  and  $Cl_y$  families; water vapor is predicted in the stratosphere and is fixed in the troposphere (but changed seasonally). The following long-lived species are predicted:  $N_2O$ ,  $CH_4$ ,  $CH_3Cl$ ,  $CCl_4$ ,  $CH_3CCl_3$ ,  $CF_{11}$ ,  $CF_{12}$ ,  $CF_{113}$ ,  $CF_{114}$ ,  $CF_{115}$ ,  $CH_2$ . The diurnal cycle is parameterized, but not explicitly calculated. The two-dimensional model has been fully described in Visconti and Pitari (1987), although both the chemistry and transport have been subjected to several important updates. The most important one has been the inclusion of the ozone prediction along with heterogeneous chemistry on both sulfate and polar stratospheric clouds (PSC) aerosols. A description of PSC parameterization can be found in Pitari and Visconti (1991) and Pitari et al. (1992b). Essentially, no attempt is made to model PSC microphysics: a fixed size distribution is imposed for both PSC-1 and PSC-2 and they are assumed to be formed when temperature is low enough that local mixing ratios of  $HNO_3$  and  $H_2O$  are larger than saturation mixing ratios for nitric acid trihydrate and water ice. The temperature dependence of saturation pressures is calculated using the data of

Poole and McCormick (1988). The amount of nitric acid and water vapor exceeding the saturation value is assumed to condense instantaneously, and aerosols are removed through sedimentation. Aerosol evaporation takes place when gas phase  $\text{HNO}_3$  and  $\text{H}_2\text{O}$  mixing ratios are lower than saturation.

Photodissociation coefficients are calculated using a simplified scheme for Rayleigh scattering (Pitari and Visconti, 1979). Essentially, the method adopted is based on the combination of reflectivity and transmission of two layers, one above and one below the height considered, and is inspired by the method developed by Lacis and Hansen (1974). Reflectivity of the bottom layer takes into account both the ground albedo and the atmospheric reflectivity, which is calculated using published data and tables on Rayleigh scattering. Schumann-Runge bands are treated using equivalent mean absorption cross-sections, following the method developed by Park (1974). Solar fluxes are taken from WMO (1986) and cross sections (as well as rates for chemical reactions) from JPL (1990). The diurnal average is obtained by averaging the instantaneous photodissociation coefficients at 10 zenith angles and weighting for the length of the day.

## REFERENCES

- Jet Propulsion Laboratory, *Chemical Kinetics and Photochemical Data for Use in Stratospheric Modeling*, JPL Publication 90-1, NASA/JPL, Pasadena, CA, 1990.
- Lacis, A. A., and J. E. Hansen, A parameterization for the absorption of solar radiation in the Earth's atmosphere, *J. Atmos. Sci.*, 31, 118, 1974.
- Park, J. H., The equivalent mean absorption cross sections for the  $\text{O}_2$  Schumann-Runge bands: Application to the  $\text{H}_2\text{O}$  and  $\text{NO}$  photodissociation rates, *J. Atmos. Sci.*, 31, 1893, 1974.
- Pitari, G., and G. Visconti, A simple method to account for Rayleigh scattering effects on photodissociation rates, *J. Atmos. Sci.*, 36, 1803, 1979.
- Pitari, G., and G. Visconti, Ozone trend in the northern hemisphere: A numerical study, *J. Geophys. Res.*, 96, 10931, 1991.
- Pitari, G., S. Palermi, G. Visconti, and R. Prinn, Ozone response to a  $\text{CO}_2$  doubling: Results from a stratospheric circulation model with heterogeneous chemistry, *J. Geophys. Res.*, 97, 5953-5962, 1992a.
- Pitari, G., G. Visconti, and M. Verdecchia, Global ozone depletion and the antarctic ozone hole, *J. Geophys. Res.*, 97, 8075, 1992b.
- Poole, L. R., and M. P. McCormick, Polar stratospheric clouds and the antarctic ozone hole, *J. Geophys. Res.*, 93, 8423, 1988.
- Ramanathan, V., Radiative transfer within the Earth's troposphere and stratosphere: a simplified radiative convective model, *J. Atmos. Sci.*, 33, 1330, 1976.
- Sasamori, T., The radiative cooling calculation for application to general circulation experiments, *J. Appl. Met.*, 7, 721, 1968.
- Tung, K. K., *Modeling of tracer transport in the middle atmosphere, dynamics of the middle atmosphere*, J. R. Holton and T. Matsuno, eds., Terra Scientific Publishing, pp. 417-444, 1984.

Vardavas, I. M. and J. H. Carver, Solar and terrestrial parameterizations for radiative-convective models, *Planet. Space Sci.*, 32, 1307, 1984.

Visconti, G., and G. Pitari, Seasonal and latitudinal distribution of trace gases in the stratosphere: Results from a 2D residual circulation model, *J. Atmos. Chem.*, 5, 255, 1987.

World Meteorological Organization, *Atmospheric Ozone 1985*, Global Ozone Research and Monitoring Project, Report No. 16, WMO, Geneva, 1986.

## LLNL Two-Dimensional Chemical-Radiative-Transport Model

Don Wuebbles, Peter Connell, Keith Grant,  
Doug Kinnison, and Doug Rotman  
Lawrence Livermore National Laboratory

The LLNL zonally averaged two-dimensional chemical-radiative transport model currently determines the atmospheric distributions of 54 chemically active atmospheric trace constituents in the troposphere and stratosphere. The model domain extends from pole to pole and from ground to 60 km. The sine of latitude is used as the horizontal coordinate, with uneven increments corresponding to approximately 10 degrees in latitude. The vertical coordinate corresponds to the natural logarithm of pressure, with the scale height being 7.2 km and surface pressure as 1013 mb. The vertical resolution is 1.5 km in the troposphere and 3 km in the stratosphere.

### MODEL CHEMISTRY

The photochemistry in the LLNL two-dimensional model represents the tropospheric and stratospheric interactions of actinic solar flux and the species families  $O_x$ ,  $NO_y$ ,  $ClO_y$ ,  $HO_y$ ,  $CH_4$  and its oxidation products, and  $BrO_y$ . The mechanism incorporates 44 transported species and 4 species for which abundance is determined through the assumption of instantaneous equilibrium. The thermal reactions considered number 105; the photolytic reactions considered number 47. Source gases used include  $NO_x$ ,  $N_2O$ ,  $CH_4$ ,  $CO_2$ , and  $CO$ ; the chlorine compounds CFC11, 12, 113, 114, 115, HCFC 22,  $CCl_4$ ,  $CH_3CCl_3$ , and  $CH_3Cl$ , and the bromine compounds  $CH_3Br$ ,  $CF_2ClBr$ , and  $CF_3Br$ . Most of the thermal reaction rates were taken from the NASA Panel recommendations provided in JPL Publication 90-1 (JPL, 1990). However, the rate constant for  $OH + CH_4$  used as part of the United Nations Environmental Program (UNEP) report (WMO, 1992) preparations was used, representing more recent work. Absorption cross section information was assembled from JPL Publication 92-20 (JPL, 1992). Emission boundary conditions were taken from the report, "Scientific Assessment of Ozone Depletion, 1991" (WMO, 1992). Water vapor is dealt with in a unique way compared with the other chemical species: the level of water vapor is assigned its climatological value, following the specific humidity of the Oort climatology, everywhere below the hygropause. Above the hygropause water vapor is calculated like to all other species, the oxidation with methane being its major source.

The photolytic loss rate constants are calculated by integrating the product of the absorption coefficient, quantum yield, and solar flux over wavelength (175 nm to 760 nm). The exoatmospheric solar flux was taken from WMO (1986). The solar flux is then calculated as a function of altitude, latitude, and season at each time step, including the effects of absorption by  $O_2$  and  $O_3$  and multiple molecular (Rayleigh) scattering. The absorption cross sections and quantum yields include temperature and pressure dependence where appropriate and available. The Schumann-Runge band region of the  $O_2$  absorption is modified to match the more recent lower cross sections of the  $O_2$  Herzberg continuum region using the technique of Allen and Frederick (1982). The photolysis of  $NO$  is also treated through the parameterization technique of Allen and Frederick.

The nonlinearity of the photochemistry with respect to diurnal averaging is accounted for through the calculation of altitude, latitude, and seasonally varying factors for each photochemical process. The full diurnal variability of each specie is calculated off line for

four seasons. The factors, relating individual process rates from the full diurnal calculation to the diurnally averaged values, are then spline interpolated for each time step.

Members of the ClO<sub>y</sub> family that are currently thought to play a role in the Antarctic spring are included, such as the ClO dimer, but the polar stratospheric aerosol surface is not currently included. A representation of background stratospheric sulfuric acid aerosol surface is included, following the recommendations from the WMO report (1992). The reactions of N<sub>2</sub>O<sub>5</sub> and ClONO<sub>2</sub> with H<sub>2</sub>O on the aerosol surface are parameterized as first-order loss processes, with rate constants determined by specified surface area density, collision frequency, and reaction probability.

## MODEL TRANSPORT

Currently two forms of the dynamics portion of the two-dimensional code exist. In the first formulation the circulation field is obtained by a diagnostic approach using a known temperature distribution. This temperature field varies continuously over the annual cycle and is based on the reference model of Barnett and Corney (1985). With the known temperature field and a calculated net heating rate (which includes latent heating), the zonally averaged transformed Eulerian mean continuity and the thermodynamic equations form a system of equations with only two unknowns: the horizontal velocity  $v^*$  and the vertical velocity  $w^*$ . The right side of the thermodynamic equation includes only the net heating rate, not any eddy diffusion of energy. Introduction of a streamfunction combines these two equations into a single equation, which is iterated to obtain a circulation field in terms of the streamfunction. The velocity fields,  $v^*$  and  $w^*$ , are then obtained from the streamfunction.

The transport of chemical species is accomplished through both advection and turbulent eddy transport. Advection terms are treated using the second-order, two-dimensional transport algorithm of Smolarkiewicz (1984). The transport caused by large eddies and very small scale motion is parameterized through the diffusion coefficients,  $K_{yy}$  and  $K_{zz}$ . Values of  $K_{yy}$  and  $K_{zz}$  do not vary with annual cycle, but are different within the troposphere and stratosphere. The value of  $K_{yy}$  in all stratospheric altitudes and latitudes is  $2 \times 10^5 \text{ m}^2 \text{ s}^{-1}$  and  $5 \times 10^6 \text{ m}^2 \text{ s}^{-1}$  in all tropospheric altitudes and latitudes. Likewise, the value of  $K_{zz}$  in the troposphere is  $5 \text{ m}^2 \text{ s}^{-1}$ , while  $K_{zz}$  in the stratosphere is based on gravity wave studies and having values of  $0.1 \text{ m}^2 \text{ s}^{-1}$  in the lower stratosphere increasing to  $16 \text{ m}^2 \text{ s}^{-1}$  near the stratopause. The tropopause is treated as an annual mean but latitude dependent function of the temperature field. The height of the tropopause varies from 8 km near the poles to 14 km at the equator.

### New Formulation of Transport

In the second formulation the circulation field is obtained using the approach of Garcia and Solomon (1983). Full implementation of this approach is not complete, therefore, we still use known temperature and zonal mean wind fields. Both the temperature and zonal mean wind field vary continuously over the annual cycle. The temperature field is based on the reference model of Barnett and Corney (1985), whereas the zonal mean wind is based on data from Fleming et al. (1988). The method used to obtain the circulation field is the zonal mean momentum equation and the thermodynamic equation combined into a form that, along with the thermal wind equation, yields a second-order diagnostic equation for the residual mean meridional streamfunction. This streamfunction is defined so that the continuity equation is solved exactly. The coefficients in front of the streamfunction terms on the left side of the equation are functions of known quantities, namely, the coriolis force, zonal mean wind, scale height, temperature field, a global reference altitude-dependent

temperature field, and the Brunt-Vaisala frequency. The model averages the known temperature fields seasonally to provide an altitude-dependent reference temperature field from which an altitude-dependent Brunt-Vaisala frequency is calculated. The right side of the streamfunction equation includes the net heating rate term and the Eliassen-Palm flux representing wave driving. The net heating rate is calculated knowing the temperature and chemical specie distribution and includes latent heating. The present code does not include a separate planetary or gravity wave calculation, but instead calculates the Eliassen-Palm flux directly from the zonal mean momentum equation. This is done by simply calculating the left side of the zonal mean momentum equation using the known zonal mean wind field and approximate values of  $v^*$  and  $w^*$ , which were obtained from a diagnostic interaction between the continuity and thermodynamic equations with a known temperature field. The right-hand side also includes a very small value of Rayleigh friction (about  $0.1 \text{ day}^{-1}$ ) to account for small-scale disturbances. With all terms known, the second-order equation for the streamfunction is evaluated and then used to obtain the velocity fields.

The transport of chemical species is accomplished through both advection and turbulent eddy transport. Advection terms are treated using the second-order, two-dimensional transport algorithm of Smolarkiewicz (1984). The transport caused by eddy motion is parameterized through the diffusion coefficients,  $K_{yy}$  and  $K_{zz}$ . Values of  $K_{zz}$  do not vary with annual cycle, but are different within the troposphere and stratosphere. The value of  $K_{zz}$  in the troposphere is  $4 \text{ m}^2 \text{ s}^{-1}$ , while  $K_{zz}$  in the stratosphere has values of  $0.1 \text{ m}^2 \text{ s}^{-1}$  in the lower stratosphere increasing to  $0.25 \text{ m}^2 \text{ s}^{-1}$  near the middle stratosphere and returning to  $0.1 \text{ m}^2 \text{ s}^{-1}$  at the stratopause. Values of  $K_{yy}$  in the stratosphere are calculated using a similar method to that of Newman et al. (1988) by dividing the zonal mean momentum equation (i.e., the Eliassen-Palm flux) by the horizontal gradient of the quasigeostrophic potential vorticity. In the stratosphere, a minimum value of  $K_{yy}$  has been established as  $1 \times 10^5 \text{ m}^2 \text{ s}^{-1}$ . The values of  $K_{yy}$  in the troposphere are assigned a value of  $1 \times 10^6 \text{ m}^2 \text{ s}^{-1}$ . The tropopause is treated as an annual mean but latitude dependent function of the temperature field. The height of the tropopause varies from 8 km near the poles to 14 km at the equator.

## **Radiative Transfer Models**

### ***Solar Model***

To capture the spectral detail needed for photodissociation calculations, our two-stream, multiple-layer, UV-visible model uses 126 wavelength bins between 175 nm and 735 nm. The two-stream approach was chosen because of the computational efficiency requirements placed on radiative transfer models designed for inclusion in atmospheric chemistry models. In this approach, solar radiation is effectively divided into direct solar radiation, downward diffuse radiation, and upward diffuse radiation. The scattering of energy from the direct solar beam within each individual layer is treated using the delta-Eddington algorithm, which includes the dependence of scattering and absorption on the solar zenith angle. The scattering of diffuse radiation (i.e., previously scattered radiation) from each individual layer is modeled using the simpler Sagan-Pollack algorithm. Both algorithms allow inclusion of the bulk optical properties of clouds and aerosols. Finally, the adding method is used to calculate irradiances throughout the vertically inhomogeneous atmosphere.

### ***Infrared Model***

The RADIR infrared model that we have been using for several years is a version of the model described by Harshvardhan et al. (1987). For our use it has been modified to

improve the accuracy in the upper stratosphere and includes absorption and emission by CO<sub>2</sub>, O<sub>3</sub>, and H<sub>2</sub>O. It is based on wide-band parameterizations fit to line-by-line calculations. Inhomogeneous absorption paths are included by pressure- and temperature-weighted scaling of trace gas absorber amounts. The model provides for specification of fractional cloud cover within each vertical model layer. Separate fractions can be specified for convective (deep, overlapping) and randomly overlapped clouds.

As part of our effort to develop a new infrared, radiative transfer model based on the correlated k-distribution technique, we have acquired a substantial capability to calculate the absorption properties of common trace gases. We have the HITRAN-91 spectroscopic data base readily available on our workstation network. Temperature-dependent absorption cross-section data for a number of CFCs are included with these data. To make use of these data, we have a version of FASCODE modified to facilitate the calculation of pressure- and temperature-dependent absorption coefficients. A final processing program is available to calculate absorption coefficient frequency distributions from these data.

## REFERENCES

- Allen, M., and J. E. Frederick, Effective photodissociation cross sections for molecular oxygen and nitric oxide in the Schumann-Runge bands, *J. Atmos. Sci.*, 39, 2066-2075, 1982.
- Barnett, J. J., and M. Corney, A middle atmosphere temperature model from satellite measurements, *Adv. Space Res.*, 5, 125-134, 1985.
- Fleming, E. L., S. Chandra, M. R. Schoeberl, and J. J. Barnett, Monthly mean global climatology of temperature, wind, geopotential height, and pressure for 0-120 km, NASA Technical Memorandum 1000697, February, 1988.
- Garcia, R. R., and S. Solomon, A numerical model of the zonally averaged dynamical and chemical structure of the middle atmosphere, *J. Geophys. Res.*, 88, 1379-1400, 1983.
- Harshvardhan, R. Davies, D. A. Randall, and T. G. Corset, A fast radiation parameterization for atmospheric circulation models, *J. Geophys. Res.*, 91, 1009-1016, 1987.
- Jet Propulsion Laboratory, *Chemical Kinetics and Photochemical Data for Use in Stratospheric Modeling, Evaluation No. 9*, JPL Publication 90-1, NASA/JPL, Pasadena, CA, 1990.
- Jet Propulsion Laboratory, *Chemical Kinetics and Photochemical Data for Use in Stratospheric Modeling, Evaluation No. 10*, JPL Publication 92-20, NASA/JPL, Pasadena, CA, 1992.
- Newman, P. A., M. R. Schoeberl, R. A. Plumb, and J. Rosenfield, Mixing rates calculated from potential vorticity, *J. Geophys. Res.*, 93, 5221-5240, 1988.
- Smolarkiewicz, P. K., A fully multidimensional positive definitive advection transport algorithm with small implicit diffusion, *J. Comput. Phys.*, 54, 325-362, 1984.
- World Meteorological Organization, *Atmospheric Ozone, 1985*, Global Ozone Research and Monitoring Project Report No. 16, WMO, Geneva, 1986

World Meteorological Organization, *Scientific Assessment of Ozone Depletion, 1991*,  
Global Ozone Research and Monitoring Research Report No. 25, WMO, Geneva,  
1992.

## MPIC Two-Dimensional Model

C. Bruehl and P.J. Crutzen  
Max Planck Institute for Chemistry

### GRID

Surface to about 60 km, log-pressure grid with about 2 km resolution in the vertical; finer grid with about 600 m resolution near the surface. 10 degrees in latitude from 85S to 85N. Dynamical quantities are given on staggered grid for the central differencing.

### TRANSPORT

The precalculated diabatic circulation in the stratosphere is based on our radiation scheme (Bruehl and Crutzen, 1988) using observed temperatures (MAP) and ozone (CIRA/Shine). In the troposphere mean winds from observations are taken, including a strong Hadley circulation. The two schemes are connected using streamfunction and global vertical mass flux. Winds are given monthly.

The eddy coefficients  $K_{yy}$ ,  $K_{yz}$  and  $K_{zz}$  are derived empirically for each season.  $K_{yy}$  typically is on the order of  $10^{10} \text{ cm}^2 \text{ s}^{-1}$ ,  $K_{yz} \pm 10^6 \text{ cm}^2 \text{ s}^{-1}$  in midlatitudes,  $K_{zz}$  larger than  $10^3 \text{ cm}^2 \text{ s}^{-1}$  with minimum at the tropopause. Usually flux boundary conditions.

### CHEMISTRY

Family technique for  $\text{O}_x$ ,  $\text{N}_x$ ,  $\text{Cl}_x$ ,  $\text{H}_x$ , and  $\text{Br}_x$ ;  $\text{HNO}_3$ , and  $\text{HCl}$  are transported separately. There are about 75 species, including chlorofluorocarbons and some intermediate decay products. Simplified scheme for non-methane hydrocarbons. In total about 150 chemical reactions including the most important heterogeneous ones on sulfate and, optionally, polar stratospheric clouds (PSCs). Combination of analytical and numerical solution methods. Rainout of  $\text{HCl}$ ,  $\text{HNO}_3$ ,  $\text{HF}$ , and some other species in the troposphere following Crutzen and Gidel (1983).

The timestep is 2 hours; fully time dependent with diurnal cycle. Monthly temperatures are fixed. Diurnal cycle of photolysis rates is calculated every 15 days.

### RADIATION

Solar radiation for photolysis rates and heating: six values for the diurnal cycle (2-hr step). Multiple scattering at air molecules, aerosol particles, and climatological clouds treated with the modified delta-two stream method of Zdunkowski (1980) (*see* Bruehl and Crutzen, 1988, 1989). Ground albedo from climatology: 176 spectral intervals, 1-nm resolution between 300 and 320 nm, Allen and Frederick (1982) scheme for Schumann-Runge bands.

### INFRARED

Modified broadband-model of Ramanathan (1976) for  $\text{CO}_2$  (Kiehl and Ramanathan, 1983),  $\text{O}_3$  and  $\text{H}_2\text{O}$ ;  $\text{CH}_4$ ,  $\text{N}_2\text{O}$ , and CFCs included.

## REFERENCES

- Allen, M. and J. Frederick, Effective photodissociation cross sections for molecular oxygen and nitric oxide in the Schumann Runge bands, *J. Atmos. Sci.*, 39, 2066, 1982.
- Bruehl, C. and P. J. Crutzen, On the disproportionate role of tropospheric ozone as a filter against solar UV-B radiation, *Geophys. Res. Lett.*, 16, 703-706, 1989.
- Bruehl, C. and P. J. Crutzen, Scenarios of possible changes in atmospheric temperatures and ozone concentrations due to man's activities, estimated with a one-dimensional coupled photochemical climate model, *Climate Dynamics*, 2, 173, 1988.
- Crutzen, P. J. and L. T. Gidel, A two-dimensional model of the atmosphere. 2. The tropospheric budgets of anthropogenic chlorocarbons, CO, CH<sub>4</sub>, CH<sub>3</sub>Cl and the effect of various NO<sub>x</sub> sources on tropospheric ozone, *J. Geophys. Res.*, 88, 6641-6661, 1983.
- Kiehl, J. T. and V. Ramanathan, CO<sub>2</sub> radiative parametrization used in climate models: Comparisons with narrow band models and laboratory data, *J. Geophys. Res.*, 88, 5191, 1983.
- Peter, T., C. Bruehl, and P. J. Crutzen, Increase in the PSC-formation probability caused by high-flying aircraft, *Geophys. Res. Lett.*, 18, 1465-1468, 1991.
- Ramanathan, V., Radiative transfer within the earth's troposphere and stratosphere: A simplified radiative convective model, *J. Atmos. Sci.* 33, 1330, 1976.
- Zdunkowski, W., An investigation of the structure of typical two-stream methods for the calculation of solar fluxes and heating rates in clouds, *Contr. Phys. Atmos.*, 53, 147-166, 1980.

## **MRI Two-Dimensional Photochemical Model**

**Toru Sasaki**  
**Meteorological Research Institute**

A tape of the results from the two-dimensional model from the Japanese Meteorological Research Institute was submitted to the Upper Atmosphere Research Program in December 1991. Dr. Sasaki was unable to attend the February Models and Measurements Workshop, but results from his model runs were included in our comparisons. Calculations from this model were presented in Section 8.3 of WMO Report No. 25 (1992), and it is assumed that the model description is the same as that presented in Section 4.13 of Conference Publication 3042 (NASA, 1988). I appreciate the participation of Dr. Sasaki in this comparison activity. (Reported by E. Remsberg.)

### **REFERENCES**

National Aeronautics and Space Administration, *Two-Dimensional Intercomparison of Stratospheric Models*, NASA Conference Publication 3042, NASA Scientific and Technical Information Division, Washington, D.C., 1989.

World Meteorological Organization, *Scientific Assessment of Ozone Depletion, 1991*, Global Ozone Research and Monitoring Project Report No. 25, WMO, Geneva, 1992.

## **NCAR Model: Specifications, Limitations, Goals**

**Guy Brasseur, Claire Granier, Ian Folkins, and Stacy Walters  
National Center for Atmospheric Research**

**Matt Hitchman  
University of Wisconsin**

**Anne Smith  
University of Michigan**

The model, described in Brasseur et al. (1990), extends from the surface to 85 km, with a vertical resolution of 1 km, and from 85S to 85N, with a latitudinal resolution of 5 degrees. Radiation, chemistry, and dynamics are treated interactively above the tropopause.

### **DYNAMICS**

A description of the dynamical aspects of the model is given in Brasseur and Hitchman (1987), Hitchman and Brasseur (1988), and Brasseur et al. (1990), and in the Fort Meyers comparison edited by Jackman et al. (1989). Temperature and tracer families are integrated semi-implicitly with a 15-day time step. Zonal winds are diagnosed from thermal wind balance and are used to determine the body forces due to Rossby and gravity waves and corresponding distributions of vertical and meridional eddy diffusivities. The body forces and net heating rates are used to diagnose the residual circulation, hence advection terms for the next time step. The streamfunction solver uses an internal boundary condition at the tropopause which may be tuned to obtain a good "Dobson diagram." It exerts a powerful control on the temperature and the circulation well into the stratosphere.

The most notable limitations at present are the tropopause boundary condition on the streamfunction and tropical dynamics. For a perturbation scenario, the circulation at the tropopause cannot change, causing spurious return flows near the tropopause. The observed behavior of aerosols and radioactive tracers highlights the need to include the quasi-biennial oscillation (QBO) and semiannual oscillation (SAO) dynamics.

A more flexible tropopause condition is being tested on the streamfunction, allowing a portion of it to change with model dynamics. To represent the QBO and SAO, we are integrating both the temperature and momentum equations, blending them at each time step. Kelvin waves and mixed Rossby gravity waves will be included in a similar fashion to gravity and Rossby waves by specifying phase speeds and forcing amplitudes within a linear WKBJ context.

Another goal is to reassess the distributions of mixing coefficients, with particular attention to the tropopause region. Rapid poleward and downward transport within a few kilometers of the tropical tropopause seen in tracer data suggest the need to include the effects of inertio-gravity waves and synoptic-scale Rossby waves that partially penetrate the stratosphere.

### **CHEMISTRY AND RADIATION**

The model calculates the distribution of 56 species. The concentrations of the long-lived species ( $\text{CO}_2$ ,  $\text{CO}$ ,  $\text{N}_2\text{O}$ ,  $\text{HNO}_3$ ,  $\text{N}_2\text{O}_5$ ,  $\text{H}$ ,  $\text{H}_2$ ,  $\text{H}_2\text{O}_2$ ,  $\text{H}_2\text{O}$ ,  $\text{CH}_4$ ,  $\text{HCN}$ ,  $\text{CH}_3\text{CN}$ ,  $\text{CCl}_4$ ,  $\text{CFCl}_3$ ,  $\text{CF}_2\text{Cl}_2$ ,  $\text{CH}_3\text{CCl}_3$ ,  $\text{CH}_3\text{Cl}$ , CFC-113, CFC-114, CFC-115, CFC-22, Halon 12-

11, Halon 13-01,  $\text{CCl}_2\text{O}$ ,  $\text{CClFO}$ ,  $\text{CF}_2\text{O}$ ,  $\text{HF}$ ,  $\text{CH}_3\text{Br}$ ,  $\text{OCS}$ ,  $\text{SO}_2$ ,  $\text{HSO}_3$ ,  $\text{H}_2\text{SO}_4$ ) are calculated by solving a full continuity/transport equation for each of them. The short-lived species are grouped into long-lived families ( $\text{O}_x = \text{O}_3 + \text{O}(1\text{D}) + \text{O}(3\text{P})$ ,  $\text{NO}_y = \text{N} + \text{NO} + \text{NO}_2 + \text{NO}_3 + \text{HO}_2\text{NO}_2 + \text{ClONO}_2 + \text{HNO}_3 + 2 \text{N}_2\text{O}_5$ ,  $\text{Cl}_x = \text{Cl} + \text{ClO} + \text{HOCl} + \text{HCl} + \text{ClONO}_2 + \text{OCIO} + 2 \text{Cl}_2\text{O}_2$ ,  $\text{Br}_x = \text{Br} + \text{BrO} + \text{BrONO}_2 + \text{HBr} + \text{HOBr}$ ) for which a full continuity/transport equation is solved. The concentration of each individual fast reacting species is derived by assuming photochemical equilibrium for the fastest reacting species, and by using a time integration method (Hesstvedt et al., 1978) for the other compounds. The model calculates the 24-hour average of the concentration of each specie from the surface to 85 km altitude.

The rate of the reactions is based on JPL Publication 90-1 (1990). The photodissociation rates are calculated by spectral integration, using the 171 wavelength intervals specified by Ackerman (1972). These correspond to a resolution of  $500 \text{ cm}^{-1}$  (wavenumber) between 117 and 308 nm, of 2.5 nm (wavelength) between 310 and 645 nm, and of 5 nm between 650 and 730 nm. The solar irradiances are specified according to Brasseur and Simon (1981). The absorption cross sections are from JPL (1990). The absorption cross sections as a function of temperature for  $\text{N}_2\text{O}_5$  and for the CFCs are from Simon et al. (1988). The method used to calculate the photodissociation coefficients includes multiple scattering and albedo and is based on the methodology of Fred Luther (private communication): six orders of scattering are considered together with absorption by  $\text{O}_2$  and  $\text{O}_3$ . The surface albedo is specified. Penetration of solar UV in the Schumann-Runge bands is calculated by the parameterization of Nicolet and Kennes (1989); for the photolysis of  $\text{NO}$ , the parameterization of Nicolet (1979) is used. The diurnal average of the photodissociation rates is approximated by a 4-point integral between sunrise and sunset (Cunnold et al., 1975). This procedure allows one to calculate accurate mean photodissociation rates for different altitudes, latitudes, and season with minimum computer costs.

The mixing ratios of the transported species are solved in a two-stage process. First, a system of algebraic equations is formed by replacing all spatial operators with second-order, centered, finite differences and by approximating the temporal derivative with a backward Euler (fully implicit) analogue. Second, the system of nonlinear, algebraic equations is solved via an iterative fixed-point method that allows each specie to be independently computed over the spatial domain. At each time step the "photochemical" species are solved before the transported species via a fixed point method.

The net diabatic rate is calculated by using the radiative code of the NCAR community model (CCM1, Kiehl et al., 1987). The radiation code uses the  $\text{CO}_2$ ,  $\text{H}_2\text{O}$ , and  $\text{O}_3$  distributions calculated by the chemistry/transport model. Below the tropopause, temperatures are specified from the monthly mean climatology of Randel (1987).

The water vapor in the troposphere is calculated as a function of the temperature for a specified relative humidity. Above the tropopause  $\text{H}_2\text{O}$  is calculated as a regular chemical species.

Parameterizations of the heterogeneous processes occurring on the surface of the polar stratospheric clouds (PSCs) are included: type I PSCs are assumed to be formed in less than 1 time step as soon as the temperature decreases to below 195K. Type II PSCs are assumed to be present in the regions where the temperature drops below 191K. These temperatures are higher than the thermodynamical ones to account for the fact that the temperature calculated by the two-dimensional model represents zonal averages, which are higher than that of the coldest air masses at a given latitude. The conversion of  $\text{HCl}$  and  $\text{ClONO}_2$  into

chlorine radicals is assumed to take place in less than a time step. Inside PSCs II, dehydration and denitrification are assumed to occur with a 5-day time constant. Where PSCs I are present, no dehydration takes place, but a weak denitrification is assumed to occur, with a time constant of 30 days. When the sun returns over the polar regions, ozone is destroyed by the classic catalytic cycles and through cycles involving  $\text{Cl}_2\text{O}_2$  and  $\text{BrO}$ .

For the calculations concerning the effects of sulfate aerosols, the values of the mass accommodation coefficients and of the aerosol surface area densities recommended in the UNEP report have been used.

One important limitation of the model is that only 24-hour average values of the concentrations are presently calculated. We are now in the process of including the effect of diurnal cycles. The model will occasionally calculate the diurnal variations of species by going to a much smaller time step of about 15-30 minutes. Based on Turco and Whitten (1978), we will calculate diurnal factors that enhance reaction rates between species that have positively correlated diurnal variations and diminish reaction rates between negatively correlated species.

## REFERENCES

- Ackerman, M., in *Mesospheric Models and Related Experiments*, pp. 149-159, 1972.
- Brasseur, G., and P. C. Simon, *J. Geophys. Res.*, **86**, 7343-7362, 1981.
- Brasseur, G., and M. H. Hitchman, in *Transport Processes in the Middle Atmosphere* (G. Visconti and R. Garcia, eds.) pp. 215-227, D. Reidel, Hingham, MA., 1987.
- Brasseur, G., M. H. Hitchman, S. Walters, M. Dymek, E. Falise, and M. Pirre, *J. Geophys. Res.*, **95**, 5639-5655, 1990.
- Cunnold, D. F., N. Alyea, N. Phillips, and R. G. Prinn, *J. Atmos. Sci.*, **32**, 170-194, 1975.
- Hesstvedt, E., O. Hov, and I. S. A. Isaksen, *Int. J. Chem. Kinetics*, **10**, 971-994, 1978.
- Hitchman, M. H., and G. Brasseur, *J. Geophys. Res.*, **93**, 9405-9417, 1988.
- Jackman, C. H., R. K. Seals, and M. J. Prather, Two-dimensional intercomparison of stratospheric models, *NASA Conference Publication 3042*, NASA, Washington D.C., 1989.
- Jet Propulsion Laboratory, *Chemical Kinetics and Photochemical Data for Use in Stratospheric Modeling, Evaluation No. 9*, JPL Publication 90-1, NASA/JPL, Pasadena, CA, 1990.
- Kiehl, J. T., J. Wolski, B. P. Briegleb, and V. Ramanathan, NCAR Tech. Note, NCAR/TN-288+IA, National Center for Atmospheric Research, Boulder, CO, 1987.
- Nicolet, M., Photodissociation of nitric oxide in the mesosphere and stratosphere: Simplified numerical relations for atmosphere model calculation, *Geophys. Res. Letts.*, **6**, 866-869, 1979.

Nicolet, M., and R. Kennes, Aeronomic problems of molecular oxygen photodissociation - VI. Photodissociation frequency and transmittance in the spectral range of the Schumann-Runge bands, *Planet. Space Sci.*, 37, 459-491, 1989.

Randel, W. J., NCAR Technical Note, NCAR/TN-295+STR, 1987.

Simon, P. C., D. Gillotay, N. Vanlaethem-Meuree, and J. Wisenberg, *J. Atmos. Chem.*, 7, 107-135, 1988.

Turco, R. P., and R. C. Whitten, *J. Atmos. Terr. Phys.*, 40, 13-20, 1978.

## NOCAR Two-Dimensional Model

Rolando Garcia and Susan Solomon  
National Oceanic and Atmospheric Administration  
National Center for Atmospheric Research

Species distributions for the selected present-day atmosphere comparisons in Volume II were performed with the model version described in Conference Publication 3042 (NASA, 1989). The model runs for N<sub>2</sub>O and CH<sub>4</sub> (section E) and for the XI/X2 tracer experiment (section O) were conducted with an updated version of the NOCAR model (Garcia, 1991; Garcia et al., 1992). It is a wave-mean flow, interaction model. The zonal mean dynamics are derived from the momentum equation plus the transformed Eulerian mean meridional circulation. The temperature field is obtained from the zonal wind assuming a gradient wind balance. A single planetary wave model is coupled to the zonal mean equations, and there is a parameterization for planetary wave breaking. (Reported by E. Remsberg.)

### REFERENCES

- Garcia, R. R., Parameterization of planetary wave breaking in the middle atmosphere, *J. Atmos. Sci.*, 48, 1405-1419, 1991.
- Garcia, R. R., F. Stordal, S. Solomon, and J. T. Kiehl, A new numerical model of the middle atmosphere. I. Dynamics and transport of tropospheric source gases, *J. Geophys. Res.*, 97, 12967-12992, 1992.
- National Aeronautics and Space Administration, *Two-Dimensional Intercomparison of Stratospheric Models*, NASA Conference Publication 3042, NASA Scientific and Technical Information Division, Washington, D.C., 1989.

## OSLO Two-Dimensional Transport Chemistry Model

Ivar Isaksen  
University of Oslo

Frode Stordal  
Norwegian Institute for Air Research

Total ozone from the OSLO model was included in the comparisons for section C. These model results were obtained from calculations described in section 8.3 of the report entitled "Scientific Assessment of Ozone Depletion: 1991" (WMO, 1992). It is assumed that the description of the model in Section 4.15 of Conference Publication 3042 (NASA, 1989) is still appropriate for this model. (Reported by E. Remsberg.)

### REFERENCES

National Aeronautics and Space Administration, *Two-Dimensional Intercomparison of Stratospheric Models*, NASA Conference Publication 3042, NASA Scientific and Technical Information Division, Washington, D.C., 1989.

World Meteorological Organization, *Scientific Assessment of Ozone Depletion, 1991*, Global Ozone Research and Monitoring Project Report No. 25, WMO, Geneva, 1992.

## WASH Two-Dimensional Model

K.K. Tung, H. Yang, and E. Olaguer  
University of Washington

The model has coupled dynamics, radiation, and chemistry, requiring only the observed temperature as input, and the specification of lower boundary conditions. The version of the model used for the current intercomparison has been extensively documented in the literature (see Yang et al., 1990, 1991 and Olaguer et al. 1992).

### DYNAMICAL ASPECTS OF THE MODEL

The dynamical transport formulation is as given in Tung (1982, 1986) and Yang et al. (1990, 1991). The model is based on a self-consistent, non-geostrophic formulation in isentropic coordinates. The isentropic mixing coefficient,  $K_{yy}$ , is calculated from the zonal momentum equation using the same National Meteorological Center (NMC) input temperature as that used in the calculation of advective transport from radiative transfer. The model year corresponds to the temperature input year. The vertical coordinate is  $\log(\text{potential temperature})$  above 350K and  $\log(\text{potential temperature/surface potential temperature})$  below 350K. The lower surface is currently specified to be at  $P = 1000$  mb, but an actual (variable) surface pressure can be specified, if desired. The zonal average is taken on the surfaces of constant vertical coordinate.

No gravity wave cross-isentropic mixing is incorporated. Consequently there is no vertical diffusion in the model stratosphere  $K_{zz}$ . No  $K_{zz}$  is included, even in the troposphere.

The Prather advection scheme (Prather, 1986) is used. The meridional domain of the model is from pole to pole in increments of 10 degrees of latitude. The vertical domain is from ground to 8 pressure scale-heights in increments of about 2 km.

### RADIATIVE TRANSFER CODE

A detailed documentation of the radiative-transfer code can be found in Olaguer et al. (1992), where comparison with line-by-line calculations were made and error quantified. The errors in heating rates are generally about 5% or 0.05K per day in the lower stratosphere, when comparisons with line-by-line results are available. The model's net heating is globally balanced to within 0.1K per day in the lower stratosphere using observed inputs, and less when ozone is model generated. The imbalance is uniformly subtracted from the local net heating in the stratosphere. In the troposphere, latent heating, which is uncertain, is decreased or increased to enforce strict mass balance. Three layers of clouds are assumed in the troposphere.

Some relevant information for the current intercomparison experiments are given below.

Photochemical reaction rates and cross sections are from JPL Publication 90-1, except for the following:

- (1)  $k[\text{OH} + \text{CH}_4] = 3.9\text{E} - 12 \exp(-1885/T)$ , as recommended for intercomparison.

- (2) Thermal decomposition rate of  $N_2O_5$  and photodissociation cross sections for  $H_2O$  and  $CClF_2CCl_2F$  are from Baulch et al. (1982).
- (3) Zenith angle-dependent cross sections for  $NO$  and  $O_2$  are computed from the parameterization of Allen and Frederick (1982), with Herzberg continuum cross sections taken from WMO (1986).
- (4) Rayleigh scattering and ozone photodissociation cross sections are from WMO (1986).

## PHOTOCHEMISTRY

Details of the photochemical package can be found in Yang et al. (1991). Family grouping is adopted for the  $O_x$ ,  $NO_y$ ,  $HO_x$ , and  $ClO_y$ . The long-lived species are advected (and diffused) by model-calculated transports, while short-lived species (except the diurnal species) are calculated algebraically under the assumption of photochemical equilibrium. All photochemical processes are assumed to take place only in daylight.

## SPECIFIC TO THE INTERCOMPARISON EXPERIMENTS

For the current intercomparison experiments, some shortcuts were taken, e.g., tropospheric chemistry was switched off and water vapor was specified from observation: Limb Infrared Monitor of the Stratosphere (LIMS) in the stratosphere and Oort's climatology in the troposphere. [Only the January and April data for LIMS were used, which cover 64S to 84N and from 100 mb to 1 mb. Data are extrapolated beyond 64S and 84N, and above 1 mb using the constant value from the last grid point. The poles are reversed for July and October (from January and April). Oort's climatology for January, April, July, and October were specified between 1000 mb and 100 mb. A sinusoidal function is used to interpolate the 4 months into an annually varying field.]

## REFERENCES

- Allen, M. and J. E. Frederick, Effective photodissociation cross sections for molecular oxygen and nitric oxide in the Schumann-Runge bands, *J. Atmos. Sci.*, 39, 2066-2075, 1982.
- Baulch, D. L., R. A. Cox, P. J. Crutzen, R. F. Hampson, J. A. Herr, J. Troe, and R. T. Watson, Evaluated kinetic and photochemical data for atmospheric chemistry: Supplement I. CODATA Task Group on Chemical Kinetics, *J. Phys. Chem. Ref. Data*, 11, 327-496, 1982.
- Olaguer, E. P., H. Yang and K. K. Tung, A reexamination of the radiative balance of the stratosphere, *J. Atmos. Sci.*, 49, 1242-1263, 1992.
- Prather, M. J., Numerical advection by conservation of second-order moments, *J. Geophys. Res.*, 91, 6671-6681, 1986.
- Tung, K. K., Nongeostrophic theory of zonally averaged circulation, Part I: Formulation, *J. Atmos. Sciences*, 43, 2600-2618, 1986.
- Tung, K. K., On the two-dimensional transport of stratospheric trace gases in isentropic coordinates, *J. Atmos. Sci.* 39, 2230-2355, 1982.

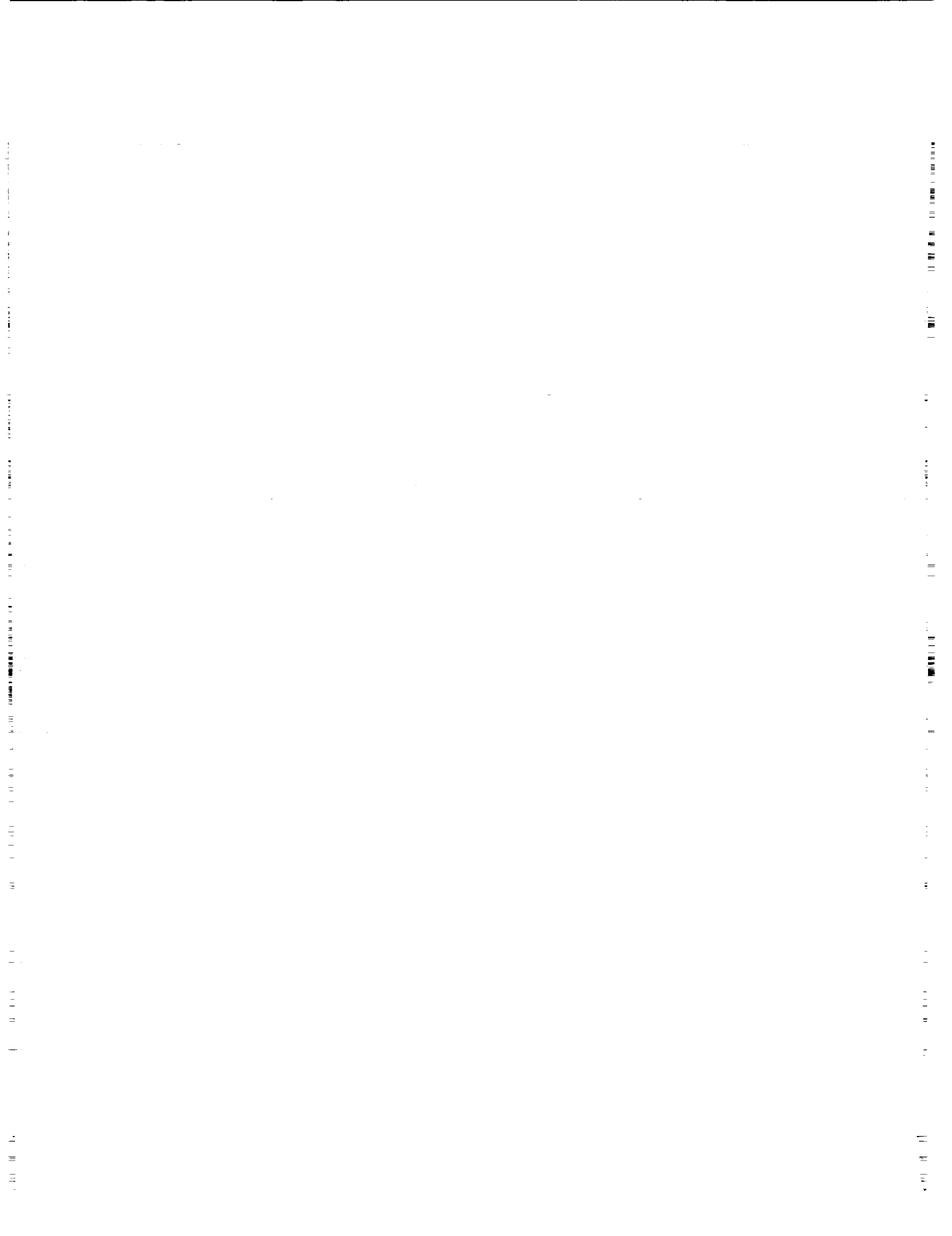
World Meteorological Organization, Atmospheric Ozone 1985: Assessment of Our Understanding of the Processes Controlling its Present Distribution and Change, WMO, Global Ozone Research and Monitoring Project, Report No. 16, Geneva, 1986.

Yang, H., E. P. Olaguer, and K. K. Tung, Simulation of the present day ozone, odd nitrogen, chlorine and other species using a coupled model in isentropic coordinates, *J. Atmos. Sci.*, 48, 442-471, 1991.

Yang, H., K. K. Tung, and E. P. Olaguer, Nongeostrophic theory of zonally averaged circulation, Part II: E-P. Flux divergences and isentropic mixing coefficients, *J. Atmos. Sci.* 47, 215-241, 1990.

## **Chapter 5**

# **Commentary on Models and Measurements Intercomparison**



*Some modeling groups have provided their "editorial commentary" of this Workshop experience. This commentary was optional, but it does represent a response concerning individual model status and performance and/or recommendations for future inter-comparison efforts.*

## **AER Model**

**Malcolm Ko, Debra Weisenstein, Run-Lie Shia, Jose Rodriguez and Dak Sze  
Atmospheric and Environmental Research, Inc**

The publication of this report marks a milestone in the intercomparison exercise. Speaking for our group, we were so overwhelmed with meeting the deadlines for turning in the data and performing analyses on our assigned section that when bits and pieces of the different versions of the three-inches-thick draft report trickled in after the workshop, we hardly had the energy to wade through the document. Our priority at that point was to make sure that the model results we submitted were correctly reproduced. With the publication of the report, we will start the real work of figuring out how the model performed and what improvements are needed.

The AER model analyzed in this report is a 2-dimensional chemical-transport model with specified circulation, temperature, and water vapor. Therefore, a useful phase of the intercomparison for us was to compare our model inputs with the "best" available global data sets of temperature, net heating (or circulation), and water vapor. The NMC temperature data set and the SAGE II water vapor data set can easily be incorporated into our model. Though we are aware that the circulation used by our model is far from ideal, how best to improve it is not straightforward, given the competition between advection and diffusion in determining model transport. Rather than improve the specified circulation in our present model, we plan to continue development of our interactive model, which has been operational for several years though it produces a less-realistic ozone distribution than the chemical-transport model.

Each model has its own strengths and weaknesses based on the emphasis of the model developers. Because our model does diurnal chemistry with 17 time points per day, we believe that it better evaluate heterogeneous mechanisms than a model that calculates only diurnal average species densities or daytime and nighttime average species densities. However, each model must strive to reproduce a wide range of atmospheric observations. Unlike the model input parameters, failure of model outputs to match observations does not immediately lead to ways for model improvements. Not surprisingly, modelers tend to spend their effort in areas where there is disagreement between model results and observations. Often, they do not ask why the model produces good results even though they know that such results may be due to fortuitous choice of parameters. Knowing how other models perform provides a benchmark to determine what needs explaining. We hope this would be a new emphasis for future publications. An ideal way to deal with this in future intercomparison exercises would be to ask one group that does well and another group that does poorly on a particular exercise to work jointly on that area.

Everyone recognized that if one is interested in how ozone responds to a perturbation, one must identify and validate the mechanisms that control the present-day ozone concentration. Thus, the exercise must go beyond mere comparison of the observed and calculated ozone. The set of diagnostic studies was designed to examine specific mechanisms. Experiments K, L, and M address the issue of photochemical interactions, making use of simultaneous measured concentrations of different photochemically-active

species. In these experiments, the role of transport is minimized. This is to be contrasted with the results from experiments E, F, G and H, in which the role of transport cannot be isolated. It is interesting to note that while the occurrence of heterogeneous conversion of  $N_2O_5$  to  $HNO_3$  seems to be supported by diagnostic studies based on in situ aircraft data, the conclusion is less certain for studies based on large-scale data (see discussion on the column abundance of  $NO_2$  in experiment G). Additional data from SPADE should help to resolve this.

The role of transport on ozone is more difficult to quantify. Experiment N is a first attempt to do this, along with other diagnostic studies (experiment O). In addition, experiments A through H all contain information relevant to this issue though it is difficult to isolate the effect of transport in interpreting the results. The same can be said about experiments I and J, which are more concerned with the transport near the tropopause and the residence time of aerosol particles. It is important that more effort should be put into studying how transport modulates the ozone response to chemical perturbations.

We plan to go ahead with our model improvements based on the results of the intercomparison exercise. Our emphasis will be on specific mechanisms and our priority will be on aspects that will affect the response of ozone to perturbations. Short-term improvements to our model, which are already underway, include an increase in the vertical resolution from 3.5 km to 1.2 km, adoption of the new parameterization of the Schumann-Runge band  $O_2$  absorption cross-sections, and incorporation of the most recent JPL-92 rate recommendations.

## Du Pont Two-Dimensional Model

D. A. Fisher, C. Miller, C. H. Hales,  
R. W. Nopper, Jr., and D. L. Filkin  
Du Pont Experimental Station

### MODEL PERFORMANCE

We made a number of revisions and improvements to our two-dimensional (2-D) model prior to the workshop, including

- New residual mean flow parameterization, based on calculated diabatic circulation, with consideration also given to observed lower stratospheric distributions of N<sub>2</sub>O and CH<sub>4</sub> from balloon measurements
- Reduced values of eddy diffusion parameters throughout the stratosphere
- Greatly increased latitudinal resolution (25 grid points pole-to-pole), and conversion from sin (latitude) coordinates to straight latitude coordinates (to obtain additional enhanced resolution near the poles)
- Improved numerical methods for handling advection dominated transport of individual species (no family grouping).

In view of these changes, we were gratified to find that the model, in our estimation, performed fairly well. It generally agreed with the vast majority of the data on long-lived tracers, and in no instances were our results excessively out of line. In key model intercomparisons of photolytic reaction rates, heating rates, and short lived tracer distributions, we were in good agreement with other models, considering the inherent differences in the transport specifications.

We attribute our good agreement with the long-lived tracer data to use of lower vertical residual mean flow velocities for the lower stratosphere, compared to other models. We believe that the diabatic circulations employed in many 2-D models overestimate the velocities in the lower stratosphere. This may be due to neglecting clouds in the thermal IR portion of the calculation when deriving the diabatic circulation. Further, we believe that the calculated net heating rates in the lower stratosphere are very uncertain and difficult to determine precisely. It may be desirable to use other tracers (besides potential temperature) to deduce the residual mean circulation.

### FUTURE MODEL DEVELOPMENTS

The current version of our model features a transport parameterization that is symmetric with respect to the equator (indexed 6 months), and therefore is not able to reproduce certain features of the observed column ozone distribution (Duetsch diagram). We intend to place high priority on modifying the eddy transport parameterization to suitably account for differences between the hemispheres.

We also intend to improve the water vapor parameterization in our model for the 10-20 km region, to better match observational data from SAGE II (water vapor is calculated as an active species above 20 km in our model).

We also plan to improve the treatment of clouds in our model in calculating solar radiation transport and photolytic reaction rates. We believe that improved methods of treating clouds are necessary for making accurate estimates of OH abundances below cloud altitudes and thus lifetimes and profiles for CFC alternatives and other hydrogenated species.

#### OVERALL VALUE OF M&M 92

We found the M&M 92 Workshop of great value. It helped to verify key portions of the model calculations, such as the determination of photolytic reaction rates. It also helped to highlight differences among models and provide a better understanding of factors that contribute to differences in results.

The development and maintenance of an observational data base for atmospheric measurements is perhaps the key product of the workshop. It provides for the first time an authoritative set of data with which to compare model results. Such comparisons at the workshop identified a number of areas in which models are not in good agreement with the observations, including

- Altitude of the ozone maximum mixing ratio
- "Smile" in the ozone mixing-ratio contour plots.

Another key advantage of the workshop was that it enabled modelers and measurement people to network in a setting that encouraged close ties and valuable communications.

We feel there is a need for more workshops of this type in the future.

## **GSFC Two-Dimensional Model**

**Charles H. Jackman and Anne R. Douglass  
NASA/Goddard Space Flight Center**

The whole models and measurements intercomparison activity, while time consuming, was extremely useful to us. Although we have tried over the years to compare our model results to measurements, the intercomparison provided far greater access and ease of comparison of our model results to familiar as well as many other datasets. We feel fortunate to have been a part of this learning experience.

The Upper Atmosphere Data Pilot, which served as the repository for all the model and measurement information, has been shown to be an extremely valuable resource. Linda Hunt and Karen Sage have eased the pain of model/measurement and model/model comparisons dramatically through their expertise in manipulating and plotting large datasets.

Our two-dimensional (2D) model, like other 2D models, is not perfect and we hope to improve it as a result of this activity. On the one hand, we were pleased with our model results compared to ATMOS measurements, measurements of Ruiz aerosol settling, and measurements of HF, HCl, and CH<sub>4</sub>. On the other hand, we were disappointed in our model comparisons to carbon-14, strontium-90, high latitude column ozone, and high latitude lower stratosphere long-lived tracers. It was also clear from this activity that some large differences among the models involved the photodissociation rates.

We plan on improving our model by 1) working on the dynamical representation of the lower stratosphere and upper troposphere, 2) improving our heterogeneous chemistry representation, and 3) evaluating our photolysis rate computation. We hope to improve our dynamical representation of the lower stratosphere and upper troposphere by determining the proper latent heat to use, the impact of the tropopause height, and the impact of vertical diffusion coefficients. We intend to add polar stratospheric cloud chemistry to our model as well as include more heterogeneous reactions that occur on stratospheric sulfate aerosols in our model. We also plan on evaluating our photodissociation rate computation, including the multiple scattering formulation, to determine if there are any apparent problems in this part of our model.

We suggest that these types of intercomparison activities be held every several years as they are useful and educational experiences. We would also suggest that more constraints be placed on certain comparisons, such as those involving the photodissociation rate computation, in order to help understand model differences.

## ITALY Two-Dimensional Model

G. Pitari, G. Visconti, and E. Mancini  
University of L'Aquila

The two-dimensional model developed at the University of L'Aquila (Italy) participated in 13 of the 15 experiments designed for the 1992 M&M campaign with encouraging results, particularly for the experiments related to species transport. Many nice features of the two-dimensional model are related to its strict interaction with a quasi-geostrophic three-dimensional model from which heating rates, diabatic circulation and diffusion coefficients are deduced. The heating rates are consistent with the ozone distribution predicted by the three-dimensional model. The two-dimensional model, in turn, has the advantage of incorporating at a relatively lower cost a much more detailed photochemical code in such a way that several different sensitivity tests for stratospheric trace species can be easily performed. The calculated, zonally averaged steady state distributions of  $\text{NO}_x$ ,  $\text{Cl}_y$  and  $\text{HO}_x$  may be used as input for the  $\text{O}_3$  photochemical code in the three-dimensional model, so that the feedback between two-dimensional and three-dimensional is complete. In general, the ozone distribution predicted by the two-dimensional model does not differ greatly from that calculated with the three-dimensional model, thus proving the consistency of the calculated set of transport parameters.

Correlation diagrams of long-lived species shows a generally larger spread of points for the ITALY model than for other models, although a clear differentiation of points by latitude is found. As would be expected, points corresponding to the tropical latitude band are the most scattered.

More work should be done on photochemistry, in particular for:

- An updated calculation of photodissociation coefficients in the Schumann-Runge bands
- A more detailed scheme for Rayleigh scattering in the lower atmosphere
- A more explicit scheme for diurnal variations.

For future experiments of model intercomparison we believe it is important to give more emphasis to heterogeneous chemistry on different kinds of stratospheric aerosol particles. Modeling groups should try to include aerosol microphysical codes of differing complexity for more meaningful experiments on ozone trends and  $\text{HNO}_3$ ,  $\text{NO}_x$ , and  $\text{HCl}$  distributions. The overall effect on ozone of heterogeneous chemical reactions over sulfate particles and PSCs may be comparable to the result of some refinements in the gas phase chemistry that have already been included in most two-dimensional models.

An effort should also be made to include QBO effects on large-scale transport using two-dimensional modeling. For example, an experiment similar to the one for the Ruiz cloud could be repeated in the future in a more meaningful way with the QBO effects included.

## LLNL Two-Dimensional Model

Douglas Kinnison and Donald Wuebbles  
Lawrence Livermore National Laboratory

The NASA HSRP/AESA model data intercomparison has been a very useful exercise for our group. Comparing model-derived species distributions to observed data is absolutely a necessary component to validating our atmospheric models. Overall we are very pleased with the agreement of the observed data with both the LLNL two-dimensional and the LLNLND two-dimensional (New Dynamics) models.

At the time of this intercomparison, the dynamics representation of the LLNL two-dimensional model was being updated (*see* Chapter 4) to a more realistic representation of eddy diffusion processes. This task was partially completed and a small subset of the requested data (column O<sub>3</sub>, CH<sub>4</sub>, N<sub>2</sub>O, and carbon-14) was submitted to the UADP data base. In general, species distributions are in better agreement with the new dynamical approach. For example, column ozone distributions from the new dynamics, which show the Southern Hemisphere ozone maximum now off the pole, are in better agreement with TOMS data. Also, the stratospheric residence time increased, showing better agreement with carbon-14 (section I).

In reviewing all the sections, the LLNL two-dimensional model differed greatly from the data and results from other models in the following two instances:

- In section A, the model-derived net heating rate showed a band of cooling across all latitudes. We ascribe this to an inconsistency in using observed temperature and model-derived ozone to calculate our net heating rates. In the future this will not be a problem when we finish updating the dynamical formalism. Our new model will involve a fully interactive model in which temperature and the radiatively active species distributions will be derived concurrently, thus giving a consistent net heating rate.
- In section G, the model-derived NO<sub>2</sub> was higher in the upper stratosphere than SAGE II data. We currently are investigating this difference.

Additional model development is continuing in order to meet the needs of the 1993 and 1995 assessments and for other studies needed by HSRP. The most important areas where model improvement are needed are listed below:

- **Heterogeneous processes:** We plan on studies to consider the sulfuric acid aerosol formation, growth, and sedimentation. Coupling this capability to the LLNL two-dimensional model will allow us to model heterogeneous chemical processes that may be affected by increased emissions of sulfur dioxide from HSCTs or volcanic eruptions.
- **Enhanced Tropospheric Chemistry:** Increased emissions of CH<sub>4</sub>, CO, NO<sub>x</sub>, and NMHC from subsonic aircraft will affect hydroxyl radical and ozone concentrations in the troposphere. Changes in the hydroxyl radical will change the amount of chlorine-containing species that reach the stratosphere. The resultant changing ozone concentrations will affect the radiative forcing, and therefore, the climate. Having a complete reaction set, including the organic nitrates, is needed to accurately represent these feedbacks.
- **Improved Dynamical Representation:** As mentioned above we are currently modifying the dynamical approach used in the LLNL two-dimensional model.

- **Seasonally-Varying Tropopause Height:** Accurate knowledge of this altitude level at all latitudes as it responds to seasonal variations in temperature profiles is essential to the proper modeling of stratospheric-tropospheric exchange.
- **Excited O<sub>2</sub> Chemistry Upper Stratosphere:** We are currently studying the effect of vibrational excited oxygen from ozone photolysis as a source of odd-oxygen in the upper stratosphere. Currently model-derived ozone is approximately 20-40% lower than observed data in this region.
- **Schumann-Runge Cross Sections:** We are developing a new fit to the Schumann-Runge band region (175-205 nm) similar to the approach used by Allen and Frederick, but using updated spectroscopic data.
- **Infrared Model:** We have designed and implemented a prototype correlated k-distribution model for the infrared transmission of the individual molecules H<sub>2</sub>O, CO<sub>2</sub>, O<sub>3</sub>, CH<sub>4</sub>, and NO<sub>2</sub>, plus a combined mixture of these molecules in the atmosphere between 0 and 60 km. The model substantially reduces computational complexity when compared to detailed line-by-line calculations while providing accuracies to within ten percent of the line-by-line calculations.
- **Cloud Properties:** We are improving our cloud parameterization using frequencies of occurrence and the amount, when present from satellite data. This is coupled with a parameterization of the cloud optical depth based on cloud type and/or cloud liquid water content.

To evaluate and understand the potential influence of subsonic and HSCT aircraft on ozone and other important species, observed global data must be available in the 15-25 km region, which currently is a very difficult region to model accurately. The model/data comparisons in this workshop did not address this region. Without observed data to validate the chemical and physical processes that occur in this region, confidence in model-derived species changes from anthropogenic perturbations will be very uncertain.

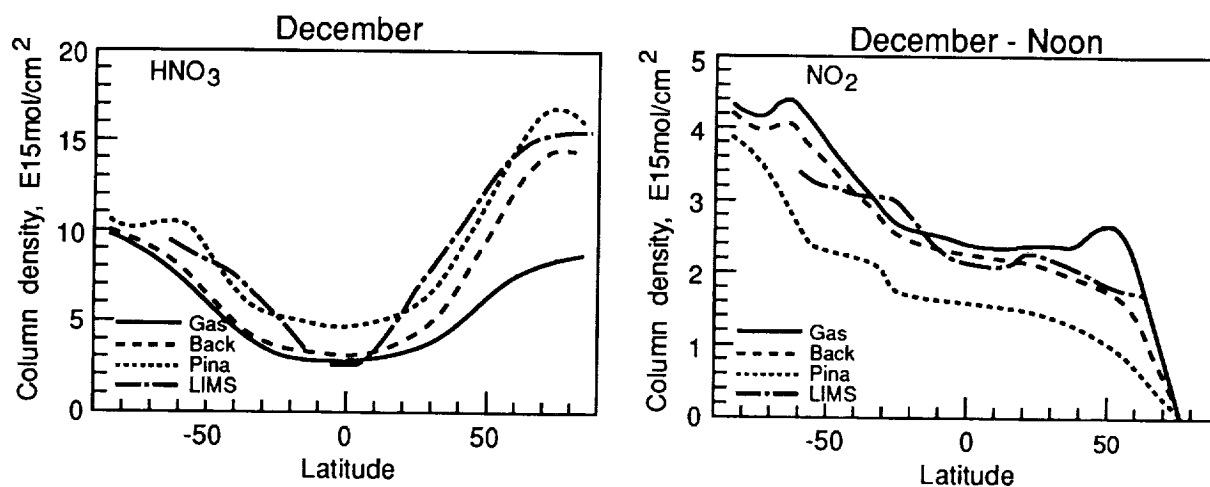
## MPI Model

Christoph Bruhl  
Max Planck Institute for Chemistry

Although other commitments prevented us from submitting all the required data to the UADP data base in time, the M&M workshop was very valuable in letting us compare the performance of our model with observations and the other models. Some comparisons have been done later based on our standard output and the drafts of the different sections. A general finding is that our model fits well into the range given in the intercomparison. The most important reason for differing from the observations appears to be that we may have too much meridional and vertical eddy diffusion in our transport scheme, a problem that was evident in the  $^{14}\text{C}$ -experiment and also in the intercomparisons for  $\text{NO}_y$ ,  $\text{N}_2\text{O}$ , and  $\text{CH}_4$ . For  $\text{NO}_y$  the magnitude and position of the maximum are about right but there is too much spread to high latitudes. In the lower stratosphere the meridional gradients in the middle latitudes are too shallow.

An important feature of the Mainz model is that it simulates the Hadley Circulation in the troposphere based on mean observed winds, with the consequence that total ozone values in the subtropics and tropics are in good agreement with observations. The diabatic circulation in the high latitude lower stratosphere has to be improved; however, there are no strong winds in the wrong direction as presented in Florida in some examples. One problem is to get a good data set of observed ozone in the lower stratosphere (below about 30hPa) to compute the monthly fixed diabatic circulation, a data set that is not available yet. For water vapor the condition at the tropical tropopause should be improved since we assume too low mixing ratios there. Eddy transport of water through the tropopause is not considered and also not recommended because of too large a dependency on the model grid.

The figure below shows  $\text{HNO}_3$  and  $\text{NO}_2$  columns calculated using the MPI model with gas phase chemistry only and with heterogeneous background (Back) and enhanced sulfate (Pina) chemistry compared to the LIMS measurements.

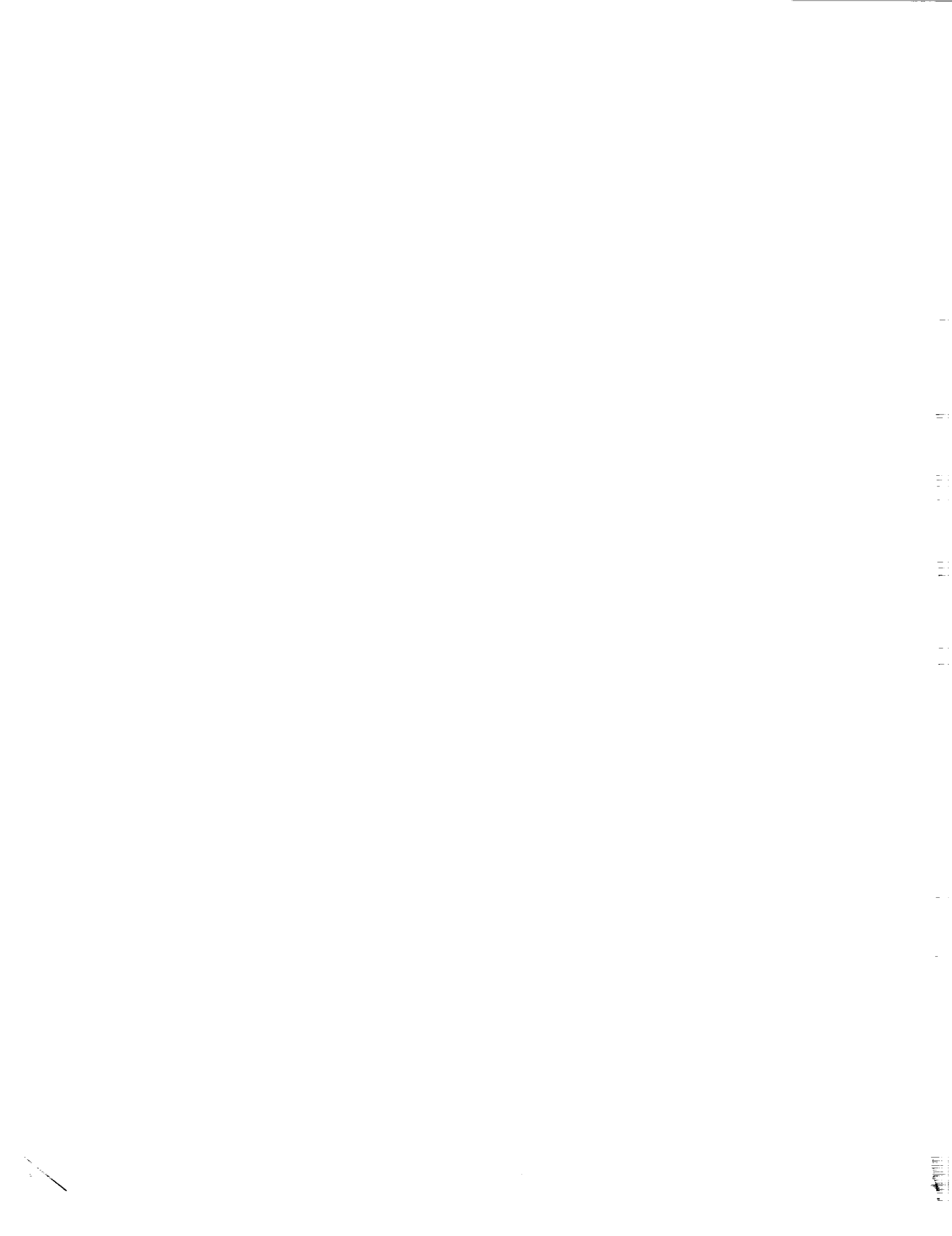


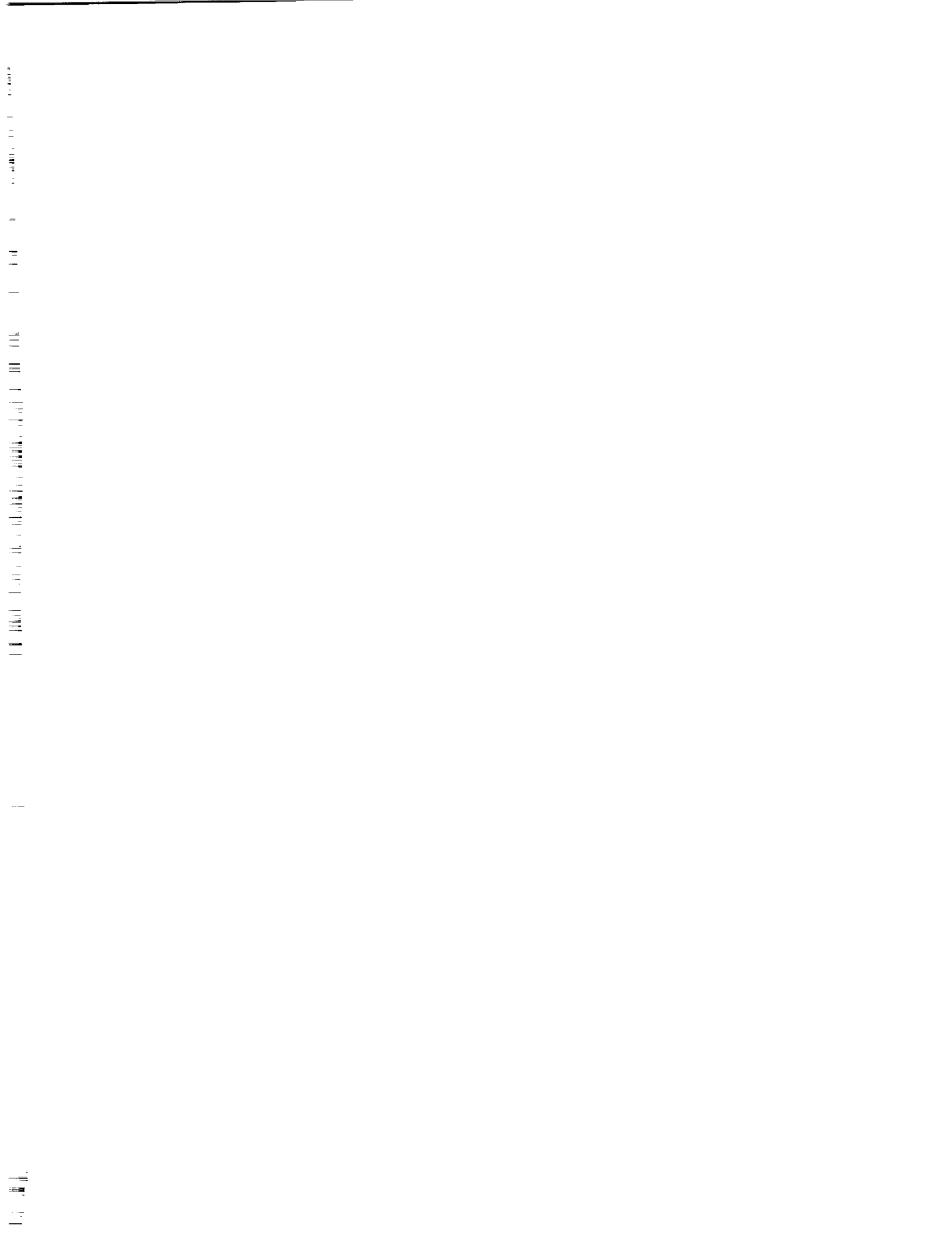
To model ozone in high latitude spring, it is essential to include PSC-chemistry, a problem we are now working on. Except in the ozone hole regions the modeled distribution of ozone is fair. By including the chemistry on sulfate aerosol, it is possible to get at least the columns of  $\text{HNO}_3$  and  $\text{NO}_2$  in agreement with observations. Column abundances for HF and HCl in 1980

are in fair agreement with the cited observations for seasonal and latitudinal dependence in Chapter G but are at the low end of the models discussed.

The photolysis rates calculated by the Mainz model are in the range of the other participating models. More differences than in Chapter K may appear if the models are intercompared in their normal operational model including scattering by cloud droplets and aerosol particles. In Europe another intercomparison of photolysis rates is now in progress which also looks for differences at large solar zenith angles, which is important for polar chemistry.

For comparisons with observations it is more reasonable to run models in a time-dependent mode than in quasi-steady-state. Especially for HF and HCl there is a significant difference. It might also be useful to model nearly inert tracers like CO<sub>2</sub>. Another useful experiment might be to prescribe the transport parameters and just intercompare the chemistry more generally than in Chapters L and M. However, this might not be possible for all participating models because of the many transport schemes.







## Report Documentation Page

1. Report No. NASA RP-1292, Vol. I	2. Government Accession No.	3. Recipient's Catalog No.	
4. Title and Subtitle  The Atmospheric Effects of Stratospheric Aircraft: Report of the 1992 Models and Measurements Workshop <i>Volume I—Workshop Objectives and Summary</i>		5. Report Date March 1993	6. Performing Organization Code
		8. Performing Organization Report No.	10. Work Unit No.
7. Author(s) Michael J. Prather and Ellis E. Remsberg, Editors		11. Contract or Grant No.	
		13. Type of Report and Period Covered Reference Publication	
9. Performing Organization Name and Address NASA Office of Space Science and Applications Earth Science and Applications Division		14. Sponsoring Agency Code	
		12. Sponsoring Agency Name and Address National Aeronautics and Space Administration Washington, DC 20546	
15. Supplementary Notes  Prather: NASA Office of Space Science and Applications, Washington, D.C.; Remsberg: Langley Research Center, Hampton, VA.			
16. Abstract  This Workshop on Stratospheric Models and Measurements (M&M) marks a significant expansion in the history of model intercomparisons. It provides a foundation for establishing the credibility of stratospheric models used in environmental assessments of chlorofluorocarbons, aircraft emissions, and climate-chemistry interactions. The core of the M&M comparisons involves the selection of observations of the current stratosphere (i.e., within the last 15 years): these data are believed to be accurate and representative of certain aspects of stratospheric chemistry and dynamics that the models should be able to simulate.			
17. Key Words (Suggested by Author(s))  The stratosphere; Observations; Chemical models; Dynamical models; Ozone		18. Distribution Statement  Unclassified - Unlimited Subject Category 45	
19. Security Classif. (of this report) Unclassified	20. Security Classif. (of this page) Unclassified	21. No. of pages 144	22. Price A07

